Fiber Dosage Effects in Asphalt Binders

And Hot Mix Asphalt Mixtures

by

Ashraf Alrajhi

A Thesis Presented in Partial Fulfillment
of the Requirements for the Degree
Master of Science

Approved November 2011 by the
Graduate Supervisory Committee:

Kamil Kaloush, Chair
Matthew Witczak
Michael Mamlouk

ARIZONA STATE UNIVERSITY

May 2012

ABSTRACT

The application of fibers and other materials in asphalt mixes has been studied and applied over the past five decades in order to improve pavement performance around the world. This thesis highlights the characteristics and performance properties of modified asphalt mixes using a blend of polypropylene and aramid fibers, The main objective of this study was to evaluate the effect of adding different fiber dosages on the laboratory performance of both asphalt binder and mixture. The laboratory study was conducted on sixteen different dosages and blends of the fibers, with various combinations of polypropylene and aramid, using binder tests as well as hot mix asphalt tests. The binder tests included: penetration, softening point, and Brookfield viscosity tests. The asphalt mixture tests included the dynamic modulus and indirect tensile strength. The binder test results indicated that the best viscosity – temperature susceptibility performance would be from the blend of three dosages of polypropylene and one dosage of aramid, the dynamic modulus test results also confirmed this finding. Overall, in almost every case, the addition of fibers resulted in an increase in mixture stiffness regardless of fiber content. From the indirect tensile strength results, the polypropylene fibers had less of an effect on post peak failure than the aramid fibers. Overall, the aramid fibers yielded better results than the polypropylene fibers.

This study has important implications for the future of pavement design and the prospect of using optimal dosages of polypropylene and aramid fibers in

further research to further determine their long-term performance and characteristics used in real world applications.

DEDICATION

This work is dedicated to the future of the field of pavement design and to my family. Thank you for your unconditional support.

ACKNOWLEDGMENTS

In the name of God, most Gracious, most Compassionate. Numerous individuals are to acknowledge for their contributions during the research and writing of this work. First, I want to acknowledge my mother, father, sisters, and brothers for their undying support and love throughout my educational experience. Their presence kept me going throughout this journey, even with 10,691 kilometers between us. Special thanks go to my mentor, Dr. Kamil Kaloush, for your wisdom, support, and encouragement, and to Dr. Matthew Witczak for providing the supplies necessary to conduct this research. My peers in the Pavement and Materials Program continuously inspired me as we learned from and assisted one another. I want to especially acknowledge my colleagues, Waleed Zeiada, Mena Souliman, Jeff Stempihar, and Kenny Witczak, for your assistance and guidance during the many hours spent in the laboratory, and my good friend and colleague, Ramadan Salim, for contributing to the first phase of the research and for his loyalty from my first day in the U.S. until the end. Finally, undying thanks goes to Katie Curiel for her support, encouragement, and knowledge throughout my entire education in the U.S.

TABLE OF CONTENTS

Page

LIST OF TABLES

Table Page

Table Page

Table Page

Table Page

Table Page

LIST OF FIGURES

CHAPTER 1 INTRODUCTION

1.1 Introduction

Due to the rapid urbanization and industrialization of the world over the last century, the construction and maintenance of transportation roadways is a constant demand in both urban and rural areas. Furthermore, due to excessive traffic loads and environmental factors, many existing pavements have already reached the end of their service life and other pavements will soon require maintenance (1). The economic impacts of roadway construction and maintenance are another major factor, with an estimated 500 million tons of hot mix asphalt being produced and placed in the United States alone, costing about $10.5 billion (2). As the world continues to urbanize and construct transportation roadways, the need for quality sustainable pavement is a constant need. Due to these demands, transportation experts and engineers are focused on improving the performance and life of pavements.

More specifically, pavement design research has focused on the application of various fibers in asphalt binders and mixtures to improve performance. Since the 1950s, research studies reported on the performance of many different fibers, from polyester to used tire shreds, which have shown success in their applications throughout various constructions (3).

The use of fibers in asphalt binders has specifically proven useful in its applications with flexible pavements, also known as hot mix asphalt (HMA). Additional use of various fibers, included: cellulose, polyester, mineral, rubber,

aramid, collagen, carbon, rock wool, geogrids, polymer/ "plastic", and polypropylene (4).

Fiber applications in HMA can provide additional reinforcement to pavement structures, improve the life of the pavement, and provide versatility in varying environmental conditions, such as repeated traffic load, climate impacts and changes, and the condition of existing pavements. However, the effects of using fibers in asphalt binders and mixtures vary widely depending on the combinations, amounts, and variables of the fibers used. Most recently, the success of fibers has been determined by those that both increase the tensile strength and also provide good lateral confinement of the reinforcement mechanism (5).

In 1978, FORTA Corporation introduced the concept of three-dimensional synthetic fiber reinforcement to the construction market worldwide. FORTA-FI products are proprietary blends containing aramid and polyolefin fibers and other materials, known for their strength, durability, and binding properties. The application of FORTA fibers in HMA have proven several advantages, such as improving the reinforcement of both conventional and modified asphalt mixtures, as well as stability-related problems (6).

Previous research also includes a City of Tempe neighborhood street overlay project with research work conducted by Arizona State University (ASU) in 2008, an overlay street project over 2,200 meters-long conducted by the City of Bautou, China in 2005, and the latest project, the Jackson Hole Airport runway rehabilitation project conducted in 2009 in Wyoming. These projects used a

typical (FORTA) fiber dosage of 1 lb./ton. The results proved that FORTA fibers improved properties such as the Marshall Stability, tensile strength, compressive strength, permanent deformation, and fatigue life. FORTA fibers have also proven to reduce the propagation of load-induced reflective cracking. HMA modified with FORTA fibers is generally expected to last up to 20% longer than untreated pavements if subjected to the same loading and environmental conditions (6).

1.2 Study Objective

The objective of this study was to compare the effects of different dosages of FORTA fibers (polypropylene and/or aramid) on the performance of an asphalt binder and HMA mixtures. Nine different dosages were evaluated for one source of asphalt binder, and sixteen different dosages were evaluated for the effect of fibers on HMA mixture performance.

1.3 Scope of Research

The different combinations included a control asphalt binder and mixture with no fibers added, and three fiber modified asphalt binder and HMA mixtures at 1 lb./ton, 2 lbs./ton, and 3 lbs./ton. of the FORTA fibers. The fiber combinations also included a blend of the of the polypropylene and aramid fibers. that the binder Performance Grade PG 58-28 was used in this study. Binder consistency tests were conducted on the PG 58-28 binder to develop the ASTM A_i-VTS_i viscosity-temperature relationships. The following tests were performed at various temperatures: penetration, ring and ball softening point, and Brookfield viscosity. Moreover, the advanced material characterization tests conducted on

the control and modified HMA mixtures included: dynamic (complex) modulus and indirect tensile strength tests.

1.4 Thesis Organization

This thesis is composed of seven chapters. Chapter one includes the introduction, study objective, and scope of work. Chapter two contains a literature review discussing the background and existing research on fiber reinforced asphalt concrete mixtures. Chapter three includes details on the laboratory mixtures. Chapter four summarizes the binder characterization tests. Chapter five presents the dynamic modulus tests. Chapter six discusses the indirect tensile test. Finally, chapter seven provides a summary of the research, conclusions, and recommendations for future work.

CHAPTER 2 LITERATURE REVIEW

2.1 Modified Mixtures

2.1.1 Polymer Modified Mixtures

Polymer additives are generally thought of as "plastic" fibers. Polymers are large molecules created by joining together many small molecules. There are two actions that occur in order for the polymerization processes to occur, namely the "addition" and "condensation" processes. "Addition" polymers are produced by covalently joining the individual molecules, producing very long chains. When two or more types of molecules are joined by a chemical reaction, a byproduct (such as water) is released, called "condensation" polymers. A lattice within the asphalt cement is created by combining small molecules into larger ones. The larger molecule lattice is more stable under high and low temperatures, thus resists thermally induced cracking in the winter and permanent deformation or rutting in the summer (7).

The addition of polymers to asphalt has been shown to improve performance. Researchers showed benefits such as greater resistance to rutting and thermal cracking, decreased fatigue damage, improved stripping and temperature susceptibility (8, 9, and 10). Polymer modified binders have been used with success at locations of high stress, such as intersections of busy streets, airports, vehicle weigh stations, and race tracks. Various types of polymers are used to modify the asphalt binder. Examples are styrene–butadiene–styrene (SBS), styrene butadiene rubber (SBR), Elvaloy, rubber, ethylene vinyl acetate (EVA), polyethylene, and others. Desirable characteristics of the polymer

modified binders include greater elastic recovery, a higher softening point, greater viscosity, greater cohesive strength and greater ductility (8, 9, and 10). Low-temperature cracking can be controlled through use of low-viscosity based asphalt (11).

In a 2003 US Army Corps of Engineers study, it is pointed out that polymer modified binders provided resistance to multiple distresses, such as rutting, fatigue, thermal cracking and water damage (10, 12). Novophalt is a specific type of polymer modified asphalt cement that was developed in Europe in 1976, and later introduced in the United States ten years later. It is known for increasing resiliency and durability, and stops asphalt rutting and shoving at elevated temperatures. It is also known for its ability to increase the cohesion and adhesion of the binder to the aggregate, thereby reducing stripping and raveling (13). Research studies indicated that a mixture with Novophalt was approximately seven times more resistant to rutting than the control at 60 °C/140°F. About 4% to 6% (by weight of binder) of polyethylene is added to asphalt cement in a high shear mixer to acquire the Novophalt modified mixture. In 1990, about 92% of the resin used by Novophalt came from recycled material. Polyolefin, the original source of polyethylene, is one of the resins used by Novophalt that is found in many commonly used plastic materials such as, milk jugs, trash bags, and sandwich bags. (14, 15, 16)

2.1.2 Asphalt Rubber

Asphalt rubber is defined as a blend of ground tire rubber with conventional asphalt cement. This involves heating the asphalt cement to high

temperatures and adding rubber until the desired mixture is obtained. The term “reclaimed rubber” refers to raw or unprocessed tire rubber, while “recycled rubber” refers to processed tire rubber. One characteristic of rubber's beneficial qualities is its flexibility and rutting resistance (17, 18).

The discarding of waste tires from vehicles is a major global environmental issue. Civil engineering researchers discovered methods for recycling and reusing waste tires through their use as a pavement modifier. The use of Crumb Rubber (CR) as a binder for pavement mixtures has proven to be more successful than previous attempts to enhance the properties of pavement mixtures that led to better performance of paving mixes. In various studies of Crumb Rubber's performance, characteristics, such as fatigue and permanent deformation, temperature and moisture susceptibility, and oxidative aging were tested. Several attempts utilized in the past to enhance the properties of mixture that led to better performance of paving mixes (19). Results of one study in India illustrated that crumb rubber modified asphalt mixture yielded more positive results for fatigue and permanent deformation characteristics compared to conventional mixture. Furthermore, there was lower temperature susceptibility and greater resistance to moisture damage than the conventional mixture (19). There are two fundamental methods utilizing crumb rubber in asphalt pavements which are the wet and dry methods. In the wet method, a ground rubber is added to hot asphalt cement, producing a modified binder named asphalt rubber. Two technologies are used to accomplish this blending, the McDonald and the continuous blending technologies. The McDonald technology is sometimes called

the Saguaro, or Arizona, technology. This method is the most widely used process because of its success in achieving the desired modification of the asphalt rubber binders and mixtures. The other method for utilizing crumb rubber is the dry method which involves blending rubber particles with the aggregate before incorporating the liquid asphalt. This method has received less attention due to its ineffectiveness in achieving the desired modification for the binders and mixtures. The crop product is called Rubber Modified Hot Mix Asphalt. PlusRide is one common trade name for this product (18, 20).

Hanson, et al., assessed the proportional field performance of conventional and rubber modified hot mix and related performance to laboratory testing. They assessed the performance of the rubber-modified hot mix used in very fine granules (80 meshes). Laboratory properties measured included resilient modulus, indirect tensile strength, densification properties, stripping resistance and confined dynamic creep. The test results in these studies showed the rubber modified hot mix asphalt had improved stripping resistance, resilient modulus and resistance to rutting compared to the conventional hot mix asphalt. While the tensile strength ratio of the RMHMA was higher than the control, it should be noted that it was still only 50%, versus 38%, for the control, which may indicate the mix was prone to stripping with or without the rubber. The results of the tensile strength test showed no difference, and field performance after two years showed no cracking and only minimal rutting. (18, 21)

The addition of rubber allows higher asphalt content to be used in open-graded mixes, leading to the expectation of increased durability for those mixes.

Increased costs of at least 10% are expected. However, the increase is expected to be offset by the additional life of the asphalt pavement. (18, 22)

2.1.3 General Fiber Studies

For over six decades, fibers have been widely used in several civil engineering applications. Fiber reinforcement refers to incorporating materials with desired properties within some other materials lacking those properties. With its foundations dating back to the 1950s, the practice of using fiber-reinforced bitumen is not new to the industry. A multitude of fibers and fiber materials are being introduced in the market regularly (3).

Fibers are primarily used as reinforcement in order to provide additional tensile strength in the resulting composite, which can increase the amount of strain energy that can be absorbed during the fatigue and fracture process (23). Since fibers have higher tensile strengths compared to bituminous mixtures, they have the possibility to enhance the cohesive and tensile strength of bituminous mixes. Fibers have the ability to impart physical changes to bituminous mixtures, such as reinforcement and toughening (24). Divided fibers provide a high surface area per unit weight, and behave much like filler materials which bulk the bitumen eliminating aggregate run off during construction (23).

Both natural and synthetic fibers have been utilized in various hot mix asphalt applications. Natural fibers include asbestos, cellulose, and rock wool. While synthetic fibers include polypropylene, polyester, and aramid. Fibers do not react chemically with the asphalt but rather reinforce and stiffen the asphalt mastic. The possible advantages of using fibers to reinforce asphalt paving

mixtures include reduced fatigue, thermal and reflective cracking; increased service life; and economic benefits (17, 25, 26)

Rapid advances in technology have caused the development of construction materials allowing research to be focused on increasing the serviceability and safety of concrete structures using fibers as reinforcement. Several different types of fibers, such as asbestos, steel, glass carbon, Kevlar, polypropylene, and nylon, have been widely utilized. Each varies considerably in properties, effectiveness and cost (27).

In one study, the dynamic characteristics of fiber-modified asphalt mixture were investigated using cellulose, polyester, and mineral fibers. Each fiber type was tested along the following dosages: 0.3%, 0.3%, and 0.4%. A gyratory compactor was used to prepare samples for the dynamic modulus test. The testing focused on uncovering the characteristics of the dynamic modulus (E^*) and the phase angle (δ) for the control asphalt mixtures and the fiber-modified ones at various temperatures and frequencies. The results illustrated that all fiber-modified asphalt mixtures had a higher dynamic modulus compared with the control mixture. The results indicated that the fatigue and rutting resistance properties can be improved by fiber additives (28).

Serfass and Samanos reported that two million load applications were applied to fiber modified asphalt utilized as an overlay mixture on pavements showing fatigue cracking. As a result, the macrostructure of the pavement surface had practically no cracking whatsoever, even on the flexible structural pavement, proving the effectiveness of the fiber modified asphalt concrete as an overlay

mixture. They reported that the macrostructure integrity related to maintained skid resistance over time, and the lack of fatigue cracks implied that the fatigue life of the fiber modified overlay is greater than the fatigued, unmodified pavement underneath (29, 30).

In a separate study, a fracture mechanics approach was used to evaluate the effects of fiber reinforcement on crack resistance (31). Polyester and polypropylene fibers were used to modify mixtures that were then tested for modulus of elasticity, fracture energy, and tensile strength. The study showed that toughness was increased as a result of a 50 to 100 percent increase in the fracture energy, while there was little affect on elasticity and tensile strength (30).

In 1994, Simpson conducted a study of modified asphalt mixtures in Somerset, Kentucky that utilized polypropylene and polyester fibers and polymers to modify the asphalt binder. The study evaluated two proprietary blends of modified binders. Tests also included Marshall Stability, Indirect Tensile Strength (IDT), moisture damage susceptibility, freeze/thaw susceptibility, resilient modulus, and repeated load deformation. The study concluded that mixtures including polypropylene fibers had higher tensile strengths and resistance to cracking, whereas resistance to moisture and freeze/thaw damage was not affected. IDT results predicted that the control and polypropylene mixtures will not have problems with thermal cracking, whereas mixtures made with polyester fibers and polymers may. High temperature resilient modulus testing showed that the polypropylene fiber modified mixtures were the stiffest. Decreasing of rutting

measured by repeated load deformation testing was only found for the polypropylene modified samples (30, 32).

2.1.3.1 Polypropylene Fiber

Polypropylene fibers are widely used as a reinforcing agent in concrete. A major benefit to using polypropylene fibers, especially in the United States, is to provide three-dimensional reinforcement of the concrete. However, wire mesh reinforcement cannot be replaced by these fibers. Using polypropylene fibers as a secondary reinforcement can decrease an expected cost by partially replacing steel fibers. A study at the Ohio Department of Transportation (ODOT) made a standard for the use of polypropylene fibers in high-performance asphalt mixture (33). According to ODOT's standard, high performance hot asphalt mix concrete is composed of three materials: aggregates, bitumen and polypropylene fibers.

The polypropylene fibers should be added to the asphalt mix in a ratio of about 2.7 kg/ton. However, this ratio can be changed in order to satisfy the desired mechanical properties of asphalt pavement. The fibers are added to the heated aggregate prior to introduction of the asphalt cement. The aggregate and fibers are mixed dry for additional 10 seconds after the introduction of the fibers. (34).

In a 1993 study, Jiang et al. utilized polypropylene fibers in an attempt to reduce reflection cracking in asphalt overlays. A reduction or delay in reflection cracking was not observed, although the frequency of cracking was less on the fiber modified overlay sections. Sections in which the concrete was cracked and

seated before the overlay were found to have less reflection cracking when fibers were used in either the base or binder layers (35).

In 1996, a study of asphalt overlays modified with polypropylene fiber was conducted by Huang et al. There were mixtures with fiber and others without fiber that were prepared and cored for further analysis. Tests concluded that the fiber modified mixtures were stiffer and demonstrated enhanced fatigue life. The biggest problem encountered with polypropylene fibers is the inherent incompatibility with hot asphalt binder due to the low melting point of the fiber. Huang also expressed that the viscoelastic properties of fiber modified asphalt mixtures needed further research in order to fully understand their properties and functionalities (30, 36).

2.1.3.2 Polyester Fiber

Polyester is the polymerized product of components from crude oil of which asphalt is also a component. Polyester fibers should be used if strong and durable reinforcement of bitumen-fiber mastics is needed at higher temperatures. When tested for rheological characteristics and fatigue properties, the use of polyester fibers indicates that the viscosity of asphalt binder increases with the increase in polyester fiber contents, especially at lower temperatures and lower stress levels (37).

In this 1989 study, the effect of loose fibers in overlay mixtures was investigated by Maurer et al. Due to its higher melting point, polyester fibers were selected over polypropylene fibers. It was observed that the production of the hot mix asphalt was done without complexity or extra equipment. The performance of

the polyester fiber modified mixture was compared with several types of fiber reinforced interlays and a control section. Each tested section was rated for ease of construction, cost, and resistance to reflection cracking. It was observed that sections using loose modified fiber tested best overall (38).

2.1.3.3 Cellulose Fiber

In this study, the effects of cellulose fibers were investigated by Decoene et al. (1990) on bleeding, void content reduction, abrasion, and drainage in porous asphalt. While significantly decreasing bleeding of the binder, cellulose fibers in the hot mix asphalt also increased asphalt contents. There were no remarkable changes in either abrasion with the addition of cellulose fibers or void content. For six months, all test sections were observed for drainage. Sections containing fibers retained the same drainage quality, while the drainage time doubled in sections without fibers (39).

In a second study by Stuart et al. (1994) loose cellulose fibers, pelletized cellulose fiber and two polymer fibers, were assessed for binder drain-down, resistance to rutting, low temperature cracking, aging and moisture damage. Drain-down test results indicated that mixtures with polymers or the control drained remarkably more than those with fiber. The control samples were found to have excellent resistance to rutting and no significant difference was observed between the control and mixtures with a modified binder. It was also observed that resistance to aging was greater when using polymer modified mixtures. There were no good results for low temperature and moisture damage (40).

Various contents of cellulose fibers in a mix of Stone Matrix Asphalt (SMA) were studied by Partl et al. (1994). The thermal stress controlled specimen tests and indirect tensile tests were conducted and evaluated. The results were impacted due to fiber clumping that occurred during the mixing process. This was improved by increasing the mixing temperate and duration although some clumps remained. Results of this study concluded that the mix based on the two tests conducted was not remarkably improved by using SMA with cellulose fiber. The authors think the poor distribution of fibers may have caused the limited improvement, but recommend further investigation to prove this theory (41).

In another study of SMA, the effects of cellulose fibers were investigated by Selim et al. (1994). There were some tests conducted on binder drain-down, moisture susceptibility (reported as tensile strength ratio), static creep modulus, and recovery efficiency. Fibers were added to mixtures including standard and polymer modified binders. From results, remarkable improvement in all mixtures containing the cellulose fibers was illustrated by the binder drain-down test. Mixtures with plain asphalt binder and fibers exhibited the highest indirect tensile strength and tensile strength ratio after conditioning compared to polymer modified mixtures containing fibers that showed the lowest tensile strength and resistance to moisture induced damage of all the mixtures tested. Researchers showed that recovery efficiency and creep modulus tests were comparatively superior in mixtures containing fibers and plain binder rather than with fibers and polymer modifier (42).

2.1.3.4 Geogrid

Geogrid is a type of geosynthetic fiber commonly used as a reinforcing agent in soil, but can be also used for asphalt pavements. They are made of different fiber reinforced materials, such as glass fibers and/or polymeric fibers and are usually stiff materials formed into a grid-like structure with large apertures (43). The fibers are formed into a matrix to serve as binders in order to transfer loads to the fibers and to shield the fibers against degrading conditions such as chemical substances. Not only they increase the tensile strength, but also provide good lateral confinement for the reinforcement mechanism (5, 44).

In Chang's (1999) study, several geogrids were applied to investigate the formation and development of fatigue cracks in asphalt concrete beams. The test results of a beam reinforced with geogrids, indicated the fatigue life of the pavement overlay improved five to nine times more than an unreinforced beam (27).

In another study, polyoxymethylene fibers were used as geogrids to reinforce asphalt concrete. The durability, such as plastic flow resistance and crack resistance of the geogrid-reinforced asphalt concrete, was investigated in reduced scale using the wheel tracking test. Tests indicated a remarkable increase in the durability by using the geogrid reinforced asphalt concrete in comparison with the control without geogrids. The viscosity of the asphalt concrete was also significantly increased by using geogrid-reinforcement. The crack resistance was directly connected to the plastic flow resistance. Decreasing geogrid-mesh size and a strong adhesion to the asphalt concrete were strong signs of improved

durability. This was because the stress concentration applied by a wheel load was greatly reduced by the high stiffness and small meshes of the thin geogrid inserted in the asphalt concrete (45).

2.1.3.5 Fabric and Carpet Fiber

A carpet typically consists of two layers of backing (usually polypropylene) filled styrene-butadiene latex rubber (SBR), and face fibers (the majority being nylon 6 and nylon 6.6) tufted into the primary backing. The nylon face fiber is often in the form of a heavily crimped loose filament bundle known as a textured yarn. In one study, the effects of nylon fiber were investigated (27). Tests showed that asphalt concretes reinforced by nylon fibers can improve fatigue cracking resistance by increasing the fracture energy, a fundamental mechanical property through IDT strength tests. Moreover, 85% of the fracture energy of the fiber composite asphalt concrete with a fiber length of 12 mm and a volume fraction of 1% were improved rather than that of conventional mixture. Also, due to higher fracture energy, nylon fiber reinforced asphalt mixture indicates better crack resistance. Furthermore, a single nylon fiber begins to rupture at approximately 9.7 mm, indicating the minimum embedded fiber length (27). Serfass and Samanos (1996) concluded that the incorporation of fiber in asphalt concrete is a practical and dependable technique for improving the durability and performance of asphalt concrete. Special emphasis was focused on the importance of accurate proportions of fibers and bitumen, as this can yield resistance to moisture, aging, and fatigue cracking (29)

Maurer and Malasheskie (1989) investigated the impact of using geotechnical fabrics and fibers to hinder reflective cracking in a hot mix asphalt overlay. Among paving fabrics, fiberized-asphalt membrane and fiber-reinforced asphalt concrete better performed over non-reinforced samples in comparisons of construction, maintenance costs, ease of placement, and the ability to prevent or hinder reflective cracking. 0.3% of volume fiber content was added to the asphalt mixture. Their analysis indicated that beams reinforced with woven grid and nonwoven fabric composites performed significantly better than beams containing nonwoven paving fabric alone (27, 38).

2.1.3.6 Carbon Fiber

There are many resources to extract fiber carbon such as, polyacrylonitrile (PAN), or rayon, but only fibers derived from mesophase pitch were considered. Pitch is generally cheaper, making it the lowest cost carbon fiber in production. Furthermore, it uses less energy compared to other fiber types, and there is a low percentage of N2, H2, and other non-carbons to drive off carbonization. These two factors contribute to the 75% yield of fiber from precursor fiber the highest of the three fiber types (46). From 1968 to 1972; the Federal Highway Administration (FHWA) sponsored the use of carbon black fibers as reinforcement in hot mix asphalt. The results of this research conducted at the laboratories of Materials Research and development in Oakland, California showed that an 11 to 16 weight percent of carbon black in asphalt cement gave significant improvements in durability, wear resistance, low-temperature cracking, high temperature distortion, and temperature – viscosity properties of

the asphalt. These improvements are due to the carbon black stiffening and increasing the toughness of the asphalt. Carbon black is easily dispersed in the asphalt by first being pelletized and then being subjected to the shearing action between aggregate particles during mixing. Careful selection of asphalt binder allows for the basic characteristics of the asphalt to remain unchanged after the addition of carbon black (47, 48).

Aren Cleven investigated two aspects of carbon fiber modified asphalt mixtures (30):

i. The feasibility of achieving improvements in mechanical behavior with the addition of carbon fibers

ii. The parameters that contribute to the new behavior

Carbon fibers were found to create improvements in high temperature and low temperature behavior. HMA samples containing 0.5% to 0.8% weight carbon fiber in the asphalt cement binder showed an improvement in resistance to repeated load deformation ranging from 38% to 182 %. Also, fiber length was a concern after field trials revealed a reduction in average final carbon fiber length from 2.54 cm to between 0.2 mm and 0.65 mm due to the need to improve carbon fiber length in the final asphalt cement by protecting it during mixing. Potential problems identified by this study were final fiber length, even distribution of fibers, and initial asphalt quality (30). The final optimal fiber length was determined to be 6 mm in order to improve mechanical properties such as, control micro cracks and educe creep (48).

In a study by Cleven, characteristics and properties of carbon fiber reinforced asphalt mixtures were investigated. Samples with and without fibers were tested to assess the effect of fiber contents on asphalt mixtures. During the course of this study, various tests were conducted, such as the Marshall Test, indirect tensile test, creep test, and repeated load indirect tensile test. Carbon fiber exhibited consistency in results, and as such, it was observed that the addition of fiber does affect the properties of bituminous mixtures (e.g. an increase in its stability and a decrease in the flow value as well as an increase in voids in the mix). Overall, the addition of carbon fiber improved some of the mechanical properties like fatigue and deformation in the flexible pavement (3).

2.1.3.7 FORTA Fibers

FORTA Corporation is a U.S.-based company that has numerous functions and productions focusing on the future of pavement materials. Synthetic fibers are one of its primary products for civil engineering applications. Synthetic fibers are a defined blend of collated fibrillated polypropylene and aramid fibers, which are fairly new fibers being considered and tested for their impacts on modifying hot mix asphalt. Both kinds of fibers have different properties that yield different results when utilized in hot mix asphalt. Polypropylene fiber is chemically inert, and both are non-corrosive and non-absorbent. Aramid fiber has a high tensile strength and a high temperature resistance, while remaining non-corrosive (6, 49). TABLE 1 shows the physical characteristics of FORTA fibers.

TABLE 1 Physical Characteristics of FORTA Fibers (49)

Materials	Polypropylene	Aramid
Form	Twisted Fibrillated Fiber	Monofilament Fiber
Specific Gravity	0.91	1.45
Tensile Strength (MPa)	483	3000
Length (millimeter)	19.05	19.05
Acid/Alkali Resistance	inert	inert
Decomposition Temperature (Celsius)	157	>450

In a recent ASU study, polypropylene and aramid fibers were used in the asphalt mixture to evaluate the performance characteristics of a modified asphalt mixture. A designated road section in Tempe, Arizona was used as the test site to perform the project. Two asphalt mixtures were used: a control mix with no fibers, and a mixture that contained one pound of fibers per ton of asphalt concrete. Triaxial shear strength, dynamic modulus, repeated load permanent deformation, beam fatigue, crack propagation, and indirect diametral tensile tests were conducted in the ASU lab to compare the performance of the fiber modified mixture to the control. From the lab results, it was observed that the fibers enhanced the mixture's performance in numerous unique methods against the anticipated major pavement distresses: permanent deformation, fatigue cracking, and thermal cracking (50).

The Department of Civil, Environmental and Sustainable Engineering at Arizona State University (ASU) has been involved with different major asphalt mixtures characterization studies taking place at the ASU Advanced Pavements Laboratory. The nationally recognized National Cooperative Highway Research

Program (NCHRP) 9-19 project (1), dealt with the development of Simple Performance Tests (SPT) for permanent deformation and cracking potential evaluation of asphalt mixtures. The results from these advanced tests were utilized as input in the Mechanistic-Empirical Pavement Design Guide (MEPDG). ASU has the largest database of hot mix asphalt mix engineering properties in the United States, which contains tests conducted on asphalt mixtures from national and international test sites (51).

CHAPTER 3 LABORATORY SPECIMENS FOR DYNAMIC MATERIALS LAB CHARACTERIZATION

All processes and sample preparation in this study were conducted at ASU's Advanced Pavement Laboratory. The asphalt mixtures evaluated utilized cylindrical plug specimens prepared using the Gyratory compactor. The following brief summary addresses the steps taken for the preparation and evaluation of the asphalt concrete mixtures prepared:

1) Separate aggregates into different aggregate size fractions

2) Select a mix design

3) Calculate fiber percentages per the experimental design

4) Prepare and batch aggregates per the mix design

5) Heat and mix the aggregates, fibers and asphalt

6) 7) Short term aging of the specimens in the oven

8) Compact the specimens using a gyratory compactor

9) Calculate the Theoretical Maximum Specific Gravity (G_{mm})

10) Calculate the air void from trial mixtures

3.1 Aggregates

Salt River aggregates were provided by CEMEX in Phoenix, Arizona. The following aggregate sizes were obtained: 3/4″, 1/2″, 3/8″, Sand, and Crushed Fines. The aggregates of each barrel / source were separated into trays and were dried overnight at 110 ºF. The dried aggregates were then blended and sieved by percentages shown in TABLE 2.

TABLE 2 Aggregate Blends

Sieves	**Percentages %**
3/4 ″	15%
1/2 ″	34%
3/8 ″	15%
Sand	15%
Crushed Fines	21%

After blending aggregates at the determined percentages, three or four full load shovels were placed on top of the TM-4 Floor Sieve Shaker that separated aggregates into different sized particles. Sieves typically used for the sieve analysis were: 3/4 inch, 1/2 inch, 3/8 inch, No. 4, No. 8, No. 16, No. 30, No. 50, No. 100 and No. 200. The TM-4 was run for a 15-minute period and once completed, the contents of each size sieve were placed separately into plastic buckets. These plastic buckets were transferred to another laboratory to be used in the batching process.

3.2 Mix Design

A 19 mm Superpave High Traffic Asphalt Concrete mix design was used for this study. This mix design, prepared by Mactec according to ADOT standard specifications, was previously used in another ASU project. The dense graded asphalt mix utilized a PG 58-28 binder. TABLE 3 shows the designed aggregate gradation distribution curve.

TABLE 3 Composite Aggregate Gradation

Size	% Passing		
	Design	**Minimum**	**Maximum**
1	100.0	100.0	100.0
¾	95.0	90.0	100.0
½	80.0	43.0	89.0
3/8	59.0		
No. 4	39.0		
No. 8	29.0	24.0	36.0
No. 16	23.0		
No. 30	17.0		
No. 50	10.0		
No. 100	5.0		
No. 200	3.3	2.0	6.0

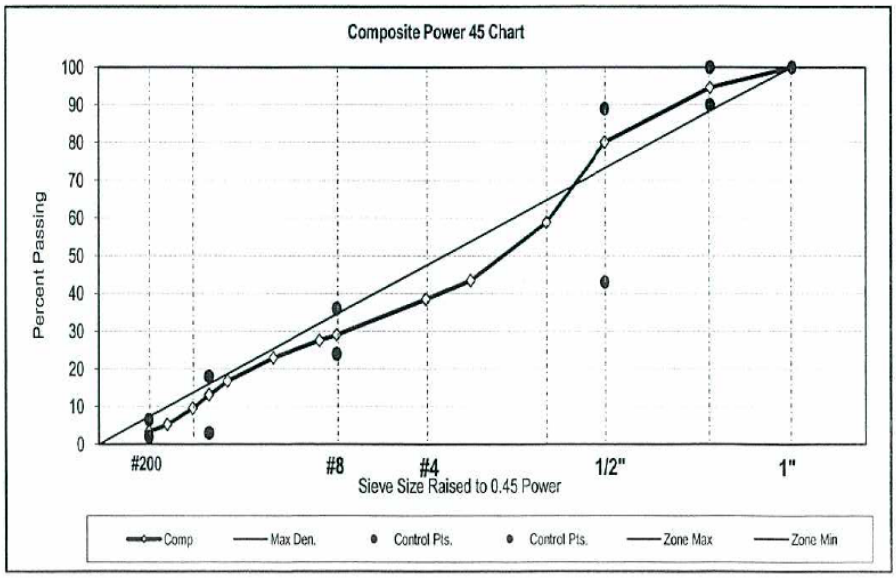

FIGURE 1 Designed aggregate gradation distribution curve.

TABLE 4 includes composite aggregate properties that were conducted by Mactec. The summary of the key volumetric properties from the mix design results are presented in TABLE 5.

TABLE 4 Composite Aggregate Properties

Property	Value	Max Specs
Sand Equivalent Value	71	Min 50
Fractured Face One (%)	99	Min 85
Fractured Face Two (%)	96	Min 80
Flat & Elongation (%)	1.0	Max 10
Un-compacted Voids (%)	46.8	Min 45
L.A. Abrasion @ 500 Rev.	16	Max 40

TABLE 5 Summary of the Volumetric Mix Design

Volumetric Property	Binder Type	Max Specs
Asphalt Type	PG 58-28	
Target Asphalt Content (%)	4.7	4.5 ~ 5.5
Bulk Specific Gravity (G_{mb})	2.365	N/A
Theoretical Max. Sp. Gr. (G_{mm})	2.461	N/A
Design Air Voids (%)	8.50	7.75 ~ 9.15
VMA (%)	13.9	Min. 13
VFA (%)	71.9	N/A

3.3 Fiber Percentages

The dosages of fibers used in the experimental program included four dosage combinations of the polypropylene and aramid fibers as shown in TABLE 6.

TABLE 6 Experimental Design for the Use of Different Combinations of Fibers

Dosage		Polypropylene			
		0	1	2	3
Aramid	0	A1	A2	A3	A4
	1	A5	A6	A7	A8
	2	A9	A10	A11	A12
	3	A13	A14	A15	A16

Each dosage (1, 2, or 3) represents a proprietary blend of aramid and polypropylene fibers percentages that were kept constant per one pound of fibers. Each dosage represents the amount of fibers added per one ton of asphalt mixture. A dosage of zero represents the control mixture with no fibers added. Dosage of 1:1, 2:2 or 3:3 are the proprietary blends of both fibers types added as 1, 2, and 3 pounds per ton respectively. A dosage of 1 aramid and 2 polypropylene represents the percentage of proprietary aramid fibers modified in the proprietary blend to keep the same dosage of the aramid fibers and increase the polypropylene fibers by twice the amount in the blend. A dosage of three triples the percentage of fibers in reference to the percentages used in dosage one. TABLE 7 shows a summary of the mixture code along with the total fiber content used (combination of the proprietary polypropylene/aramid blend) for each mixture.

3.4 Batching Aggregates and Mix Preparation

The amount of aggregate required to make one gyratory sample was determined by the mix design gradation and as shown in TABLE 8.

TABLE 7 Fiber Dosage Amount for Each Mixture

Sample ID	Mixture Weight (g)	Fiber Weight (g)
A1	6500	0
A2	6500	2.91
A3	6500	5.82
A4	6500	8.73
A5	6500	0.4
A6	6500	3.31
A7	6500	6.22
A8	6500	9.13
A9	6500	0.8
A10	6500	3.71
A11	6500	6.62
A12	6500	9.53
A13	6500	1.2
A14	6500	4.11
A15	6500	7.02
A16	6500	9.93

TABLE 8 Aggregate Batching per Mix Design

Sieve Size	Total Passing (%)	Retained (%)	Weight per Core Batch (g)
3/4	95.0	5.0	325
1/2	80.0	15.0	975
3/8	59.0	21.0	1365
No. 4	39.0	20.0	1300
No. 8	29.0	10.0	650
No. 16	23.0	6.0	390
No. 30	17.0	6.0	390
No. 50	10.0	7.0	455
No. 100	5.0	5.0	325
No. 200	3.3	1.7	110.5
Pan (<No. 200)		3.3	214.5
Total		100	6500

The batched aggregates were kept in the oven (155 ºC) overnight. The asphalt was brought to the mixing temperature (150 ºC) for approximately one hour, and the mixing tools and equipment used were also preheated to the mixing temperature.

The aggregate was transferred to the preheated mixing bucket. The pre-weighted fibers were then spread as widely as possible to cover the aggregate. The heated asphalt was carefully poured into the mixing bucket until the weight gets to the desired amount of asphalt content per the mix design. The bucket was then directly placed into the mixing machine for three minutes of mixing time as shown in FIGURE 2.

FIGURE 2 The HMA mixture process: (top left to bottom right) batched heated aggregates, pouring in mixing buckets, adding distributing pre-weighted fibers, mixing fibers and aggregates, adding binder, final HMA mixture.

Once the mixing is completed, each mixture sample was spread out on a heated metal tray and placed inside the oven for four hours at the compaction temperature (135 ºC), while stirring the mix every hour. This procedure is specified in the American Association of State Highway and Transportation Officials (AASHTO) PP2 aging procedure for Superpave mixture performance testing. Also the mould and all other equipment used in the compaction process are also placed in the oven at this time at the same compaction temperature. In the last 20 minutes of the four hours, the mould was filled with mix at the compaction temperature and the desired weight in order to compact a specimen to the target air void. The mould was then returned to the oven for about 20 minutes to achieve the proper compaction temperature before being compacted as showed in FIGURE 3.

FIGURE 3 The aging process.

3.5 Compact the Specimens Using a Gyratory Compactor

Once the mould is filled and returned to an oven to arrive at the compaction temperature, the mould is placed in a Servopac gyratory compactor

for compaction. Next, the compactor is set with a vertical stress of 600 kPa at a rate of 38 gyrations per minute, with a 1.25º gyration angle, a standardized height of 170 mm, and a standardized diameter of 150 mm. Finally, coring and cutting are conducted on each sample to obtain the required dimensions, which are 100 mm diameter and 150 mm height, as shown in FIGURE 4.

Super pave machine

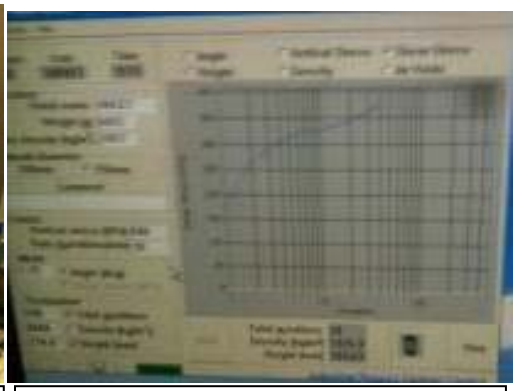

Shear strength during compaction

Sample after compaction

Size of sample 100*150 mm

FIGURE 4 Compacting in the gyratory compactor.

3.6 Determine the G_{mm} of Bituminous Paving Mixtures

AASHTO T209 is used to determine the theoretical maximum specific gravity and density of un-compacted bituminous paving mixtures at 25º C. These values can be used in the calculation of air void in the compacted bituminous paving mixture, in calculating the amount of bituminous absorbed by the aggregate, and to provide target values for the compaction of paving mixtures. The apparatus used are showed in FIGURE 5.

Scale

Hammer

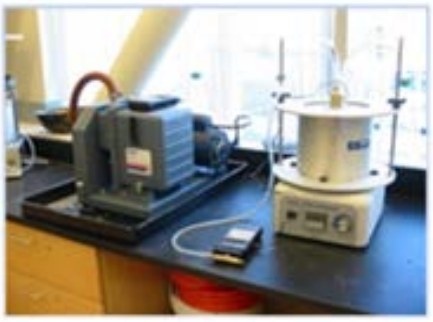

Vacuum and Container

FIGURE 5 Instruments for determining the G_{mm}.

The following procedures are used in according to the AASHTO T209 Pycnometer (52).

1. Prepare the sample in the laboratory as mentioned above, and while it is still warm, separate the particles of the sample of paving mixture by hand to get acceptable separation degree and monitor so as to not fracture the mineral particles.
2. Cool the sample to room temperature. After that, place the sample directly into the container or volumetric flask.
3. Weight the container with the dry sample and designate the net mass as "A" and record it in the chart. Pour the water at temperature 25^{o}C in the empty container so that it is full and then weight the container with water and record it in the chart as "B".
4. Place the dry sample weighting in the container and add adequate water at temperature 25^{0}C to submerge the sample completely almost (2.5cm) above the sample. After that, place the cover on the container and attach the vacuum line.
5. Start the vacuum for almost 15 minutes to remove air trapped in the sample. Once this is achieved, tap the sides of the container with the rubber hummer to help remove any remaining air.
6. Slowly open the release valve, turn off the vacuum pump, and remove the cover, add water until the container is full, place the cover on top, and make sure that the container is properly sealed. Weight the container with the dry sample, water and cover, and record it in the chart as "C".
7. Repeat this experiment two more times in order to make sure that there is not excessive mistake.

Note: The cover and container should be the same one used during each experiment. Also it should clean spot after experiment, clean the container after remove sample, and calibrate measurement apparatus.

3.6.1 Calculation and Results

$G_{mm} = A/(A+B-C)$

Where:

A = mass of dry sample in air, gm

B = mass of bowl + cover +water in air, gm

C = mass of bowl + cover +water + mix in air

The G_{mm} for the control mixture is shown in TABLE 9.

TABLE 9 G_{mm} for Control Mixture

Sample ID	Mass of Mix in Air	Mass of Bowl+Lid+Water in Air	Mass of Bowl+Lid+Water+Mix in Air	G_{mm}
	A[gm]	B[gm]	C[gm]	D[gm/cm-^{3}] A/(A+B-C)
1	1500.2	7740.9	8636.9	2.4829
2	1500.2	7740.9	8637.3	2.4845
3	1500.2	7740.9	8636.5	2.4813

$G_{mm\,1} = 1500.2/(1500.2+ 7740.9 – 8636.9) = 2.4829 gm/cm^3$

$G_{mm\,2} = 1500.2/(1500.2+ 7740.9 – 8637.3) = 2.4845 gm/cm^3$

$G_{mm\,3} = 1500.2/(1500.2+ 7740.9 – 8636.5) = 2.4813 gm/cm^3$

Average G_{mm} for control = 2.4829 gm/cm^3

The results are within acceptable procedure variations, and therefore, the Maximum Specific Gravity of Bituminous Paving Mixtures was approved.

Similarly, the G_{mm} of the fiber mixtures were determined. TABLE 10 shows an example for the mixture with 3lbs/ton dosage.

TABLE 10 G_{mm} for 3lbs. of Fiber Mixture

Sample ID	Mass of Mix in Air	Mass of Bowl+Lid+Water in Air	Mass of Bowl+Lid+Water+Mix in Air	G_{mm}
	A[gm]	B[gm]	C[gm]	D[gm/cm-^{3}] A/(A+B-C)
1	1500.2	7740.9	8636.6	2.4817
2	1500.2	7740.9	8636.1	2.4796
3	1500.2	7740.9	8636.3	2.4804

$G_{mm\ 1}$ = 1500.2/(1500.2 + 7740.9 – 8636.6) = 2.4817gm/cm^3

$G_{mm\ 2}$ = 1500.2/(1500.2 + 7740.9 – 8636.1) = 2.4796gm/cm^3

$G_{mm\ 3}$ = 1500.2/(1500.2 + 7740.9 – 8636.3) = 2.4804gm/cm^3

Average G_{mm} for 3lbs. of fiber mixture = 2.4805gm/cm^3

G_{mm} for all mixtures = 2.4817gm/cm^3

The results have acceptable variability per the test procedure, so the Maximum Specific Gravity of Bituminous Paving Mixtures was approved.

3.7 Air Voids

After the coring and cutting of samples is complete, the samples are left out in the air for enough time (at least 36 hours) to dry. An important factor in determining the air void is the theoretical maximum specific gravity (G_{mm}) of the mix, which was calculated above. The air voids (Va %) of the dried specimens are then obtained using the Bulk Specific Gravity of Bituminous Mixtures using the Saturated Surface Dry Specimens method (AASHTO T166- 93)(53).

TABLE 11 Air Void for the Mixtures

Sample ID	Mass in Air (gm)	Mass in Water (gm)	SSD Mass (gm)	Volume (cm3)	Gmb (gm/ cm3)	Water Abs. (%)	Air Voids (%)
(0P,0A)	2611.0	1487.0	2633.2	1146.2	2.278	1.94	8.21
(0P,0A)	2711.1	1539.3	2733.0	1193.7	2.271	1.83	8.48
(0P,0A)	2687.9	1506.2	2697.5	1191.3	2.256	0.81	9.08
(0P,1A)	2647.7	1491.9	2664.4	1172.5	2.258	1.42	9.01
(0P,1A)	2623.5	1496.8	2653.6	1156.8	2.268	2.60	8.62
(0P,1A)	2710.5	1524.3	2720.1	1195.8	2.267	0.80	8.66
(0P,2A)	2795.3	1575.2	2813.4	1238.2	2.258	1.46	9.03
(0P,2A)	2706.5	1524.0	2722.3	1198.3	2.259	1.32	8.99
(0P,2A)	2708.1	1533.3	2731.1	1197.8	2.261	1.92	8.90
(0P,3A)	2765.9	1564.0	2790.9	1226.9	2.254	2.04	9.16
(0P,3A)	2797.3	1573.2	2811.4	1238.2	2.259	1.14	8.97
(0P,3A)	2575.3	1446.2	2587.7	1141.5	2.256	1.09	9.09
(1P,0A)	2684.2	1518.7	2694.2	1175.5	2.283	0.85	7.99
(1P,0A)	2649.6	1483.6	2657.5	1173.9	2.257	0.67	9.05
(1P,0A)	2657.7	1497.4	2674.6	1177.2	2.258	1.44	9.03
(1P,1A)	2721.6	1528.0	2734.5	1206.5	2.256	1.07	9.10
(1P,1A)	2689.9	1503.2	2696.3	1193.1	2.255	0.54	9.15
(1P,1A)	2663.1	1499.6	2686.6	1187.0	2.244	1.98	9.60
(1P,2A)	2617.1	1467.1	2626.2	1159.1	2.258	0.79	9.02
(1P,2A)	2709.5	1526.3	2721.1	1194.8	2.268	0.97	8.62
(1P,2A)	2705.8	1529.6	2727.5	1197.9	2.259	1.81	8.98
(1P,3A)	2642.7	1489.3	2657.5	1168.2	2.262	1.27	8.84
(1P,3A)	2653.7	1504.0	2665.5	1161.5	2.285	1.02	7.94
(1P,3A)	2744.2	1557.0	2771.2	1214.2	2.260	2.22	8.93
(2P,0A)	2669.1	1498.8	2677.0	1178.2	2.265	0.67	8.72
(2P,0A)	2601.5	1463.9	2617.2	1153.3	2.256	1.36	9.11
(2P,0A)	2704.1	1534.3	2732.6	1198.3	2.257	2.38	9.07
(2P,1A)	2667.2	1503.9	2676.6	1172.7	2.274	0.80	8.35
(2P,1A)	2572.3	1444.2	2584.7	1140.5	2.255	1.09	9.12
(2P,1A)	2690.2	1523.9	2715.9	1192.0	2.257	2.16	9.06
(2P,2A)	2677.8	1508.7	2690.8	1182.1	2.265	1.10	8.72
(2P,2A)	2569.5	1443.8	2583.0	1139.2	2.256	1.19	9.11
(2P,2A)	2649.2	1496.7	2669.3	1172.6	2.259	1.71	8.96
(2P,3A)	2626.8	1483.4	2648.3	1164.9	2.255	1.85	9.14
(2P,3A)	2648.7	1491.9	2665.4	1173.5	2.257	1.42	9.05
(2P,3A)	2675.2	1513.4	2692.6	1179.2	2.269	1.48	8.58
(3P,0A)	2637.5	1489.1	2657.9	1168.8	2.257	1.75	9.07
(3P,0A)	2797.3	1576.2	2813.4	1237.2	2.261	1.30	8.89
(3P,0A)	2636.8	1483.4	2651.8	1168.4	2.257	1.28	9.06
(3P,1A)	2712.1	1538.1	2730.0	1191.9	2.275	1.50	8.31
(3P,1A)	2713.8	1539.0	2737.2	1198.2	2.265	1.95	8.74
(3P,1A)	2592.5	1472.6	2616.0	1143.4	2.267	2.06	8.64
(3P,2A)	2678.3	1503.1	2690.6	1187.5	2.255	1.04	9.12
(3P,2A)	2760.9	1563.0	2784.4	1221.4	2.260	1.92	8.92
(3P,2A)	2706.7	1534.7	2722.8	1188.1	2.278	1.36	8.20
(3P,3A)	2766.1	1557.2	2783.7	1226.5	2.255	1.43	9.12
(3P,3A)	2709.5	1525.0	2727.0	1202.0	2.254	1.46	9.17
(3P,3A)	2646.0	1495.9	2667.5	1171.6	2.258	1.84	9.00

CHAPTER 4 ASPHALT BINDER MODIFICATION STUDY

The goal of this study is to compare the effects of varying the dosages of polypropylene and aramid fibers, in blends or individually, on the properties and characteristics of the selected binder. Various binder tests were performed, such as the penetration test, the softening point test, and the Brookfield viscosity test. The PG binder, as mentioned earlier, was PG58-28.

Partial factorials of the combinations of nine different fiber dosages (discussed in the previous chapter) are shown in TABLE 12. These represent nine different modified binder combinations.

TABLE 12 Partial Experimental Design for the Use of Different Combinations of Fibers

Dosage		**Polypropylene**			
		0	**1**	**2**	**3**
Aramid	**0**	A 1	A 2		A 4
	1	A 5	A 6		A 8
	2				
	3	A 13	A 14		A 16

A dosage of one represents an existing proprietary blend aramid and polypropylene fibers, where one pound of the combined fibers are added per one ton of asphalt mixture. A dosage of three triples the percentage of fibers in reference to the percentages used in dosage one. Since some research has been conducted on the use of dosage two in the previous ASU study, the performance trends can be evaluated without including this dosage in this experimental design. This will also reduce the total number of mixtures and the amount of tests that,

otherwise, would have to be included. TABLE 13 shows the amount of fibers determined for each condition.

TABLE 13 Amount of Fiber Dosages Used

Sample ID	Binder Weight (W_b)gm	Fiber Weight (W_f) gm = W_b*454.7/51000
A6	579	5.162
A2	578.8	5.160
A5	510.2	4.549
A14	684.5	6.103
A1	503.6	4.490
A4	597.8	5.330
A13	638.9	5.696
A8	586.1	5.225
A16	558.2	4.977

4.1 The Mixing Processes

The processes to mix the fibers and asphalt cement are as follows:

8. Heat the can of asphalt in the oven around 15-20 minutes at 150 to 160 $^{\circ}C$.
9. At the same time, heat the mixing fan.
10. Weight the fiber dosage that will be added to the asphalt.
11. Turn the heater on and prepare the mixer.
12. Take the sample out from the oven and set it on the mixer.
13. Verify that the temperature is between 160 to 180°C.
14. Start to add the fiber in small amounts (piece by piece).

These steps take between 40 to 60 minutes. FIGURE 6 demonstrates some of these steps.

FIGURE 6 The binder-fibers mixing steps.

The following briefly describes the test methodology of the different binder tests.

4.2 Standard Penetration Test

The penetration test is an empirical test used to measure the consistency of asphalt binder and the test is typically performed at 13 °C and 25 °C (54). The standard test method is performed in accordance with ASTM D5 which is summarized below (55):

1. Samples are conditioned to test temperatures for one to two hours.
2. A sample of binder is placed under a specified needle which is loaded with 100 g for five seconds.
3. The depth of penetration is measured in 0.1 mm increments.

FIGURE 7 The penetration test steps.

4.3 Softening Point Test

The softening point test is a simple test to determine when a phase change occurs in the asphalt binder. The softening point is measured by a ring and ball method in accordance with ASTM D 36 which is summarized in the following steps (54):

1. Heat the asphalt and pour it into brass rings.
2. Allow the heated asphalt to cool and use a hot knife to trim the excess asphalt flush with the top of the rings.
1. Assemble the test apparatus and place it in a water bath.
2. Add ice and cool the water bath to 5±1 °C for 15 minutes before starting the test.
3. Using a heat plate, heat the water bath at a rate of 5 °C per minute.

4. Record the temperatures when the right and left asphalt samples sink and touch the bottom plate.

The softening point is indicative of the tendency of the binder to flow at elevated temperatures while in use. For most asphalt binders, the ring and ball softening point match to a viscosity of 13,000 Poise.

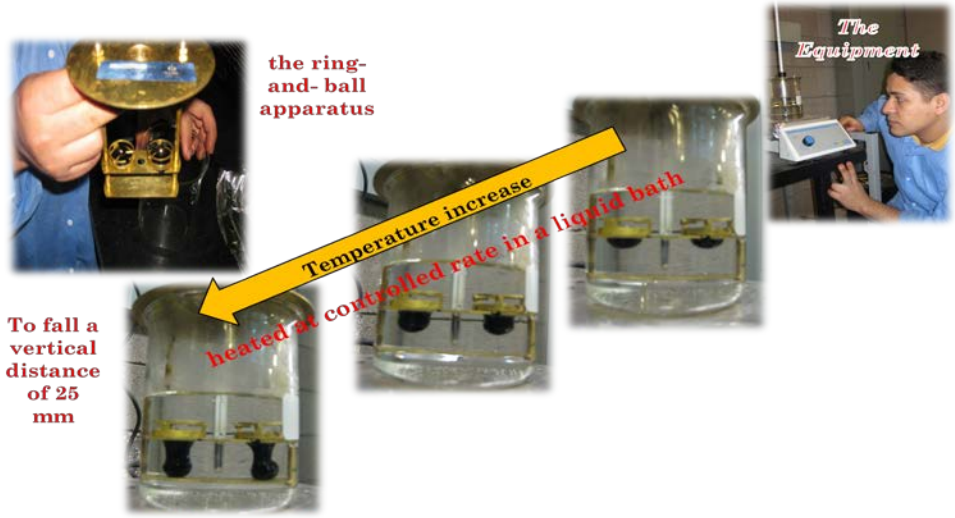

FIGURE 8 The softening point test steps.

4.4 Brookfield Viscosity Test

The viscosity of asphalt binder is an important measurement to understand how the binder is going to perform during pumping and mixing. Asphalt binders perform as Newtonian fluids and have a totally viscous response at high temperatures and thus, the measurement of viscosity represents the workability of the binder. Superpave has adopted the rotational viscometer (RV) for determining

binder viscosity at high construction temperatures (54). The Brookfield viscometer was used for the ASTM D4402 procedure, as summarized below (55).

1. Heat the binder, tube and spindle to the test temperature.
2. Fill the tube with approximately eight to ten milliliters of binder.
3. Insert the tube in the viscometer and attach the spindle.
4. Allow the temperature to stabilize for 15 minutes.
5. Begin the test and record the viscosity at one-, two-, and three-minute intervals.
6. Adjust the temperature controller to the next temperature.
7. Allow the temperature to stabilize and repeat the test.

FIGURE 9 The Brookfield Viscosity test steps.

4.5 Temperature – Viscosity Relationship

Binder testing data described in this study was used to construct a temperature viscosity relationship for the modified asphalt binder. In order to develop a relationship, all binder test results must be expressed as viscosity (cP) units. Shell Oil Company researchers have determined that all asphalts will have a viscosity of 13,000 P at their softening point (56). Also, research conducted at the University of Maryland developed the following model to convert penetration (pen) values into viscosity (*n*) units (56).

$$\text{Log n} = (10.5012 - 2.2601(\log(\text{pen})) + 0.00389(\log(\text{pen}))^2)$$

Most asphalt binders exhibit a linear relationship between log-log viscosity (cP) and log temperature (°Rankine = °F+459.7) (3). TABLE 14 summaries all combinations of penetration, softening point and temperature-viscosity relationships for all nine combinations of the modified binders. .

FIGURE 10 represents the results and the Temperature –Viscosity Relationships for all samples in one plot.

TABLE 14 Combinations of Temperature-Viscosity Relationships

SAMPLE		Penetration (0.1 mm)	Softening Point (^{o}C)	VISCOSITY (cP)		
				250	300	350
A1	**0P, 0A**	60	42.75	578	202	64
A2	**1P, 0A**	54	44	1000	250	109
A4	**3P, 0A**	30.625	39.25	6974	3233	1141
A5	**0P, 1A**	34.75	44	12276.	6514	4890
A6	**1P, 1A**	35	45	6584	3093	2724
A8	**3P, 1A**	33.25	50	29837	16325	9737
A13	**0P, 3A**	35.25	52.25	3351	1500	719
A14	**1P, 3A**	37.75	48.5	16132	9298	4819
A16	**3P, 3A**	31.25	49.75	17875	6802	1781

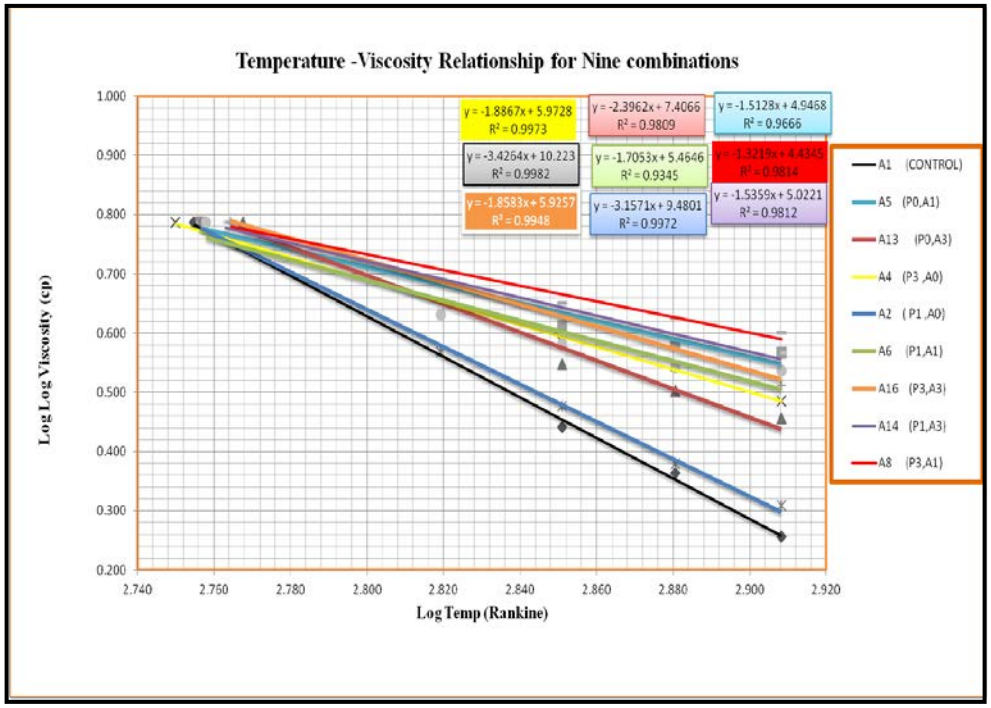

FIGURE 10 Results and temperature of viscosity relationships for nine combinations.

In general, as the amount of the fibers increases, the slope decreases which indicates a better desired binder modification characteristics. The penetration remarkably decreases as the amount of polypropylene increases. However, there is no significant change in the case of increasing aramid due to the difficulty of getting a homogeneous mix suitable for the tests. At all temperatures, the viscosity generally increases as the polypropylene increases.

From the results shown, the A8 sample, which has three dosages of polypropylene and one dosage of aramid, has the highest viscosity indicating the least temperature susceptibility to both permanent deformation and thermal cracking. When the amount of aramid is increased, the viscosity starts increasing, but it suddenly and unexpectedly drops down because the fiber does not melt in the binder and starts accumulating. As the temperature increases, the rank of the sample A16 goes down due to the excessive amount of polypropylene, which makes the mix loses its viscosity at high temperature.

TABLE 15 and 16 show the improvement that was obtained for the Temperature –Viscosity relationship without and without the penetration results. The penetration results were determined to be the most problematic in testing and may have affected the regression results.

TABLE 15 R^2 and Temperature –Viscosity Relationship With and Without Penetration Results

Sample ID	Temperature-Viscosity Relationship with Penetration	Temperature –Viscosity Relationship without Penetration
A6	y = -2.208x + 6.906 R^2 = 0.920	y = -1.705x + 5.464 R^2 = 0.934
A2	y = -3.391x + 10.15 R^2 = 0.992	y = -3.157x + 9.480 R^2 = 0.997
A5	y = -2.044x + 6.476 R^2 = 0.921	y = -1.512x + 4.946 R^2 = 0.966
A14	y = -2.026x + 6.431 R^2 = 0.939	y = -1.535x + 5.022 R^2 = 0.981
A1	y = -3.636x + 10.82 R^2 = 0.995	y = -3.426x + 10.22 R^2 = 0.998
A4	y = -2.392x + 7.427 R^2 = 0.946	y = -1.886x + 5.972 R^2 = 0.997
A13	y = -2.759x + 8.452 R^2 = 0.977	y = -2.396x + 7.406 R^2 = 0.980
A8	y = -1.859x + 5.979 R^2 = 0.921	y = -1.321x + 4.434 R^2 = 0.981
A16	y = -2.291x + 7.171 R^2 = 0.965	y = -1.858x + 5.925 R^2 = 0.994

TABLE 16 Slope of the Temperature –Viscosity Relationship With and Without Penetration Results

Sample ID	Slope With Penetration	Slope Without Penetration
A8	-1.859	-1.321
A14	-2.026	-1.535
A5	-2.044	-1.512
A6	-2.208	-1.705
A13	-2.759	-2.396
A16	-2.291	-1.858
A4	-2.392	-1.886
A2	-3.391	-3.157
A1	-3.636	-3.426

CHAPTER 5 DYNAMIC MODULUS TEST

The main purpose of the dynamic modulus (E*) test in this study is to summarize test data and master curve parameters obtained from the E* testing and analysis conducted for sixteen different combinations (control and fifteen different dosages of fibers) at different temperatures and different frequencies

5.1 E* Background

The dynamic modulus is based on linear viscoelasticity concepts, measured by applying a compressive sinusoidal loading. For linear viscoelastic materials, such as AC mixes, the stress-to-strain relationship under a continuous sinusoidal loading is defined by its complex dynamic modulus (E*) (57, 58, 59). The complex modulus is defined as the ratio of the amplitude of the sinusoidal stress (at any given time, t, and angular load frequency, ω), $\sigma = \sigma 0 \sin(\omega t)$ and the amplitude of the sinusoidal strain $\varepsilon = \varepsilon 0 \sin(\omega t - \varphi)$, at the same time and frequency as explained in Figure 11.

$$E* = \frac{\sigma}{\varepsilon} = \frac{\sigma o \sin \omega x}{\varepsilon o \sin(\omega x - \phi)}$$

Where,

σo = peak (maximum) stress

εo = peak (maximum) strain

φ = phase angle, degrees

ω = angular velocity

t = time, seconds

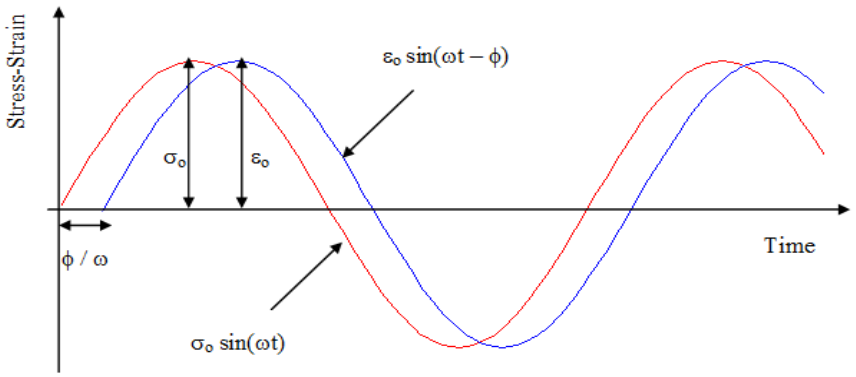

FIGURE 11 Dynamic (complex) modulus tests (60).

For elastic material, the phase angle φ = 0, means the complex modulus is equal to the dynamic modulus while, for viscous materials, φ = 90, the dynamic modulus testing is carried out using a uniaxially applied sinusoidal stress.

$$|E^*| = \frac{\sigma_o}{\varepsilon_o}$$

The dynamic modulus is considered the most important property needed for HMA that is affected by important parameters, such as temperature and time of loading, frequency, and phase angle. It is also determined by components of the mixture. The test is conducted at three temperatures and six frequencies, and controlled stress levels for a given test temperature were selected to produce resilient strains of less than 150 micro strains. This limit on the resilient strain ensured that the response of the material would be linear.

5.2 Master Curve

The values of the complex modulus and phase angle were collected for various combinations of strain level, temperature, and frequency of loading. The time rate of the load is constructed by the master curve at a reference temperature (generally taken as 70 °F). The data at various temperatures are shifted with respect to time until the curves merge into single smooth function (60).

The tests were performed at additional strain levels to evaluate the nonlinear response. In general, the master modulus curve can be mathematically modeled by a sigmoidal function described as (56):

$$\text{Log } |E^*| = \delta + \frac{\alpha}{1+e^{\beta+\gamma(\log tr)}}$$

Where,

tr = reduced time of loading at reference temperature

δ = minimum value of E*

$\delta+\alpha$ = maximum value of E*

β, γ = parameters describing the shape of the sigmoidal function

The shift factor can be shown in the following form:

$$a(T) = \frac{t}{tr}$$

Where,

a (T) = shift factor as a function of temperature

t = time of loading at desired temperature

tr = time of loading at reference temperature

T = temperature

The MEPDG uses the laboratory measured E* data for the Level 1 design analysis, while it uses E* values predicted from the Witczak E* predictive equation in Levels 2 and 3. The master curve for the Level 1 analysis is developed using numerical optimization to shift the laboratory mixture test data into a smooth master curve. Prior to shifting the mixing data, the relationship between binder viscosity and temperature must be established. This is done by first converting the binder stiffness data at each temperature to viscosity using the following equation. The parameters of the ASTM Ai-VTSi equation are then found by linear regression of the next equation after log-log transformation of the viscosity data and log transformation of the temperature data (56).

$$\eta = \frac{G^*}{10}\left(\frac{1}{\sin\delta}\right)^{4.8628}$$

log log η = A + VTS log TR

Where,

η= binder viscosity, cP

G* = binder complex shear modulus, Pa

δ = binder phase angle, degree

A, VTS= regression parameters

TR = temperature, ºRankine

The master curve for the Level 2 analysis is developed using the Witczak et al Dynamic Modulus Predictive Equation from specific laboratory test data. The Level 3 analysis requires no laboratory test data for the AC binder but requires those mixture properties for Witczak's predictive equation, which are as follows (60):

$$\text{Log}\,|E^*| = \delta + \frac{\alpha}{1 + e^{\beta + \gamma(\log t_r)}}$$

Where,

$|E^*|$ = dynamic modulus, 10^5 psi

$\delta = -1.249937 + 0.02923(\rho_{200}) - 0.001767(\rho_{200})^2 - 0.002841(\rho_4) - 0.058097(V_a)...$

$$- 82208\left(\frac{V_{beff}}{V_{beff} + V_a}\right)$$

$\alpha = 3.871977 - 0.0021(\rho_4) + 0.003958(\rho_{38}) - 0.000017(\rho_{38})2 + 0.00547(\rho_{34})$

$\beta = -0.603313 - 0.313532 \log(\eta Tr)$

$\gamma = 0.313351$

Tr = reduced time of loading at reference temperature

V_a = air void content, %

V_{beff} = effective binder content, % by volume

ρ_{34} = cumulative % retained on 19 mm sieve

ρ_{38} = cumulative % retained on 9.5 mm sieve

ρ_4 = cumulative % retained on 4.76 mm sieve

ρ_{200} = % passing 0.075 mm sieve

ηTr = binder RTFOT viscosity at the reference temperature, 106 Poise

5.3 Test Specimen Preparation and Conditioning

All test specimens were prepared in the ASU Advanced Pavements Laboratory according to AASHTO TP 62-03, and 16 different combinations of fiber mixtures were carried out to evaluate the Dynamic Modulus and to investigate properties of mixtures (61). For each combination, three replicates were prepared for testing at three different temperatures (40 ºF, 70 ºF, and 100 ºF) and six different frequencies (25 Hz, 10 Hz, 5 Hz, 1 Hz, 0.5 Hz, 0.1 Hz). Test specimens were cored from Gyratory plugs to arrive at samples 100 mm diameter and 150 mm height gyratory (sawed ends) Forty-eight cylindrical mixtures were tested. The target air voids were 8.5 ± 0.75 %. A controlled stress was used for all specimens, which generated recoverable axial micro-strain between 30 and smaller than 150 to guarantee a linear relationship at different temperatures. The deformations were measured through two spring loaded Linear Variable Differential Transformers (LVDT) as shown in FIGURE 12.

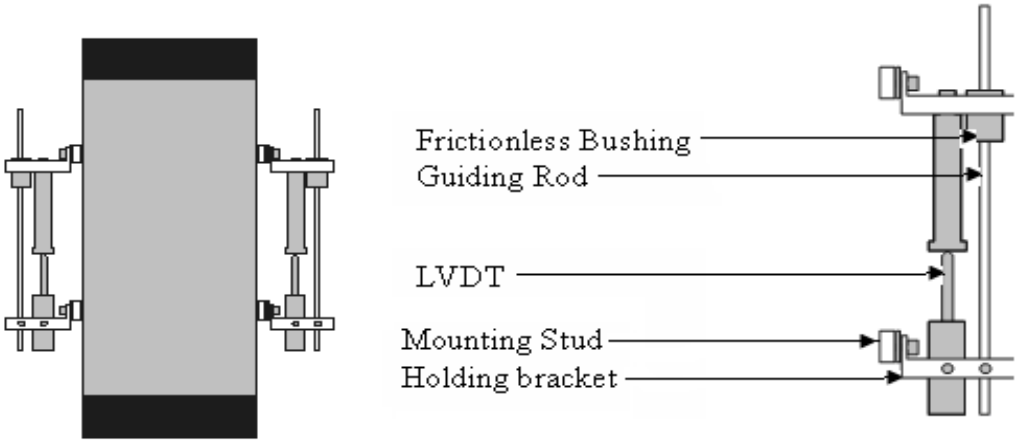

FIGURE 12 Specimen instrumentation of E* testing (60).

5.4 Test Results and Analysis for the Dynamic Modulus

The results obtained for the dynamic modulus tests for the sixteen different combinations of fiber mixtures were summarized in spreadsheets for comparison purposes and to run ANOVA statistical analysis using statistical package in Excel. The Master Curve parameters are reported in TABLE 17. FIGURE 13 through 34 show a graphical summary of the results.

TABLE 17 E* Master Curve Parameters of Mixtures

Mixture Type	**Parameters**						
	δ	**α**	**β**	**γ**	**a**	**b**	**c**
Control	3.3688	3.0638	-1.024	0.4755	0.000	-0.0853	5.6145
0 P, 1 A	3.5769	2.9340	-0.6411	0.4456	0.0002	-0.0959	5.8817
0 P, 2 A	3.6190	2.8557	-0.7875	0.4499	0.0001	-0.0978	6.1790
0 P, 3 A	3.8328	2.7092	-0.5422	0.4728	0.0001	-0.0874	5.6674
1 P, 0 A	3.1184	3.5850	-0.7463	0.3374	0.0003	-0.1235	7.2159
1 P, 1 A	3.3010	3.3951	-0.7048	0.3633	0.0002	-0.0973	5.8331
1 P, 2 A	3.5151	3.0917	-0.7762	0.4053	0.0003	-0.1120	6.5250
1 P, 3 A	4.1042	2.4073	-0.7476	0.5759	-0.0003	-0.0216	2.9536
2 P, 0 A	3.7281	2.8278	-0.7983	0.5129	0.0002	-0.1017	6.0782
2 P, 1 A	2.8456	4.1799	-0.5833	0.2746	0.0002	-0.1050	6.2050
2 P, 2 A	3.6332	3.0534	-0.7591	0.3916	-0.0002	-0.0449	4.0245
2 P, 3 A	3.0618	3.7583	-0.9508	0.3211	-0.0001	-0.0769	5.6668
3 P, 0 A	3.8817	2.8422	-0.4393	0.4591	0.0004	-0.1236	6.7430
3 P, 1 A	3.0288	3.8644	-0.8580	0.2999	0.0001	-0.0944	6.3112
3 P, 2 A	3.9975	2.7174	-0.5073	0.4608	0.0001	-0.0859	5.7459
3 P, 3 A	4.1803	2.5179	-0.4154	0.5065	0.0002	-0.1091	6.5354

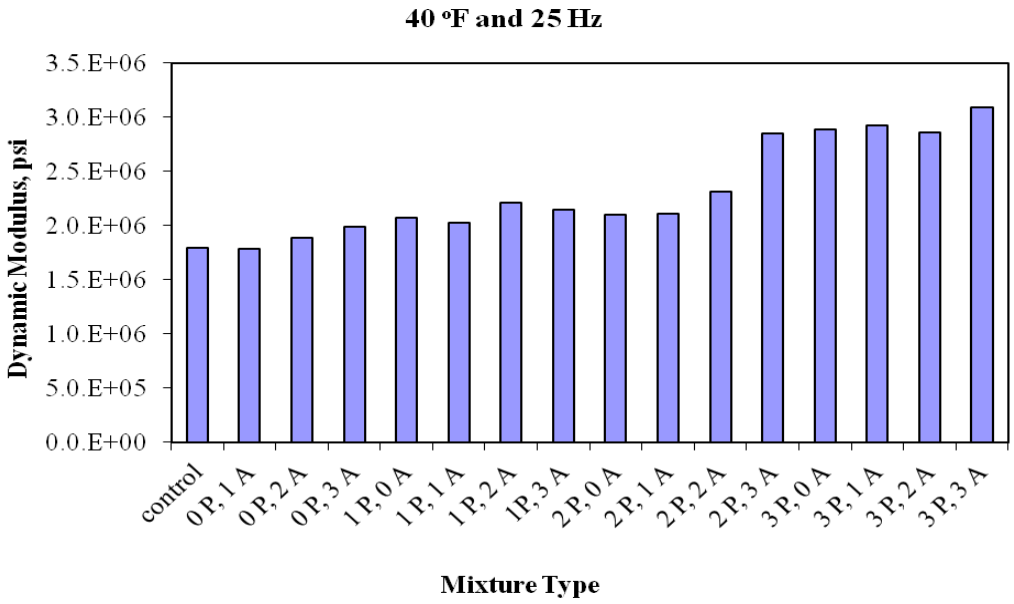

FIGURE 13 Comparison of E* based on the average of three replicates for all combinations of fibers at 40 ºF and 25 Hz.

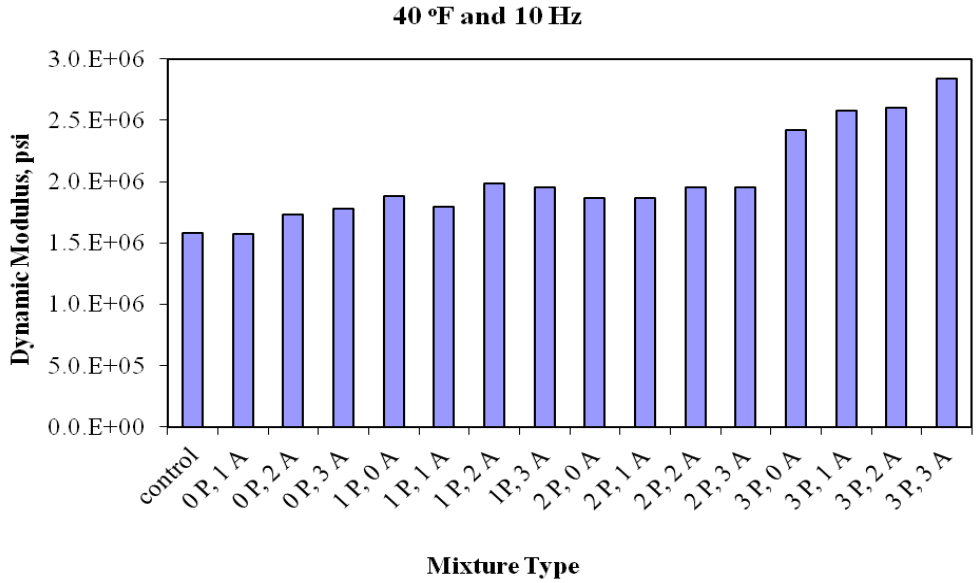

FIGURE 14 Comparison of E* based on the average of three replicates for all combinations of fibers at 40 ºF and 10 Hz.

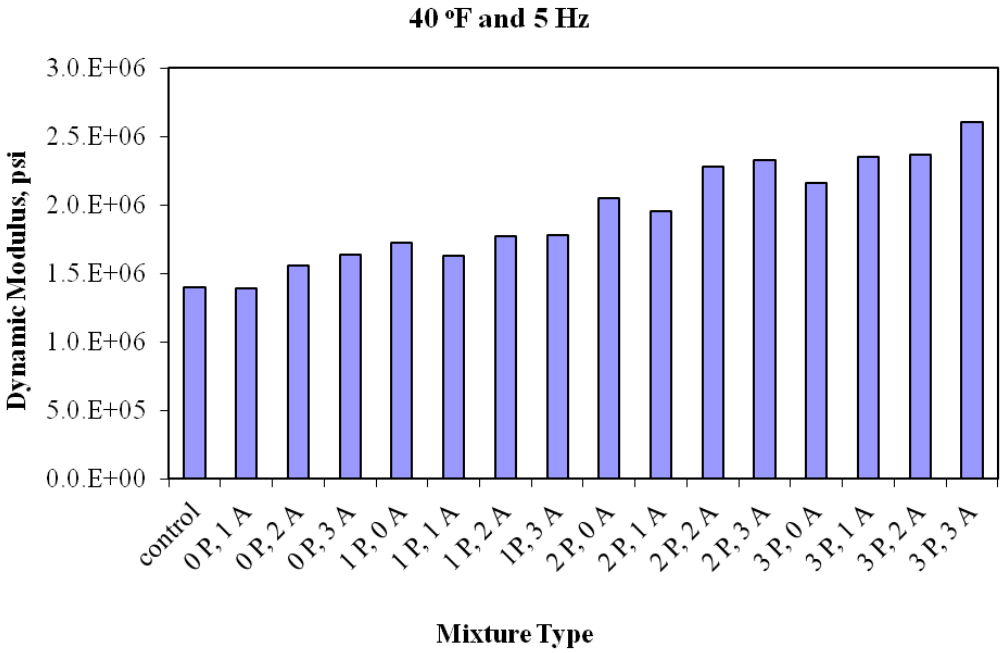

FIGURE 15 Comparison of E* based on the average of three replicates for all combinations of fibers at 40 ºF and 10 Hz.

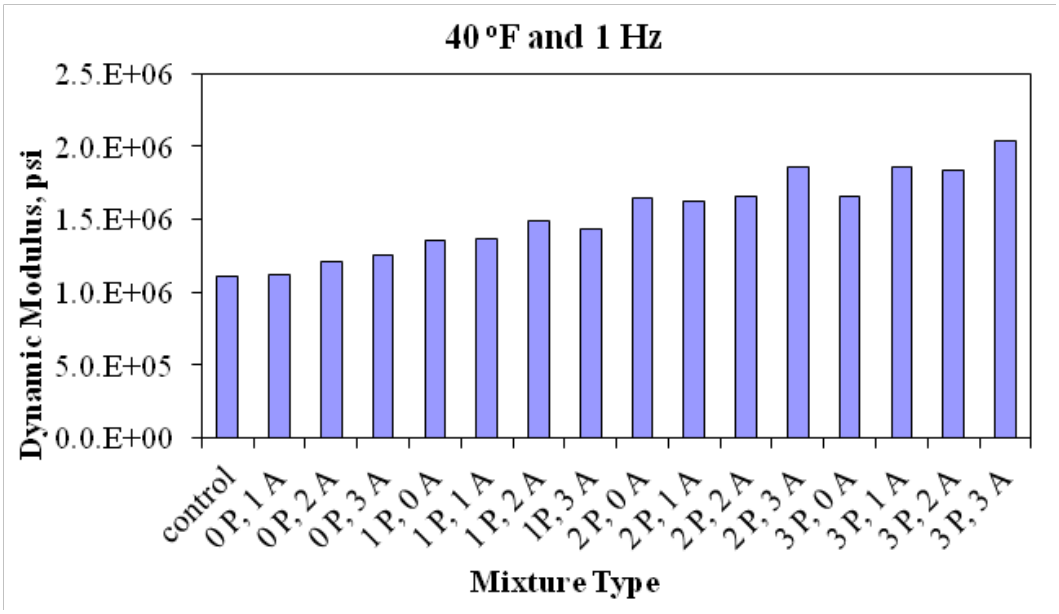

FIGURE 16 Comparison of E* based on the average of three replicates for all combinations of fibers at 40 ºF and 1 Hz.

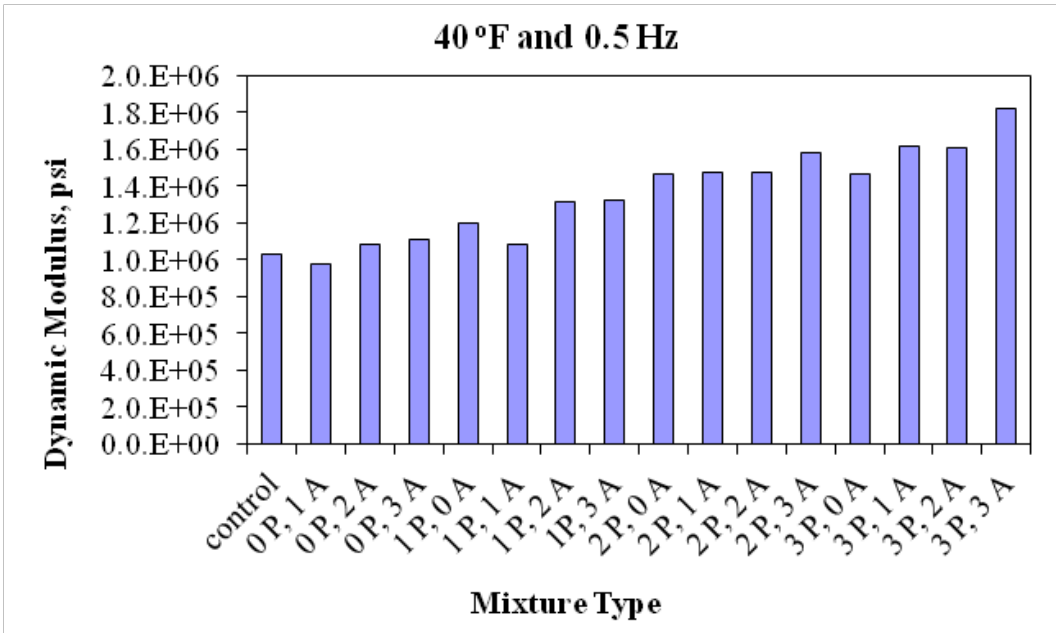

FIGURE 17 Comparison of E* based on the average of three replicates for all combinations of fibers at 40 ºF and 0.5 Hz.

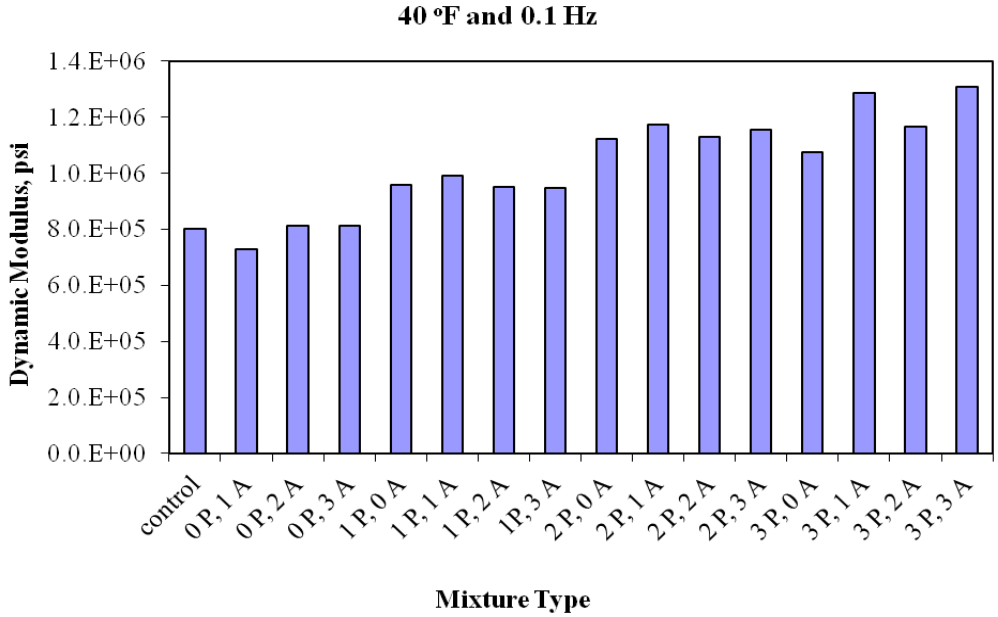

FIGURE 18 Comparison of E* based on the average of three replicates for all combinations of fibers at 40 ºF and 0.1 Hz.

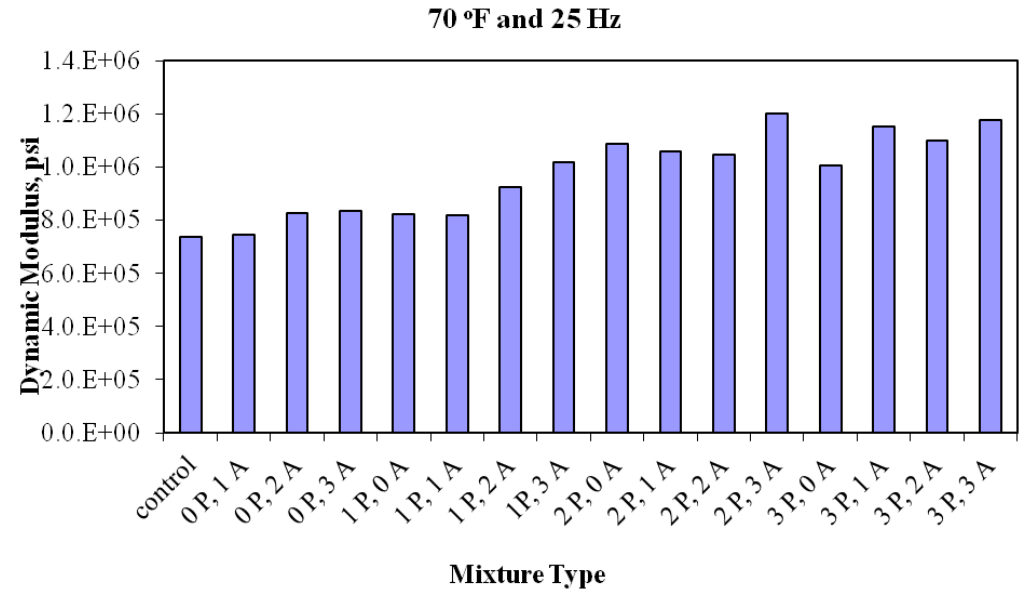

FIGURE 19 Comparison of E* based on the average of three replicates for all combinations of fibers at 70 ºF and 25 Hz.

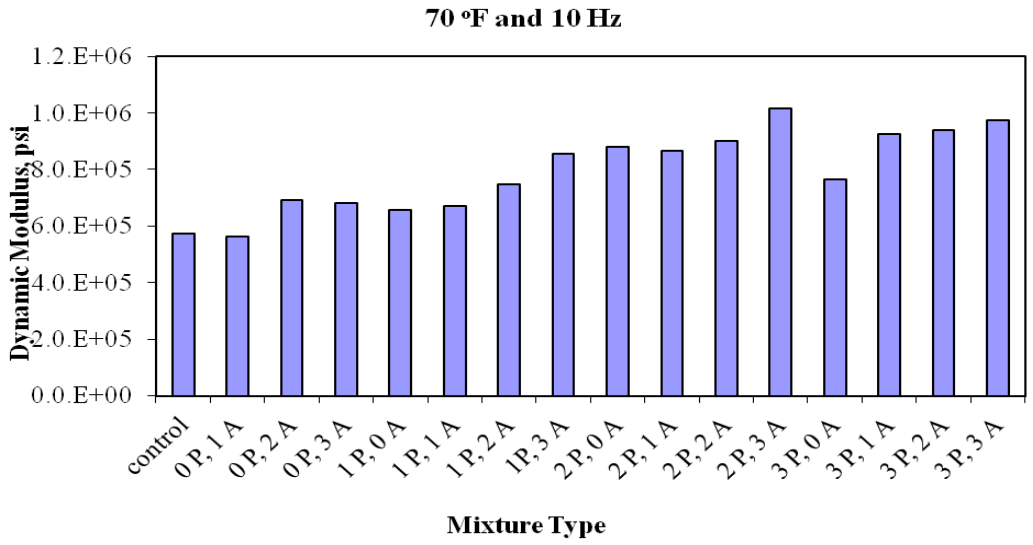

FIGURE 20 Comparison of E* based on the average of three replicates for all combinations of fibers at 70 ºF and 10 Hz.

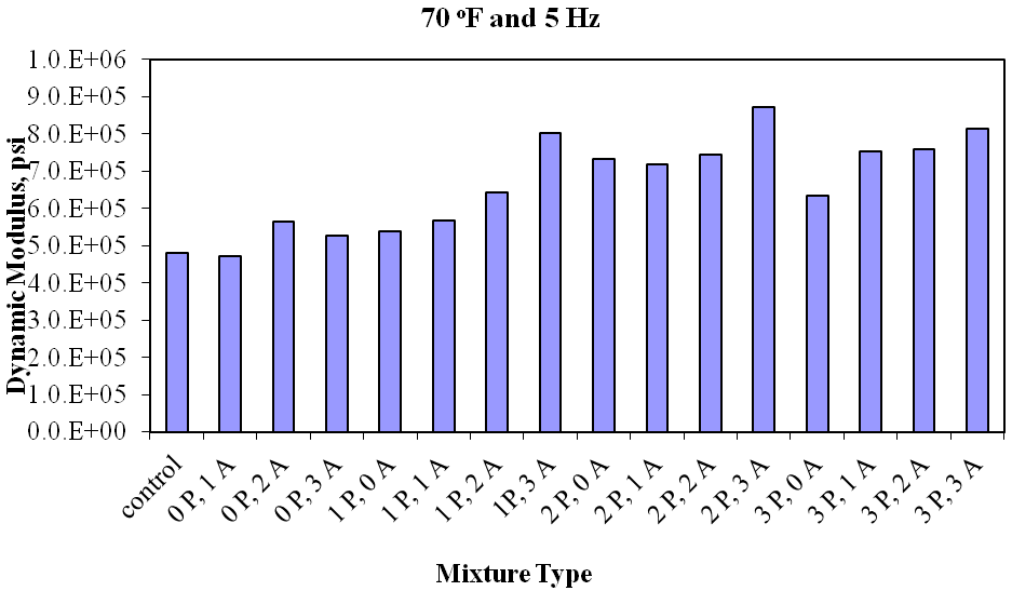

FIGURE 21 Comparison of E* based on the average of three replicates for all combinations of fibers at 70 ºF and 5 Hz.

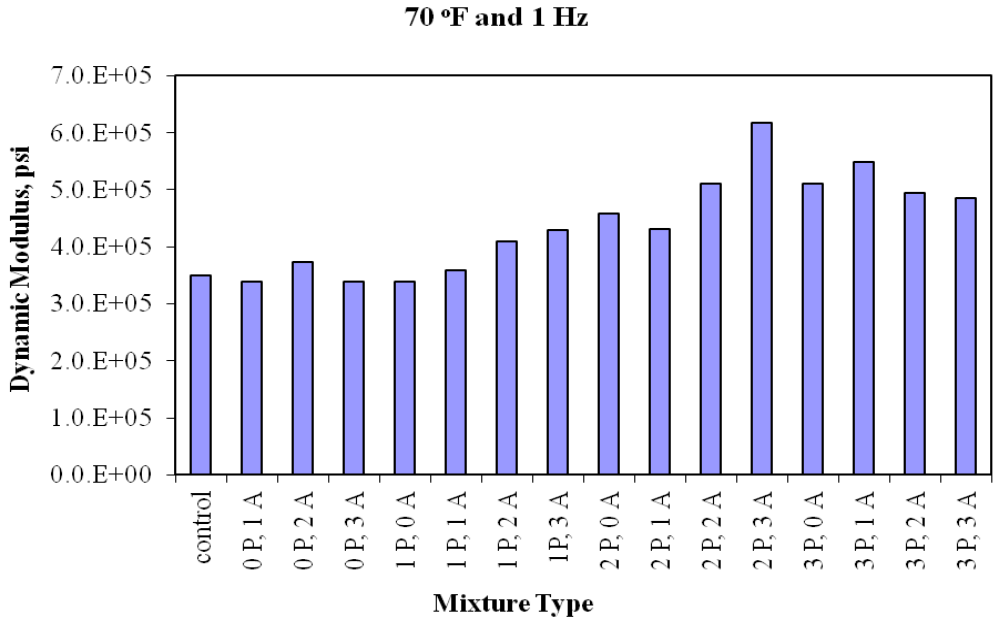

FIGURE 22 Comparison of E* based on the average of three replicates for all combinations of fibers at 70 ºF and 1 Hz.

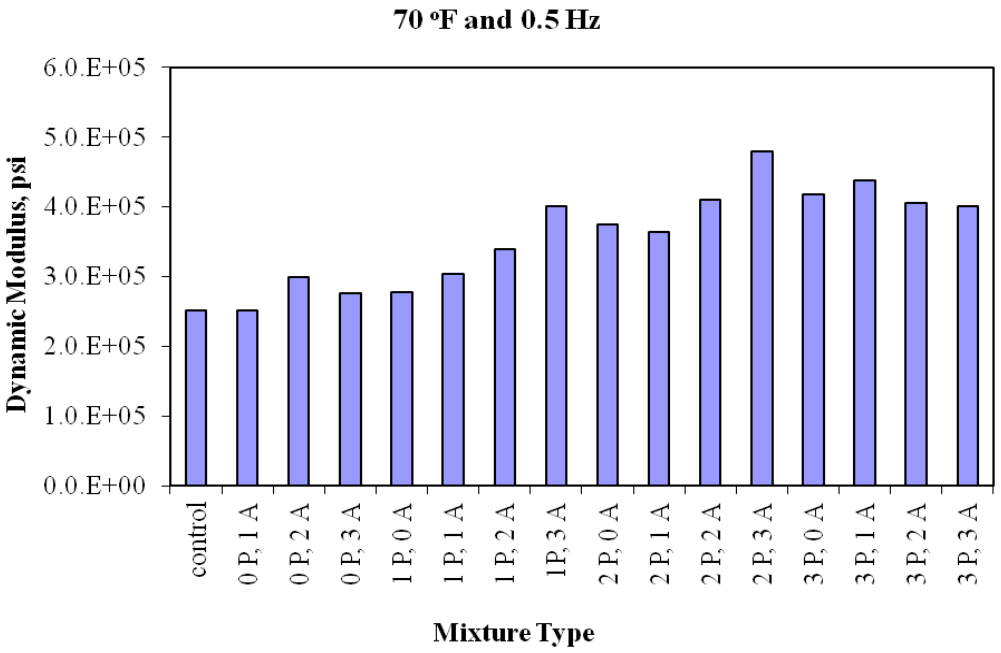

FIGURE 23 Comparison of E* based on the average of three replicates for all combinations of fibers at 70 ºF and 0.5 Hz.

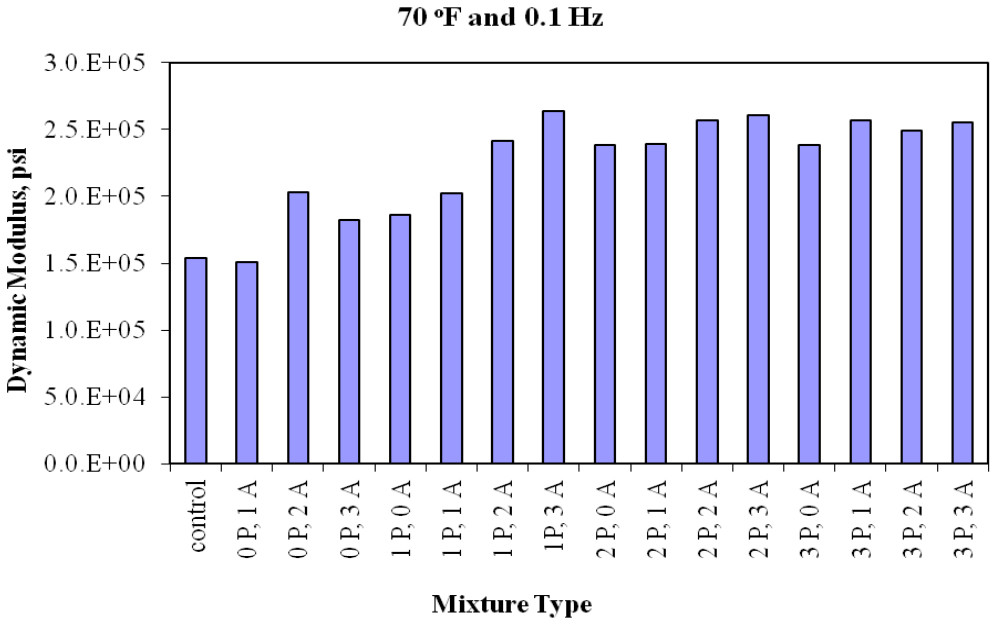

FIGURE 24 Comparison of E* based on the average of three replicates for all combinations of fibers at 70 ºF and 0.1 Hz.

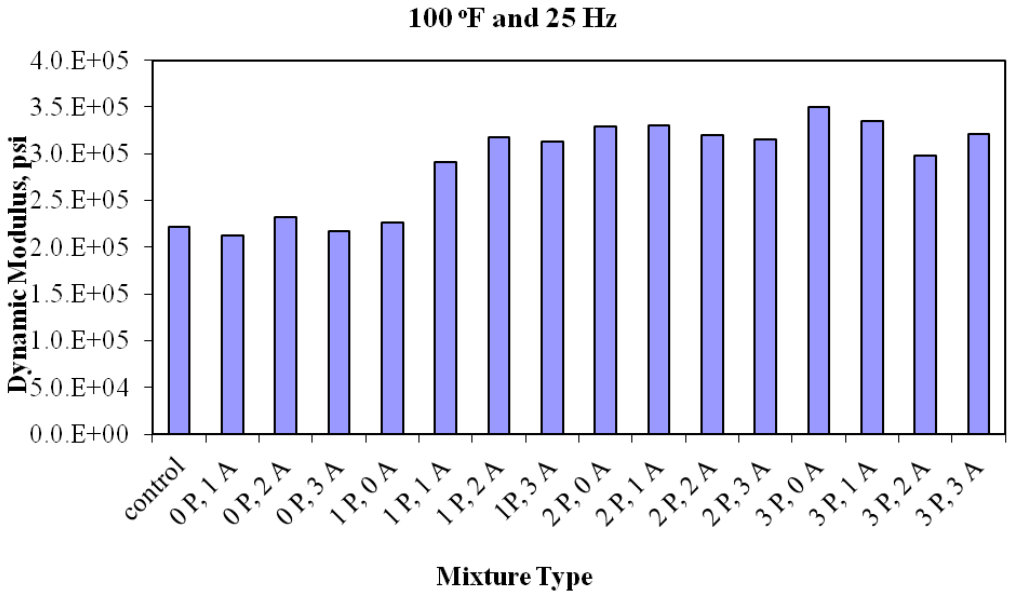

FIGURE 25 Comparison of E* based on the average of three replicates for all combinations of fibers at 100 ºF and 25 Hz.

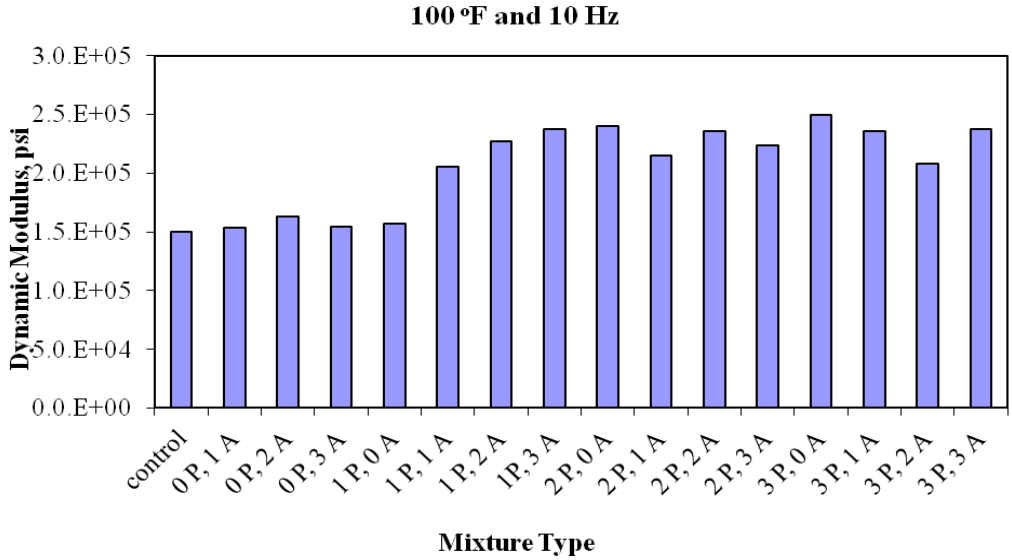

FIGURE 26 Comparison of E* based on the average of three replicates for all combinations of fibers at 100 ºF and 10 Hz.

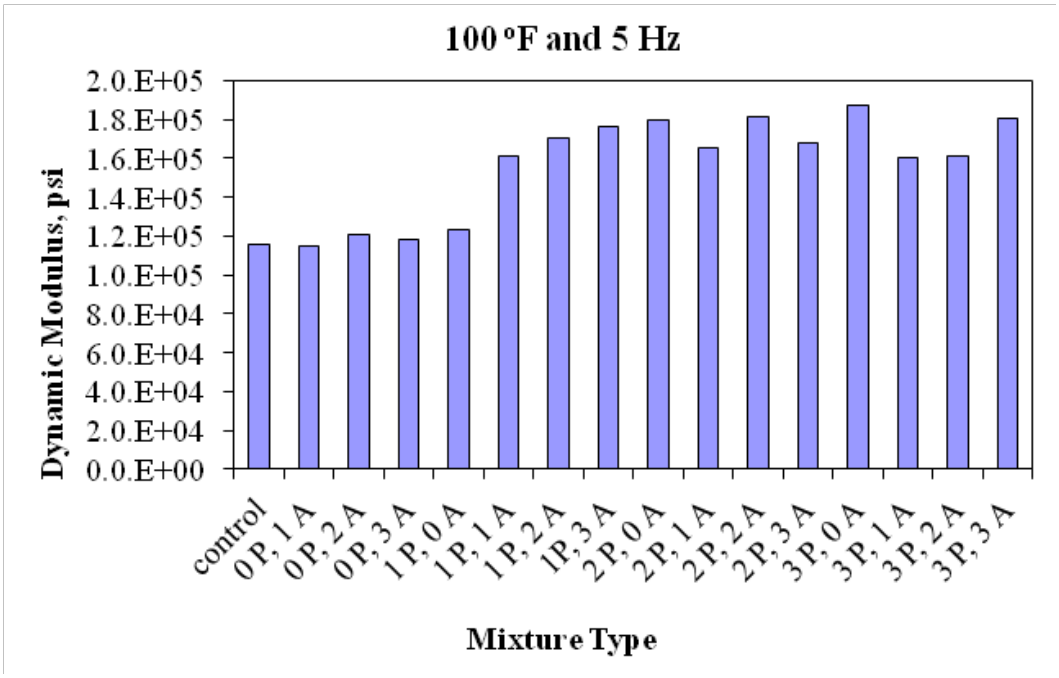

FIGURE 27 Comparison of E* based on the average of three replicates for all combinations of fibers at 100 ºF and 5 Hz.

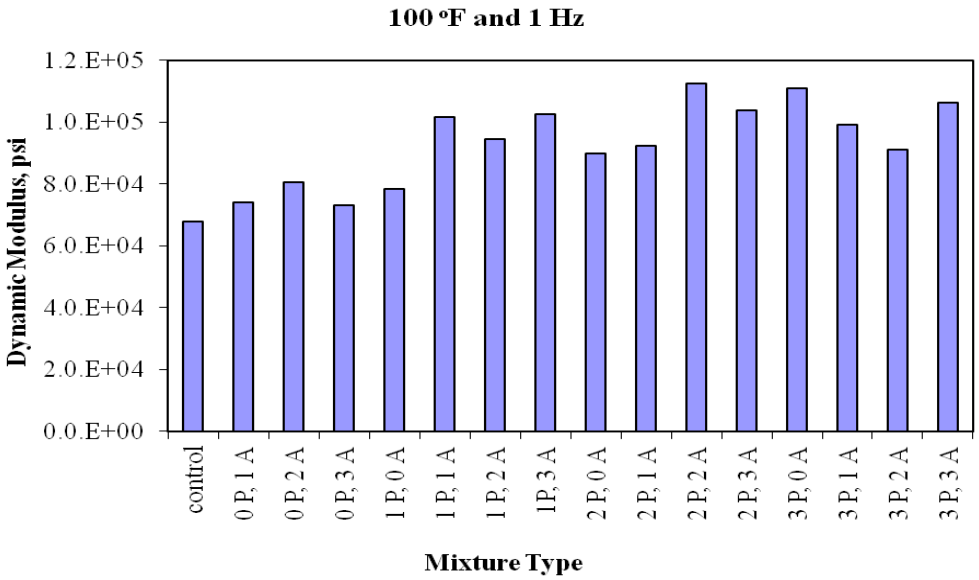

FIGURE 28 Comparison of E* based on the average of three replicates for all combinations of fibers at 100 ºF and 1 Hz.

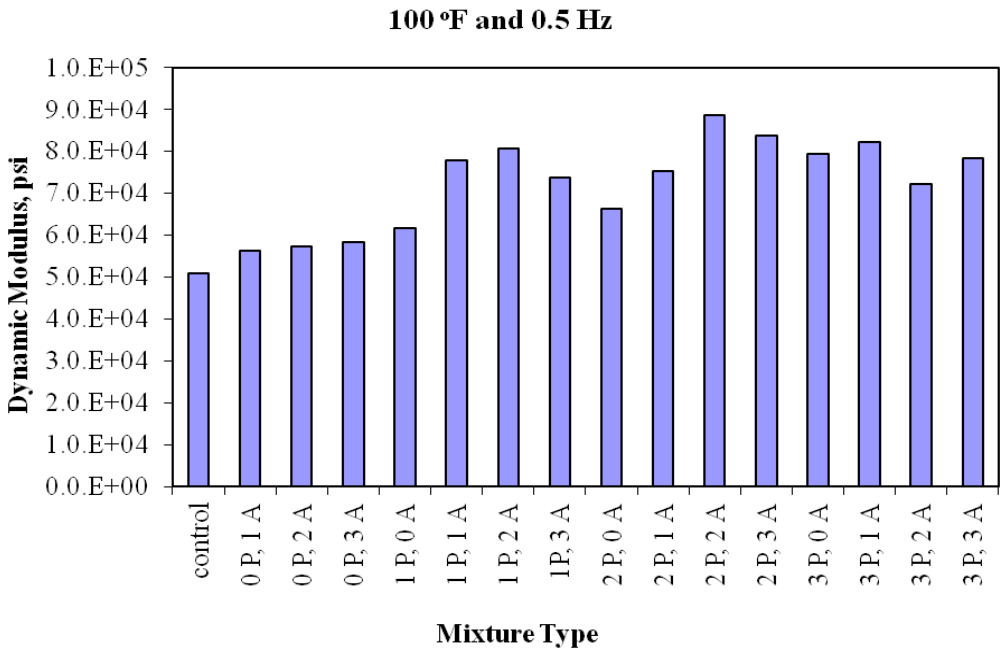

FIGURE 29 Comparison of E* based on the average of three replicates for all combinations of fibers at 100 ºF and 0.5 Hz.

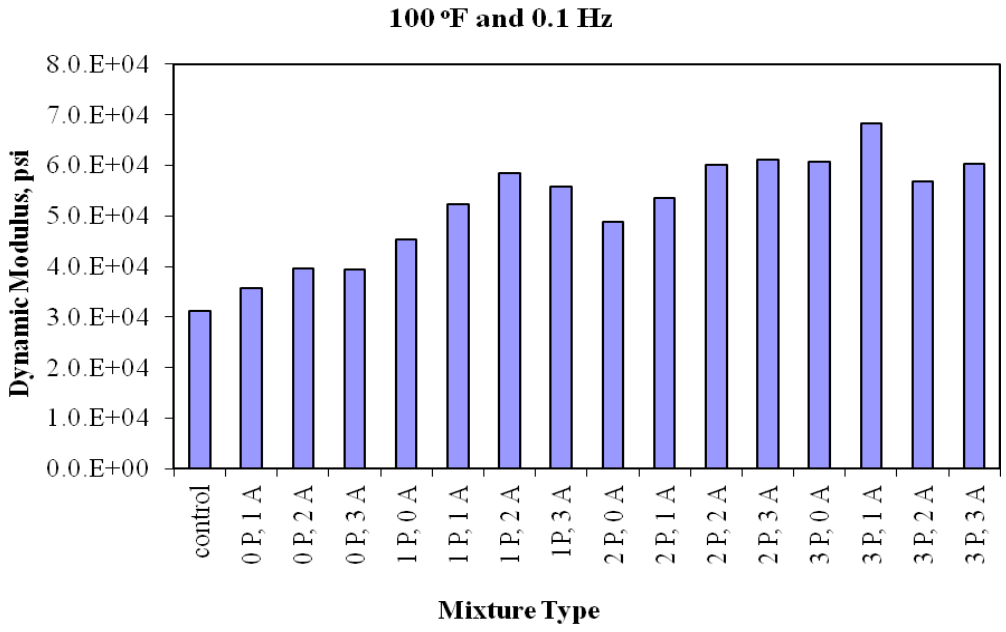

FIGURE 30 Comparison of E* based on the average of three replicates for all combinations of fibers at 100 ºF and 0.5 Hz.

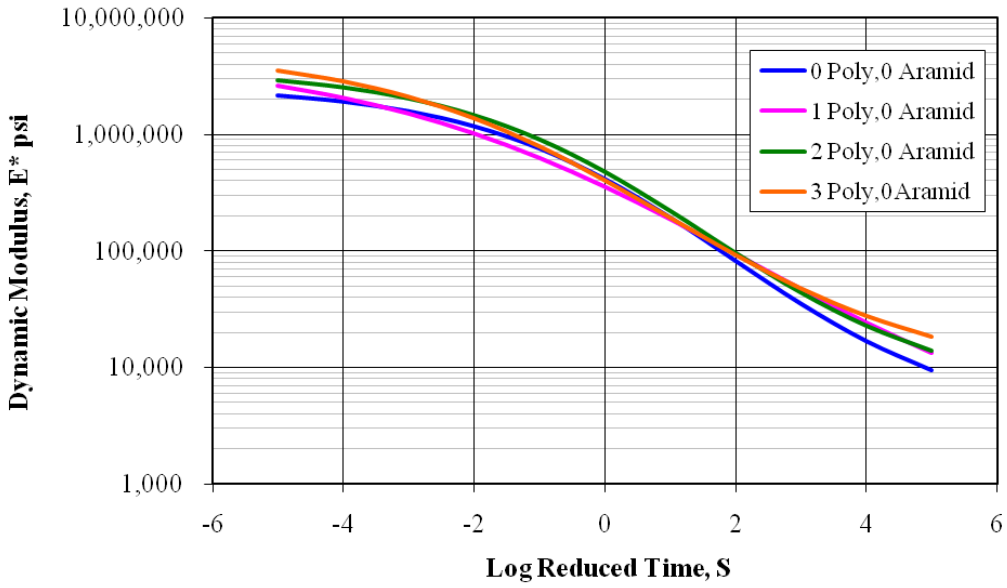

FIGURE 31 Master curves for four fiber mixtures - 1.

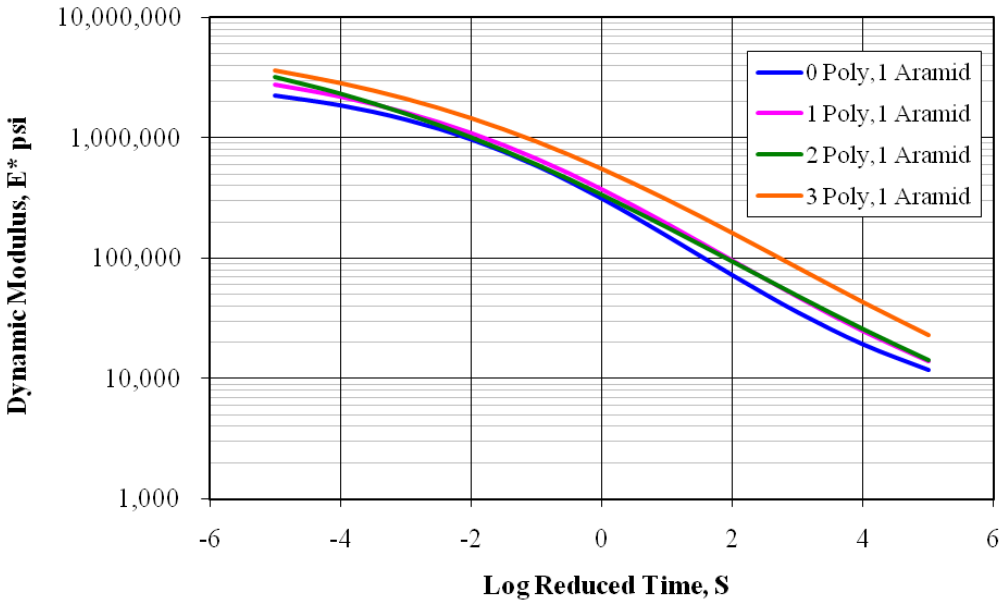

FIGURE 32 Master curves for four fiber mixtures -2.

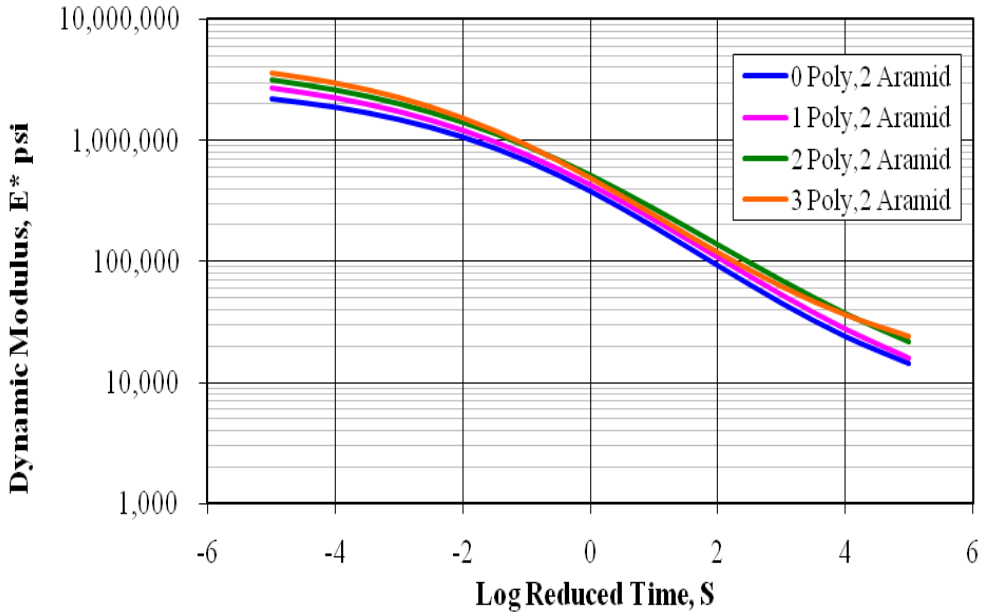

FIGURE 33 Master curves for four fiber mixtures -3.

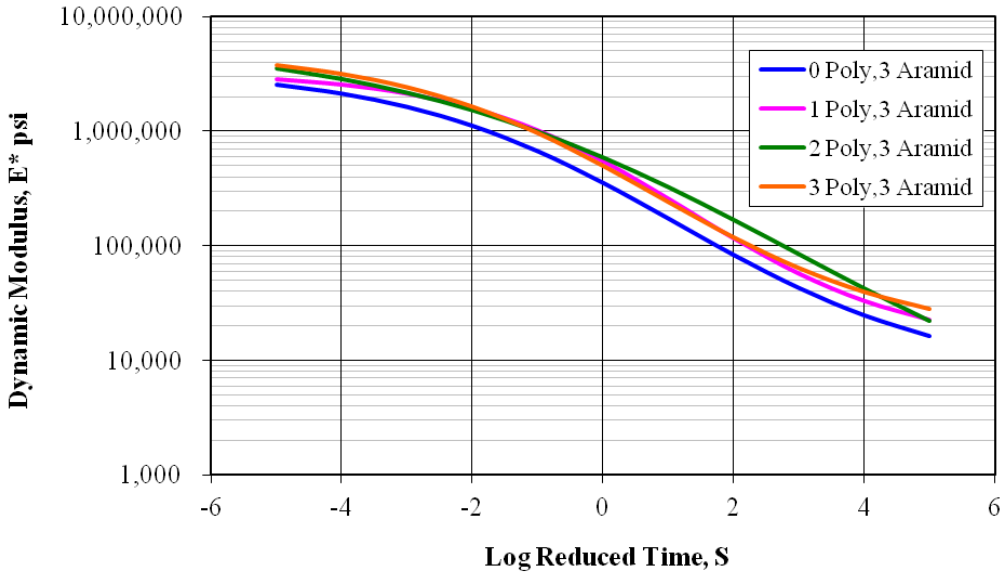

FIGURE 34 Master curves for four fiber mixtures -4.

5.5 Discussion

The Master curves using different combinations of fibers were shown in Figures 31, 32, 33 and 34. It can be observed that the dynamic modulus has a higher value when there is a low temperature and a high frequency. Also, the above figures show that when the dosage of polypropylene is increased, the dynamic modulus also increases. This also applies when using aramid fibers; however, aramid fibers have less of an effect on the dynamic modulus than polypropylene. Conversely, there are some irregular combinations that show results that do not align with the trend that may be due to uncontrolled conditions during the test preparation or testing. For example, the recoverable strain was higher than normal due to high stress in this temperature or frequency. Generally, three dosages of polypropylene in the mixture give the best performance for the dynamic modulus. Statistical comparison of the data was performed using the ANOVA test. It can be stated with 99 percent confidence that in almost every case, the addition of fibers resulted in an increase in mixture stiffness regardless of fiber content. The analysis shows a significant increase in the dynamic modulus of HMA samples by increasing polypropylene fiber compared to the control and aramid at three temperatures (4.4 °C, 21.7 °C and 37.8 °C) and all six frequencies used in the test.

CHAPTER 6 INDIRECT TENSILE TEST

6.1 Scope

The standard test method for the Indirect Tensile (IDT) Strength of Bituminous Mixtures ASMT D 6931-07 is used in laboratory procedures for preparing and testing IDT Strength. Sixteen different combinations of fibers were used in HMA with three replicates for each combination of samples with a 100 mm diameter and 50 mm thickness. The IDT loading rate on a cylindrical specimen was 0.8467 mm/s and three different test temperatures were conducted for IDT strength of bituminous mixtures.

6.2 Background

The indirect tensile test is a pavement testing method widely used to analyze and design asphalt paving mixtures by measuring the resilient modulus, creep, and indirect tensile strength. These measurements are used by many researchers to analyze the primary pavement distresses, such as fatigue, rutting and thermal cracking (30). Also, they are utilized for moisture damage.

The IDT test has been utilized by researchers since the 1960s. Most recently, however, both laboratory and field studies using the Superpave IDT tests have been used to characterize the crack growth rate of HMA mixtures (27). The test has also proven superior to conventional testing methods of the fundamental properties of asphalt mixtures at low temperatures (62).

The testing mode measures tensile properties of bituminous mixtures by applying a compressive load (0.8467 mm/s) to cylindrical specimens, resulting in

the development of tensile stresses until failure. Failure strength is defined as the stress at which first failure occurs in the specimen. This value is less than or equal to the ultimate stress realized by the specimen and is determined by analyzing deformations on specimen (63, 64).

The IDT test was used in this research to determine maximum tensile stress and fraction energy. The testing method was destructive, in that specimens were tested until their breaking point.

Parameters from the indirect tensile strength test that can be considered for mixture cracking performance include:

6.3 Tensile Strain at Failure

The tensile strain at failure is the horizontal strain corresponding to the failure strength - the stress at which failure first occurs in the specimen. Higher tensile strains at failure are favored as an indication of mix resistance to cracking. The peak load at failure is retarded and used to calculate the IDT strength of the specimen as following:

$$S_t = \frac{2000 \times p}{\pi \times t \times D}$$

S_t = IDT strength, kPa

P = maximum load, N

t = specimen average thickness, mm

D = specimen diameter, mm

6.4 Energy until Failure

The energy until failure is calculated as the area under the load-vertical deformation curve until maximum load occurs. Again, higher energy until failure is favored as an indication of the mix's resistance to cracking.

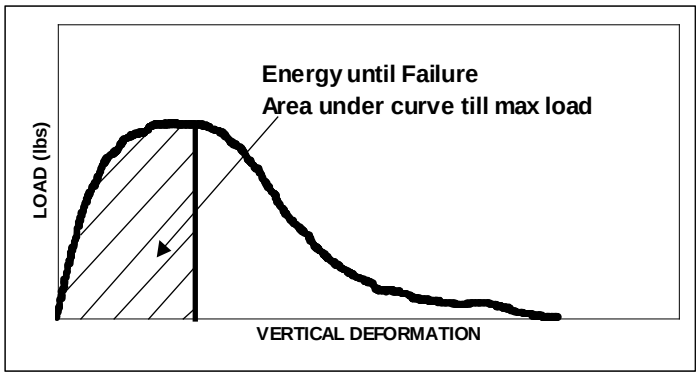

FIGURE 35 Determination of the energy until failure (63).

The total fracture energy is calculated as the area under the load-vertical deformation curve. Higher total fracture energy is favored as an indication of the mix's resistance to cracking.

Therefore, the energy approach to fracture analysis has an advantage over the tensile strength evaluation by considering not only the amount of deformation that the mixture can experience without cracking but also the maximum force that the given mixture is able to withstand.

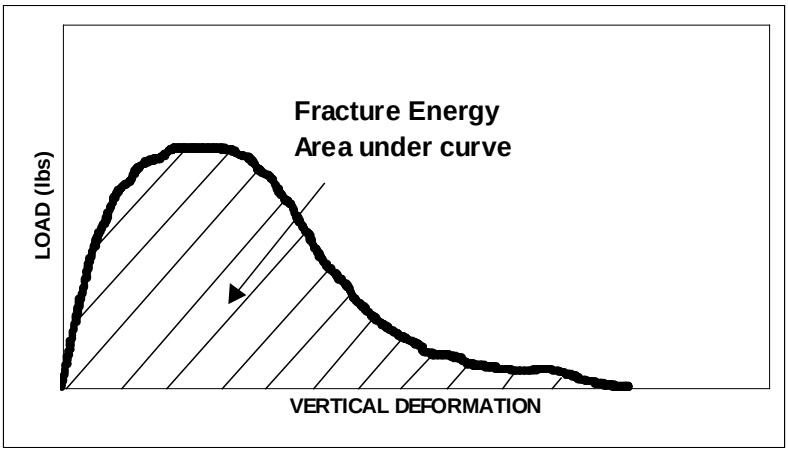

FIGURE 36 Determination of the total fracture energy (63).

6.5 Indirect Tensile Test System and Apparatuses

- Testing Machine: A hydraulic testing machine capable of producing compressive loading at controlled displacement and constant rate of ram displacement at 0.8467 mm/s.
- Environmental Chamber: A chamber for controlling the test specimen at the desired temperature. The environmental chamber shall be capable of controlling the temperature of the specimen to an accuracy of ±1.0 °C.
- Measurement System: The system shall be fully computer controlled, capable of measuring and recording the time history of the applied load and the deformations.

a. Sample before the test

b. Sample during the

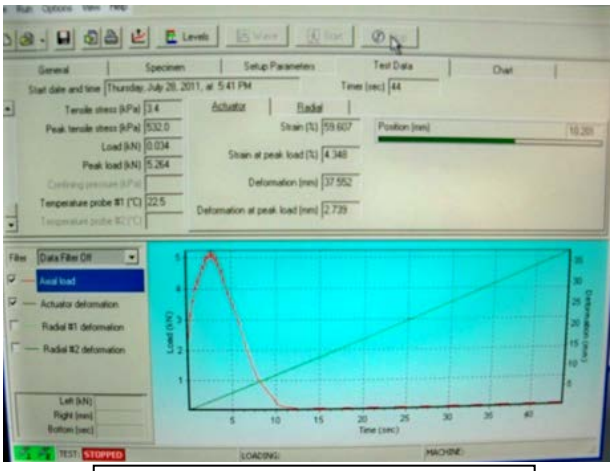

c. One result of control Sample

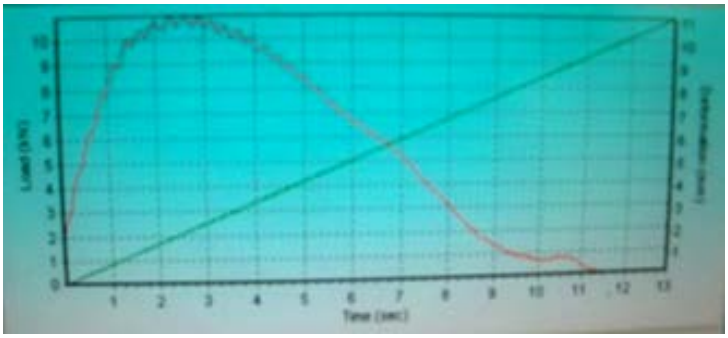

c. One result of fiber Sample

FIGURE 37 Process and results of the Indirect Tensile Strength test.

6.6 Test Specimen Preparation and Conditioning

All test specimens were prepared in the ASU Advanced Pavements Laboratory according to the Standard Test Method for Indirect Tensile (IDT) Strength of Bituminous Mixtures (ASTM D 6931-07)(65). Sixteen different combinations of fiber mixtures were used to evaluate the maximum tensile strength, pre energy, post energy and total energy. Three replicates for each combination were made on disk forms with 100 mm diameter and approximately a 50 mm thickness. IDT Strength was run at three different temperatures (4.40 ºC, 21.4 ºC, 37.8 ºC).

6.7 Test Results and Analysis for the IDT Strength

The results obtained for the IDT strength test for the sixteen different combinations of fiber mixtures were summarized and are reported in TABLES 18, 19, 20, and 21. TABLE 18 illustrates maximum tensile strength for all samples with three temperatures as demonstrated in FIGURE 38. TABLE 19 illustrates pre energy for all samples with three temperatures as demonstrated in FIGURE 39. TABLE 20 illustrates post energy for all samples with three temperatures as demonstrated in FIGURE 40. TABLE 21 illustrates Total energy for all samples with three temperatures as demonstrated in FIGURE 41.

TABLE 18 Maximum Tensile Strength for All Samples at Three Temperatures

Mixture Type	Tensile Strength, Kpa		
Temps	40 ºF	70 ºF	100 ºF
Control	1931	637	904
0 P, 1 A	2317	743	1015
0 P, 2 A	2304	841	1021
0 P, 3 A	2441	830	1045
1 P, 0 A	2074	732	950
1 P, 1 A	2287	841	1034
1 P, 2 A	2414	851	1068
1 P, 3 A	2423	841	1061
2 P, 0 A	2094	747	961
2 P, 1 A	2355	810	1068
2 P, 2 A	2407	795	1122
2 P, 3 A	2415	818	1091
3 P, 0 A	2124	768	1023
3 P, 1 A	2393	906	1195
3 P, 2 A	2455	846	1166
3 P, 3 A	2585	970	1214

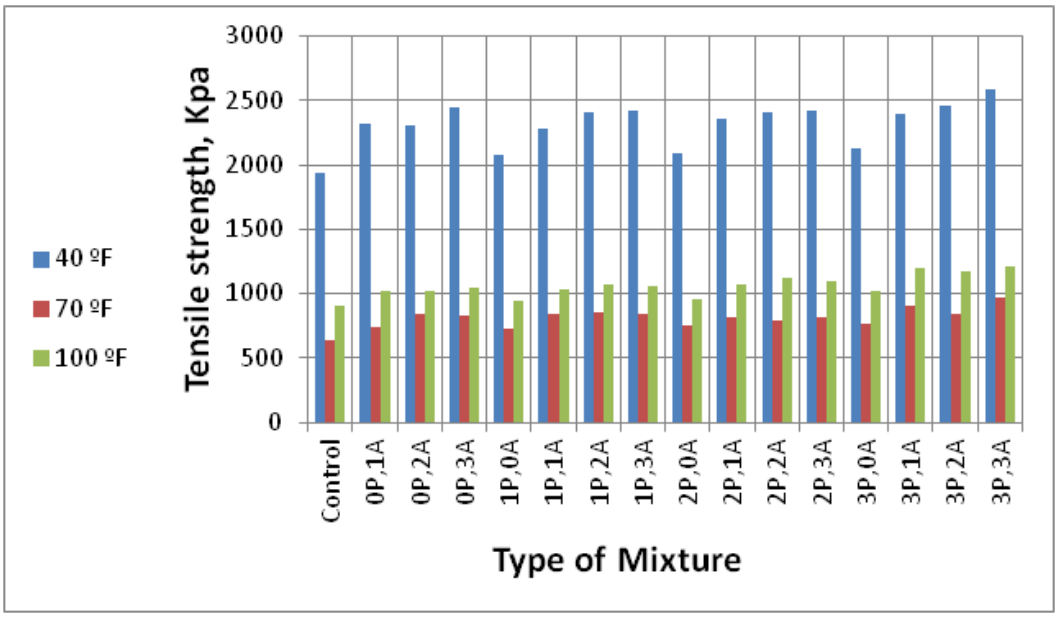

FIGURE 38 Maximum tensile strength for all samples at three temperatures.

TABLE 19 Pre-Energy for All Samples with Three Temperatures

Mixture Type	Pre Energy		
Temp.	40 ºF	70 ºF	100 ºF
Control	626	655	1361
0 P, 1 A	726	690	1421
0 P, 2 A	862	737	1415
0 P, 3 A	853	717	1531
1 P, 0 A	710	668	1371
1 P, 1 A	792	736	1443
1 P, 2 A	911	749	1516
1 P, 3 A	894	718	1479
2 P, 0 A	686	693	1413
2 P, 1 A	828	770	1473
2 P, 2 A	943	757	1549
2 P, 3 A	1094	806	1607
3 P, 0 A	776	710	1450
3 P, 1 A	863	798	1522
3 P, 2 A	863	822	1580
3 P, 3 A	1118	854	1597

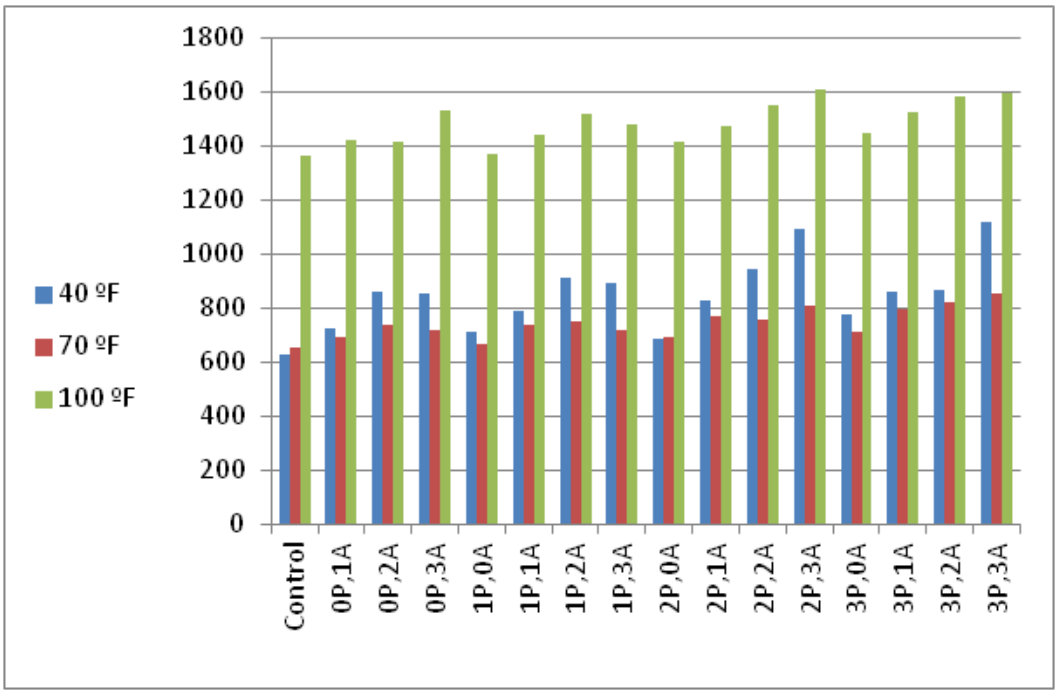

FIGURE 39 Pre-energy for all samples with three temperatures.

TABLE 20 Post Energy for All Samples with Three Temperatures.

Mixture Type	Post Energy		
Temp.	40 ºF	70 ºF	100 ºF
Control	1670	1290	3014
0 P, 1 A	1840	1467	3248
0 P, 2 A	1817	1476	3262
0 P, 3 A	1991	1543	3317
1 P , 0 A	1712	1307	3085
1 P, 1 A	1797	1411	3124
1 P, 2 A	1907	1508	3311
1 P, 3 A	2126	1662	3435
2 P, 0 A	1781	1297	3092
2 P, 1 A	1815	1514	3321
2 P, 2 A	2152	1670	3430
2 P, 3 A	2247	1632	3420
3 P, 0 A	1799	1610	3313
3 P, 1 A	1885	1603	3404
3 P, 2 A	2412	1812	3421
3 P, 3 A	2407	1917	3693

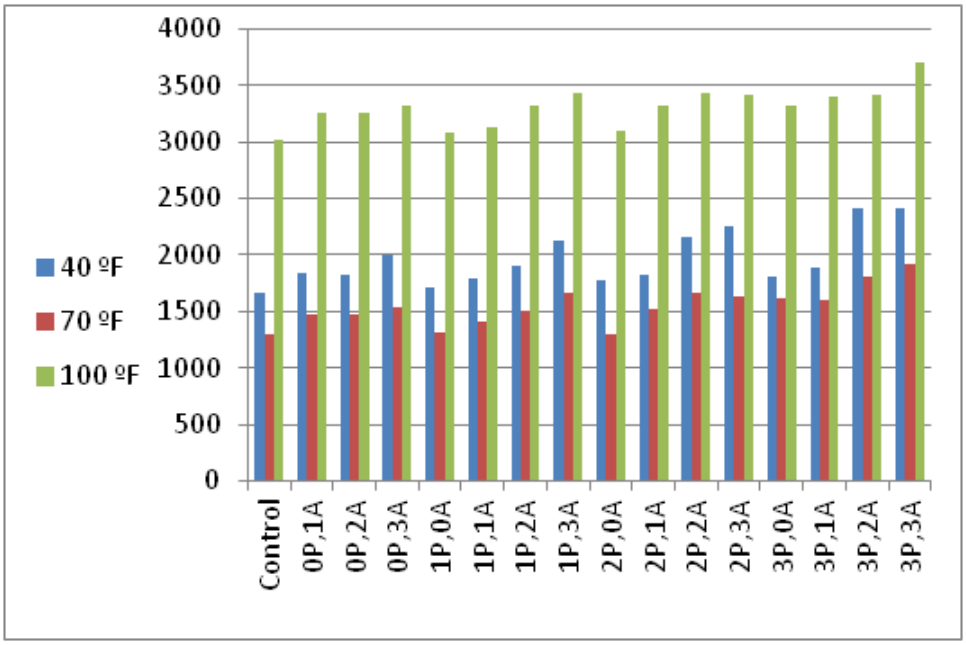

FIGURE 40 Post energy for all samples with three temperatures.

TABLE 21 Total Energy for All Samples with Three Temperatures

Mixture Type	Total Energy		
Temp.	40 ºF	70 ºF	100 ºF
Control	2295	1921	4375
0 P, 1 A	2566	2157	4669
0 P, 2 A	2680	2213	4677
0 P, 3 A	2845	2259	4848
1 P, 0 A	2422	1975	4456
1 P, 1 A	2589	2147	4567
1 P, 2 A	2818	2257	4827
1 P, 3 A	3020	2380	4914
2 P, 0 A	2467	1989	4505
2 P, 1 A	2644	2284	4794
2 P, 2 A	3096	2426	4978
2 P, 3 A	3341	2422	5027
3 P, 0 A	2575	2319	4763
3 P, 1 A	2748	2411	4926
3 P, 2 A	3275	2634	5001
3 P, 3 A	3525	2771	5291

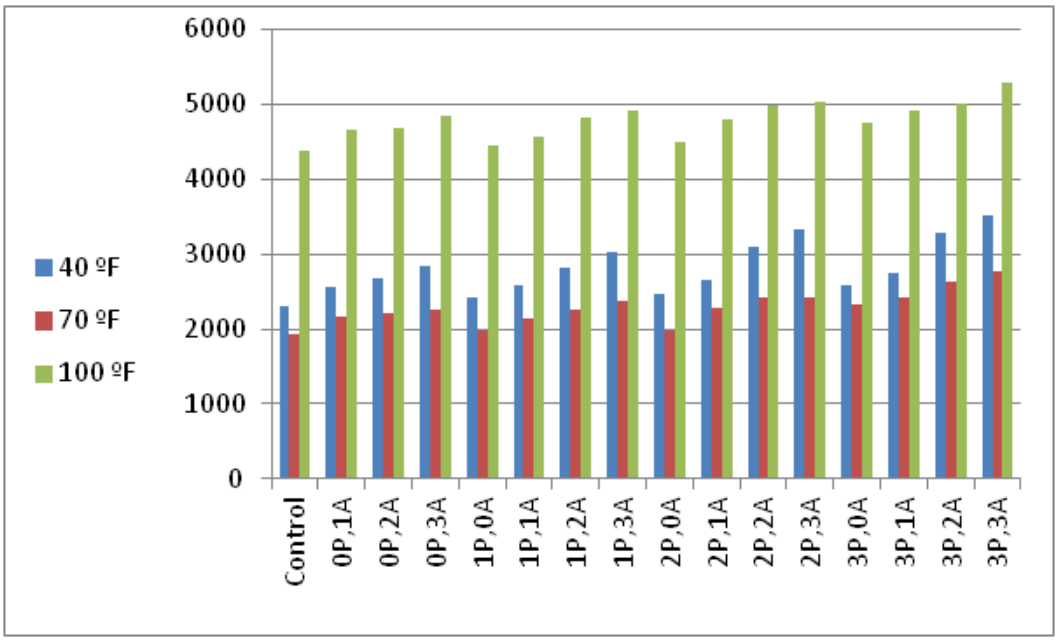

FIGURE 41 Total energy for all samples with three temperatures.

In Figure 38, it indicated when the dosage of aramid is increased, the IDT strength does too. This also applies when using polypropylene fibers; however, polypropylene fibers have less of an effect on the IDT strength than aramid. Conversely, there are some irregular combinations that show results that do not align with the trend due to certain condition. Moreover, the lowest temperature (40 ºF) has the highest IDT strength because the sample is rigid at low temperatures; therefore, it resists the load until a high limit and suddenly collapses, while the temperature at (70 ºF) has the lowest IDT strength**.**

In Figure 39, it indicated when the dosage of aramid is increased, the pre-energy does too. This also applies when using polypropylene fibers; however, polypropylene fibers have less of an effect on pre- energy than aramid.

Conversely, there are some irregular combinations that show results that do not align with the trend due to certain condition. Moreover, the lowest temperature (40 ºF) has not the highest pre- energy because the sample is rigid at low temperatures; therefore, it resists the load until a certain limit and suddenly collapses. Also, the temperature at (100 ºF) has highest pre- energy, while the temperature at (70 ºF) has lowest pre- energy.

In Figure 40, it indicated when the dosage of aramid is increased, the post energy does too. This also applies when using polypropylene fibers; however, polypropylene fibers have less of an effect on post energy than aramid. Conversely, there are some irregular combinations that show results that do not align with the trend due to certain condition. Moreover, the lowest temperature (40 ºF) has not the highest post energy because the sample is rigid at low temperatures; therefore, it resists the load until a certain limit and suddenly collapses. Also, the temperature at (100 ºF) has highest post energy, while the temperature at (70 ºF) has lowest post energy.

Total energy is a sum of pre-energy and post energy that has same results of pre-energy and post energy. Overall, the aramid yielded better results than polypropylene.

CHAPTER 7 CONCLUSION AND RECOMMENDATIONS FOR FUTURE WORK

The objective of this study was to investigate the effects of different dosages of FORTA fibers (polypropylene and/or aramid) on the performance of an asphalt binder and HMA mixtures. Nine different dosages were evaluated for one source of asphalt binder, and sixteen different dosages were evaluated for the effect of fibers on HMA mixture performance.

7.1 Binder Tests

From the results, the A8 sample, which has three dosages of polypropylene and one dosage of aramid, had the highest viscosity and the lowest VTS value indicating a lesser temperature susceptibility to both permanent deformation and thermal cracking.

When the amount of aramid is increased, the viscosity starts increasing, but it suddenly and unexpectedly drops down, probably because the fibers do not melt in the binder and starts clumping. Due to this clumping, there was high variability in the penetration test.

7.2 Dynamic (Complex) Modulus Test

All test specimens were prepared according to AASHTO TP 62-07. For each mix, at least three replicates were prepared. For each specimen, E* tests were conducted at three temperatures (40, 70, and 100 °F) and six loading frequencies (25, 10, 5, 1, 0.5 and 0.1 Hz). E* master curves of all mixtures were constructed

for a reference temperature of 70 °F using the principle of time-temperature superposition.

Results showed that the dynamic modulus of the fiber modified mixtures increased by increasing the amount fibers compared to the control mix. In general, the trend was that polypropylene fibers yielded better results than the aramid fibers.

7.3 Indirect Tensile Test

Based on the IDT test results, the control and different fiber-reinforced asphalt mixtures were compared using four different criteria; IDT strength, pre fracture energy, post fracture energy, and total energy. It was observed that the 3 lb/ton mixture (3 dosages) had the highest IDT strength most of the time, compared to the control and both 1 lb/ton and 2 lb/ton mixtures at the three test temperatures (40, 70, 100 ºF). The same trend was observed for the different fracture energy parameters. Overall, the aramid fiber yielded better results than the polypropylene fiber.

7.4 Recommendations

This study's results signify that FORTA fibers can benefit the field of pavement design by improving the performance of flexible pavements. However, this study was limited to one binder type and one asphalt mixture. Further investigation is recommended to include different aggregate gradations, fiber sizes, and asphalt binder types.

Additional laboratory performance tests, such as the flow number, flexural beam fatigue, crack propagation, and triaxial shear strength are also recommended to be incorporated into future research studies. Finally, a life cycle cost analysis should be also considered to support the use of fibers in a cost effective and financially sustainable addition to pavement mixtures.

REFERENCES

1. Siriwardane, H., Gondle, R., and Kutuk, B. *Analysis of Flexible Pavements Reinforced with Geogrids*. Department of Civil & Environmental Engineering, West Virginia University, Morgantown, WV, U.S.A. 2010.

2. Roberts, Freddy L. et al. *Hot Mix Asphalt Materials, Mixture Design, andConstruction* .2nd edition, NAPA Research and Education Foundation p 1-10, 1996.

3. Jahromi, S., and Khodaii, A. Carbon Fiber Reinforced Asphalt Concrete. Department of Civil Engineering, Amirkabir University of Technology, Tehran, Iran. The Arabian Journal for Science and Engineering, Volume 33, Number 2B, Tehran, Iran, 2008.

4. Wu, S., Ye, Q., and Li, N. Investigation of Rheological and Fatigue Properties of Asphalt Mixtures Containing Polyester Fibers. ScienceDirect: Construction and Building Materials, 2008; 22(10):2111–5. Key Laboratory of Silicate Materials Science and Engineering of Ministry of Education, Wuhan University of Technology, Wuhan 430070,China.

5. Kutuk, B. Performance of Flexible Pavements Reinforced with Geogrids. .Ph.D. Dissertation,West Virginia University, Morgantown, 1998.

6. Fiber Reinforcement Technology for Asphalt. Online website :http://www.forta- fi.com/why-fortafied-asphalt/.

7. Abdulshafi, A., Kalsoush, K. Modifiers for Asphalt Concrete. Resource International, Inc.Public Release Report, 1988.

8. King, G., King, H., Pavlovich, R. D., Epps, A. L., and Kandhal, P. Additives in Asphalt. Asphalt Paving Technology 1999, 75th Historical Review, Journal of the Association of Asphalt Paving Technologists, Vol. 68A, 1999, pp. 32-69.

9. Bates R., and Worch, R. Engineering Brief No. 39, Styrene–Butadiene Rubber Latex Modified Asphalt. Federal Aviation Administration, Washington, DC, 1987. Available from: http://www.faa.gov/arp/engineering/briefs/eb39.htm.

10. Yildirim, Y. Polymer Modified Asphalt Binders. Department of Civil Engineering, University of Texas at Austin, USA. Journal of Science Direct: Construction and Building Materials 21 (2007) 66–72.

11. Novophalt Product Information Bulletin. Bulletin #PIB-02, Novophalt America, Inc., Sterling, Virginia, February 1989, 11 pages.

12. Partl, MN, Newman, JK. Flexural Beam Fatigue Properties of Airfield Asphalt Mixtures Containing Styrene–Butadiene Based Polymer Modifiers. In Proceedings of the Sixth International Rilem Symposium, Zurich, Switzerland, 2003. p. 357–63.

13. Novophalt Permanent Deformation Laboratory Rutting Tester. Bulletin #CT-004, Novophalt America, Inc., Sterling, Virginia, February 1989, 10 pages.

14. Novophalt User Guidelines. Bulletin #PIB-01, Novophalt America, Inc., Sterling, Virginia, February 1989, 3 pages.

15. Denver's New E-470 Tests Low Density Polyethylene Modifier. Roads and Bridges, Sept 1991, p. 47.

16. Asphalt Material Garners Top Honors in PN Contest. Plastic News, Sept. 17, 1990, p. 1.

17. Terrel, R. L., and Epps, J. A. Using Additives and Modifiers in Hot Mix Asphalt (Part A). National Asphalt Pavement Association, Lanham, MD, Report No. QIP 114A, 1989.

18. McDaniel, R., and Shah, A. Asphalt Additives to Control Rutting and Cracking. Report from Joint Transportation Research Program, Purdue University, 2003.

19. Palit, S.K., Reddy, S., and Pandey, B. B. Laboratory Evaluation of Crumb Rubber Modified Asphalt Mixes. Journal of Materials in Civil Engineering, ASCE, 2004.

20. Heitzman, M. Design and Construction of Asphalt Paving Materials with Crumb Rubber Modifier. Transportation Research Record, No. 1339, Transportation Research Board, Washington, D.C., 1992, pp. 1-8.

21. Hanson, Douglas I., Foo, K. Y., Brown, E. R., and Denson, R. Evaluation and Characterization of a Rubber-Modified Hot Mix Asphalt Pavement. Transportation Research Record, No. 1436, Transportation Research Board, 1994, Washington, D. C., pp.98-107.

22. Page, G. C. Florida's Initial Experience Utilizing Ground Tire Rubber in Asphalt Concrete Mixes. Asphalt Paving Technology, Journal of the Association of Asphalt Paving Technologists, Vol. 61, 1992, St. Paul, Minnesota, pp. 446-472, 1992.

23. Mahrez, A., Karim, M. R., and Katman, H. Y. Prospect of Using Glass Fiber Reinforced Bituminous Mixes. Department of Civil Engineering, University Malaya, Malaysia. Journal of the Eastern Asia Society for Transportation Studies, Vol.5, University Malaya, Malaysia, 2003.

24. Brown, S. F., Rowlett, R. D., & Boucher, J. L. Asphalt modification. In Proceedings of the conference on the United States strategic highway research program: Sharing the benefits, ICE (pp. 181–203), 1990.

25. Button, J. W., and Epps J. A. Mechanical Characterization of Fiber-Reinforced Bituminous Concrete. Texas Transportation Institute, College Station, Texas, Report 4061-1, p. 99, February 1981.

26. Mahrez, A., and Karim, M. R. Rutting Characteristics of Bituminous Mixes Reinforced with Glass Fiber. Department of Civil Engineering, University Malaya, Malaysia. Journal of Proceedings of the Eastern Asia Society for Transportation Studies, 2007.

27. Lee, S. Long-Term Performance Assessment of Asphalt Concrete Pavements Using The Third Scale Model Mobile Loading Simulator and Fiber Reinforced Asphalt Concrete. P.h. D. Dissertation, North Carolina State University, 2003.

28. Shaopeng, w., Qunshan,Y., Ning, L., and Hongbo, Y. Effects of Fibers on the Dynamic Properties of Asphalt Mixtures. Key Laboratory of Silicate Materials Science and Engineering of Ministry of Education, Wuhan University of Technology, Wuhan 430070,China. Journal of Wuhan University of Technology-Mater. Sci. Ed, China, 2007.

29. Serfass, J.P., Samanos, J. Fiber-Modified Asphalt Concrete Characteristics, Applications and Behavior. Journal of the Association of Asphalt Paving Technologists, Vol. 65, p 193-230, 1996.

30. Cleven, M. A. Investigation of the Properties of Carbon Fiber Reinforced Asphalt Mixtures. M. S. Thesis, Michigan Technological University, 2000.

31. Jenq, Y. S., Chwen-Jang Liaw, P. L. Analysis of Crack Resistance of Asphalt Concrete Overlays. A fracture mechanics approach, Transportation Research Record n 1388 p 160-166, 1993.

32. Simpson, A. L., and Mahboub, K. C. Case Study of Modified Bituminous Mixtures: Somerset, Kentucky. Proceedings of the Third Materials Engineering Conference 804 Oct 1994, ASCE p 88-96.

33. Murali KJ, Rajagopal KR. Review of the Uses and Modeling of Bitumen from Ancient to Modern Times. Application Mech Review 2003; 56 (2): 672–5.

34. Tapkın, S. The Effect of Polypropylene Fibers on Asphalt Performance. Civil Engineering Department, Faculty of Engineering and Architecture, Anadolu University, 26555 Eskisehir, Turkey. ScienceDirect: Building and Environment 43 (2008) 1065–1071.

35. Jiang, Y., and McDaniel, R. S. Application of Cracking and Seating and Use of Fibers to Control Reflection Cracking. Transportation Research Record n 1388 p 150-159, 1993.

36. Huang, H., White, T. Dynamic Properties of Fiber-Modified Overlay Mixture. Transportation Research Record n 1545 p 98-104, 1996.

37. Shiuh, J, Kuei-Yi L. Mechanism and Behavior of Bitumen Btrength Reinforcement Using Fibers. Jornal Mater Science 2005; 40:87–95.

38. Maurer, D. A., Malasheskie, G. Field Performance of Fabrics and Fibers to Retard Reflective Cracking. Transportation Research Record n 1248 1989 p 13-23, 1989.

39. Decoene, Y. Contribution of Cellulose Fibers to the Performance of Porous Asphalts. Transportation Research Record n 1265, p. 82.

40. Stuart, K D., and Malmquist, P. Evaluation of Using Different Stabilizers in the U.S. Route 15 (Maryland) stone matrix asphalt. Transportation Research Record n.1454 p 48-57, 1994.

41. Partl, M.N., Vinson, T.S., and Hicks, R.G. Mechanical Properties of Stone Mastic Asphalt. Proceedings of the Third Materials Engineering Conference 804 Oct 1994, ASCE p 849-858.

42. Selim, A. A., Taha, R., and Bayomy, F. Laboratory Performance of Quartzite Based Stone Matrix Asphalt Mixtures (SMAM). Proceedings of the Third Materials Engineering Conference 804 Oct 1994, ASCE p 635-642, 1994.

43. Harvey, J. and Monismith, C. L. Effects of Laboratory Asphalt Concrete Specimen Preparation Variables on Fatigue and Permanent Deformation Test Results Using Strategic Highway Research Program a-003 a Proposed Testing Equipment. Transportation Research Record 1417, pp. 38-48, 1993.

44. Ling, H.I., Member, ASCE., and Liu, Z. Performance of Geosynthetic-Reinforced Asphalt Pavements. Journal of Geotechnical and Geoenvironmental Engineering, 2001.

45. Komatsua, Kikutab, Tujic,and Muramatsuc, Eijiro. Durability Assessment of Geogrid-Reinforced Asphalt Concrete. Journal of National Institute of Materials and Chemical Research, Geotextiles and Geomembranes 16 (1998) 257Ð271, Japan.

46. Buckley, John D. and Edie, Dan D. Carbon-Carbon Materials and Composites. Noyes Publications: Park Ridge, NJ. 1993.

47. Tomlinson, A. Heated Runways Using Electrically Conductive Asphalt. Superior Graphite Co. 1995.

48. Fitzgerald, R. L. Novel Applications of Carbon Fiber for Hot Mix Asphalt Reinforcement and Carbon-Carbon Pre-forms. M. S. Thesis, Michigan Technological University, 2000.

49. Kaloush, K., Biligiri, K., Zeiada, W., Rodezno, M., and Reed, J. Evaluation of Fiber-Reinforced Asphalt Mixtures Using Advanced Material Characterization Tests. Journal of Testing and Evaluation, Vol. 38, 2010.

50. Kaloush, K. Evaluation of Fiber-Reinforced Asphalt Mixtures Using Advanced Material Characterization Tests. Arizona State University,Department of Civil and Environmental Engineering PO Box 875306, Tempe, AZ 85287-5306.

51. Kaloush, K. l E. Report of Evaluation FORTA Fiber-Reinforced Asphalt Mixtures Using Advanced Material Characterization Tests. Evergreen Drive, Tempe, Arizona. Report # 200903AT101, 2008.

52. American Association of State Highway and Transportation Officials. Theoretical Maximum Specific Gravity of Bituminous Mixtures, Test Method AASHTO T 209 – 00, Standard Specifications for Transportation Materials and Methods of Sampling and Testing, Part II – Tests, Twentieth Edition, 2000.

53. Gravity of Bituminous Mixtures Using Saturated Surface Dry Specimens, Test Method AASHTO T 166 – 93, Standard Specifications for Transportation

Materials and Methods of Sampling and Testing, Part II – Tests, Twentieth Edition, 2000.

54. Roberts, Freddy, Kandhal, P. et. al. Hot Mix Asphalt Materials, Mixture Design, and Construction. 2nd ed. NAPA Research and Education Foundation, 1996.

55. ASTM Volume 04.03, Road and Paving Materials; Vehicle-Pavement Systems, 2009.

56. Kaloush, K., and at el, Final Report: Performance Evaluation of Asphalt Rubber Mixtures in Arizona – Lake HAVASU Project. Arizona State University Tempe, AZ, March, 2009.

57. Witczak, M. W., Kaloush, K. E., Pellinen, T., El-Basyouny, M., & Von Quintus, H. Simple Performance Test for Superpave Mix Design. NCHRP Report 465. Transportation Research Board. National Research Council. Washington D.C. 2002.

58. Kaloush, K. E., M. W. Witczak, G. B. Way, A. Zborowski, M. Abojaradeh, and A. Sotil. Performance Evaluation Of Arizona Asphalt Rubber Mixtures Using Advanced Dynamic Material Characterization Tests. Final Report. Arizona State University, Tempe, AZ, July 2002.

59. Sotil, A. Material Characterization of Asphalt Rubber Mixtures Using the Dynamic Modulus Test. Master of Science Thesis.Arizona State University, Tempe, AZ. May 2003.

60. Witczak, M. W., Kaloush, K. E., Pellinen, T., and Elbasyouny, M. NCHRP Report 465 Simple Performance Test for Superpave Mix Design.

61. Standard Test Method for Determining the Dynamic Modulus of Hot Mix Asphalt (HMA) Using, AASHTO TP62-03.

62. Shu, X., Huang, B., and Vukosavljevic, D. Laboratory Evaluation of Fatigue Characteristics of Recycled Asphalt Mixture. Department of Civil and Environmental Engineering, the University of Tennessee, Knoxville, TN 37996, USA, 2007.

63. Witczak, M.W., Roque, R., Hitunen, D.R., and Buttlar, W.G. Modification and Re-calibration of Superpave Thermal Cracking Model. Project Report, NCHRP 9-19 Superpave Support and Performance Models Management, Project Deliverable Task B, December 2000.

64. Roque et al. Standard Test Method for Determining the Creep Compliance and Strength of Hot Mix Asphalt (HMA) Using the Indirect Tensile Test Device. Draft Test Protocol, AASHTO TP9-02, 2002.

65. ASMT D 6931-07, Standard Test Method for the Indirect Tensile (IDT) Strength of Bituminous. American Society for Testing and Materials. Annual Book of ASTM Standards, 2010.

APPENDIX A

TABLES – FORTA FIBER DATA

TABLE 22 Summary of Penetration, Softening Point, and Viscosity Tests Results for A1

Penetration		**Softening Point**			**Viscosity**				
24 ^{0}C		Right Ring	Left Ring	Avg.	Temp. °F	2nd Min.	3rd Min.	4th Min.	Avg. cp
21.5	57.5	42	43.5	42.8	250	563	586	586	578
79									
230.5	54.5				300	210	187	211	203
285									
284	63				350	52	75	66	64
347									
13.5	65								
78.5									
62									

TABLE 23 Summary of Temperature -Viscosity Relationship Tests Results for A1

Temp. (ºF)	Log Temp (ºRankine)	Pen. (0.1 mm)	Viscosity (Poise)	Viscosity (cP)	Log Log Visc (cP)	Test
75.2	2.728	62	3.12E+06	3.12E+08	0.929	Penetration
108.95	2.755		1.30E+04	1.30E+06	0.786	Soft. Point
250	2.851			5.78E+02	0.441	Brookfield
300	2.881			2.03E+02	0.363	Brookfield
350	2.908			6.41E+01	0.257	Brookfield

TABLE 24 Summary of Penetration, Softening Point, and Viscosity Tests Results for A2

Penetration		**Softening Point**			**Viscosity**				
24 ^{0}C		Right Ring	Left Ring	Avg.	Temp. °**F**	2nd Min.	3rd Min.	4th Min.	Avg. cp
289 374	85	43.5	44.5	44	250	984	1008	1008	1000
158 214	56				300	234	258	258	250
158 216	58				350	94	117	117	109
69 118	49								
62									

TABLE 25 Summary of Temperature -Viscosity Relationship Tests Results for A2

Temp. (ºF)	Log Temp (ºRankine)	Pen. (0.1 mm)	Viscosity (Poise)	Viscosity (cP)	Log Log Visc (cP)	Test
75.2	2.728	62	2.90E+06	2.90E+08	0.928	Penetration
111.2	2.757		1.30E+04	1.30E+06	0.786	Soft. Point
200	2.819			4.93E+03	0.567	Brookfield
250	2.851			1.00E+03	0.477	Brookfield
300	2.881			2.50E+02	0.380	Brookfield
350	2.908			1.09E+02	0.309	Brookfield

TABLE 26 Summary of Penetration, Softening Point, and Viscosity Tests Results for A4

Penetration		**Softening Point**			**Viscosity**				
24 ^{0}C		Right Ring	Left Ring	Avg.	Temp. °F	2nd Min.	3rd Min.	4th Min.	Avg. cp
326	15	39	39.5	39.3	250	5228	7830	7865	6974
341									
257.5	33.5				300	3327	3163	3210	3233
291									
296	34				350	1117	1164	1141	1140
330									
330	40								
370									
62									

TABLE 27 Summary of Temperature -Viscosity Relationship Tests Results for A4

Temp. (ºF)	Log Temp (ºRankine)	Pen. (0.1 mm)	Viscosity (Poise)	Viscosity (cP)	Log Log Visc (cP)	Test
75.2	2.728	62	1.42E+07	1.42E+09	0.961	Penetration
102.65	2.750		1.30E+04	1.30E+06	0.786	Soft. Point
250	2.851			6.97E+03	0.585	Brookfield
300	2.881			3.23E+03	0.545	Brookfield
350	2.908			1.14E+03	0.485	Brookfield

TABLE 28 Summary of Penetration, Softening Point, and Viscosity Tests Results for A5

Penetration		**Softening Point**			**Viscosity**				
24 ^{0}C		Right Ring	Left Ring	Avg.	Temp. °F	2nd Min.	3rd Min.	4th Min.	Avg. cp
0	26	42	46	44	250	11271	12138	13420	12276
26									
26	38				300	6725	6397	6419	6513
64									
64	40				350	4874	4944	4851	4889
104									
160	35								
125									
34.75									

TABLE 29 Summary of Temperature -Viscosity Relationship Tests Results for A5

Temp. (ºF)	Log Temp (ºRankine)	Pen. (0.1 mm)	Viscosity (Poise)	Viscosity (cP)	Log Log Visc (cP)	Test
75.2	2.728	34.75	1.07E+07	1.07E+09	0.956	Penetration
111.2	2.757		1.30E+04	1.30E+06	0.786	Soft. Point
250	2.851			1.23E+04	0.612	Brookfield
300	2.881			6.51E+03	0.581	Brookfield
350	2.908			4.89E+03	0.567	Brookfield

TABLE 30 Summary of Penetration, Softening Point, and Viscosity Tests Results for A6

Penetration	**Softening Point**	**Viscosity**

24 ^{0}C		Right Ring	Left Ring	Avg.	Temp. °F	2nd Min.	3rd Min.	4th Min.	Avg. cp
392.5	59	44	46	45	250	6514	6608	6631	6584
333.5									
100	55				300	3351	3140	2788	3093
155									
230	40				350	2601	2855	2715	2724
270									
270	35								
305									
47.25									

TABLE 31 Summary of Temperature -Viscosity Relationship Tests Results for A6

Temp. (ºF)	Log Temp (ºRankine)	Pen. (0.1 mm)	Viscosity (Poise)	Viscosity (cP)	Log Log Visc (cP)	Test
75.2	2.728	47.25	5.34E+06	5.34E+08	0.941	Penetration
113	2.758		1.30E+04	1.30E+06	0.786	Soft. Point
200	2.819			1.88E+04	0.631	Brookfield
250	2.851			6.58E+03	0.582	Brookfield
300	2.881			3.09E+03	0.543	Brookfield
350	2.908			2.72E+03	0.536	Brookfield

TABLE 32 Summary of Penetration, Softening Point, and Viscosity Tests Results for A8

Penetration	**Softening Point**	**Viscosity**

24 ^{0}C		Right Ring	Left Ring	Avg.	Temp. °F	2nd Min.	3rd Min.	4th Min.	Avg. cp
291.5	24.5	48	52	50	250	28822	29035	31654	29837
316									
316	27				300	14606	15730	18640	16325
343									
340	36				350	6717	9607	12888	9737
376									
376	45.5								
421.5									
33.25									

TABLE 33 Summary of Temperature -Viscosity Relationship Tests Results for A8

Temp. (^{o}F)	Log Temp (^{o}Rankine)	Pen. (0.1 mm)	Viscosity (Poise)	Viscosity (cP)	Log Log Visc (cP)	Test
75.2	2.728	33.25	1.18E+07	1.18E+09	0.958	Penetration
122	2.765		1.30E+04	1.30E+06	0.786	Soft. Point
250	2.851			2.98E+04	0.651	Brookfield
300	2.881			1.63E+04	0.625	Brookfield
350	2.908			9.74E+03	0.601	Brookfield

TABLE 34 Summary of Penetration, Softening Point, and Viscosity Tests Results for A13

Penetration	**Softening Point**	**Viscosity**

24 ^{0}C		Right Ring	Left Ring	Avg.	Temp. °F	2nd Min.	3rd Min.	4th Min.	Avg. cp
288	42	53.5	51	52.3	250	3327	3374	3351	3351
330									
345	28				300	1523	1500	1476	1500
373									
2.5	41.5				350	750	726	680	719
44									
373	29.5								
402.5									
35.25									

TABLE 35 Summary of Temperature -Viscosity Relationship Tests Results for A13

Temp. (^{o}F)	Log Temp (^{o}Rankine)	Pen. (0.1 mm)	Viscosity (Poise)	Viscosity (cP)	Log Log Visc (cP)	Test
75.2	2.728	35.25	1.03E+07	1.03E+09	0.955	Penetration
126.05	2.768		1.30E+04	1.30E+06	0.786	Soft. Point
250	2.851			3.35E+03	0.547	Brookfield
300	2.881			1.50E+03	0.502	Brookfield
350	2.908			7.19E+02	0.456	Brookfield

TABLE 36 Summary of Penetration, Softening Point, and Viscosity Tests Results for A14

Penetration	**Softening Point**	**Viscosity**

24 ^{0}C		Right Ring	Left Ring	Avg.	Temp. °F	2nd Min.	3rd Min.	4th Min.	Avg. cp
341	48	47	50	48.5	250	15926	15208	17261	16132
389									
167	40				300	9328	9092	9473	9298
207									
207	36				350	4827	4804	4827	4820
243									
243	27								
270									
37.75									

TABLE 37 Summary of Temperature - Viscosity Relationship Tests Results for A14

Temp. (^{o}F)	Log Temp (^{o}Rankine)	Pen. (0.1 mm)	Viscosity (Poise)	Viscosity (cP)	Log Log Visc (cP)	Test
75.2	2.728	37.75	8.85E+06	8.85E+08	0.952	Penetration
119.3	2.763		1.30E+04	1.30E+06	0.786	Soft. Point
250	2.851			1.61E+04	0.624	Brookfield
300	2.881			9.30E+03	0.599	Brookfield
350	2.908			4.82E+03	0.566	Brookfield

TABLE 38 Summary of Penetration, Softening Point, and Viscosity Tests Results for A16

Penetration	**Softening Point**	**Viscosity**

24 ^{0}C		Right Ring	Left Ring	Avg.	Temp. °F	2nd Min.	3rd Min.	4th Min.	Avg. cp
265	38	48.5	51	49.8	250	16365	18467	18793	17875
303									
303	42				300	9303	6862	4241	6802
345									
345	13				350	1820	1773	1749	1781
358									
358	32								
390									
31.25									

TABLE 39 Summary of Temperature -Viscosity Relationship Tests Results for A16

Temp. (^{o}F)	Log Temp (^{o}Rankine)	Pen. (0.1 mm)	Viscosity (Poise)	Viscosity (cP)	Log Log Visc (cP)	Test
75.2	2.728	31.25	1.35E+07	1.35E+09	0.961	Penetration
121.55	2.764		1.30E+04	1.30E+06	0.786	Soft. Point
250	2.851			1.79E+04	0.629	Brookfield
300	2.881			6.80E+03	0.583	Brookfield
350	2.908			1.78E+03	0.512	Brookfield

TABLE 40 Summary of E* Values Based on the Average of Three Replicates for Control

(°F)	Frequency (Hz)	Dynamic Modulus E*					
		Rep. 1 (ksi)	Rep. 2 (ksi)	Rep. 3 (ksi)	Avg. (ksi)	Std. Dev.	Coeff. of Var.
40	25	2036	1760	1559	1785	240	13.4
	10	1914	1694	1486	1698	214	12.6
	5	1788	1560	1428	1592	182	11.4
	1	1399	1247	1208	1285	101	7.9
	0.5	1254	1154	1007	1138	124	10.9
	0.1	927	866	875	889	33	3.7
70	25	772	855	1003	877	117	13.4
	10	615	707	929	750	161	21.5
	5	513	616	750	626	119	19.0
	1	325	415	474	405	75	18.6
	0.5	262	350	381	331	62	18.6
	0.1	170	240	238	216	40	18.5
100	25	237	283	247	255	24	9.4
	10	169	205	168	180	21	11.7
	5	129	156	121	136	18	13.5
	1	70	87	66	74	11	14.9
	0.5	52	67	49	56	10	17.1
	0.1	32	44	30	35	8	21.3

TABLE 41 Summary of Phase Angle Values Based on the Average of Three Replicates for Control

Phase Angle, Φ							
40	25	12.6	8.1	16.8	12.5	4.4	35.1
	10	15.7	11.3	19.6	15.5	4.1	26.5
	5	17.7	13.2	21.3	17.4	4.1	23.4
	1	21.0	16.8	26.2	21.3	4.7	21.9
	0.5	22.4	18.6	29.1	23.3	5.3	22.6
	0.1	26.9	21.9	35.5	28.1	6.9	24.5
70	25	29.2	17.3	30.1	25.5	7.1	28.0
	10	29.4	23.7	32.8	28.6	4.6	16.0
	5	30.5	26.0	35.3	30.6	4.6	15.1
	1	34.9	29.3	40.2	34.8	5.5	15.7
	0.5	34.0	30.9	41.2	35.3	5.3	14.9
	0.1	36.3	36.0	42.7	38.3	3.8	9.9
100	25	35.0	29.9	40.9	35.3	5.5	15.5
	10	33.4	33.6	37.5	34.8	2.3	6.7
	5	35.1	35.7	35.3	35.4	0.3	1.0
	1	31.8	35.0	32.9	33.2	1.6	4.8
	0.5	31.1	34.0	30.4	31.8	1.9	6.0
	0.1	25.0	32.1	25.5	27.5	4.0	14.4

TABLE 42 Summary of E* Values Based on the Average of Three Replicates for (0 P, 1 A)

Temp. (°F)	Frequency (Hz)	Dynamic Modulus E*					
		Rep. 1 (ksi)	Rep. 2 (ksi)	Rep. 3 (ksi)	Avg. (ksi)	Std. Dev.	Coeff. of Var.
40	25	1732	1880	1751	1787	80	4.5
	10	1470	1611	1651	1577	95	6.0
	5	1293	1355	1524	1391	119	8.6
	1	1049	1113	1205	1122	78	7.0
	0.5	925	997	1017	980	48	4.9
	0.1	704	777	703	728	42	5.8
70	25	684	817	739	747	67	8.9
	10	542	585	566	564	21	3.8
	5	461	493	456	470	20	4.3
	1	320	392	306	339	46	13.6
	0.5	223	286	245	251	32	12.8
	0.1	129	178	146	151	25	16.6
100	25	197	246	195	213	29	13.5
	10	164	159	139	154	13	8.4
	5	117	117	109	115	5	4.0
	1	76	60	86	74	14	18.3
	0.5	54	49	65	56	8	15.0
	0.1	35	32	40	36	4	11.3

TABLE 43 Summary of Phase Angle Values Based on the Average of Three Replicates for (0 P, 1 A)

Phase Angle, Φ							
40	25	12.6	12.2	16.1	13.6	2.1	15.7
	10	15.4	16.2	19.1	16.9	1.9	11.4
	5	18.0	17.8	20.7	18.8	1.6	8.6
	1	22.0	20.8	24.7	22.5	2.0	8.9
	0.5	24.2	24.3	27.2	25.2	1.7	6.8
	0.1	30.8	30.2	32.6	31.2	1.2	4.0
70	25	25.1	25.5	28.8	26.4	2.0	7.6
	10	28.0	29.7	29.3	29.0	0.9	3.1
	5	29.4	33.4	29.4	30.7	2.3	7.6
	1	33.0	36.1	34.1	34.4	1.6	4.6
	0.5	33.6	39.6	34.8	36.0	3.2	8.8
	0.1	35.4	41.7	37.6	38.2	3.2	8.3
100	25	35.5	39.2	35.6	36.7	2.1	5.8
	10	34.8	38.3	32.9	35.3	2.7	7.7
	5	32.2	37.1	29.5	33.0	3.9	11.7
	1	27.5	35.0	25.1	29.2	5.2	17.7
	0.5	24.6	33.8	23.4	27.3	5.7	20.8
	0.1	23.3	32.1	17.6	24.3	7.3	29.9

TABLE 44 Summary of E* Values Based on the Average of Three Replicates for (0 P, 2 A)

Temp. (°F)	Frequency (Hz)	Dynamic Modulus E*					
		Rep. 1 (ksi)	Rep. 2 (ksi)	Rep. 3 (ksi)	Average (ksi)	Std. Dev.	Coeff. of Var.
40	25	1562	2396	1709	1889	445	23.6
	10	1466	2143	1577	1729	363	21.0
	5	1369	1924	1387	1560	315	20.2
	1	1098	1435	1101	1212	194	16.0
	0.5	986	1265	991	1080	160	14.8
	0.1	893	1019	921	944	67	7.1
70	25	895	908	673	825	132	16.0
	10	726	784	563	691	114	16.6
	5	620	585	485	563	70	12.5
	1	412	385	321	373	47	12.6
	0.5	341	293	262	299	40	13.3
	0.1	222	212	176	203	24	11.9
100	25	221	254	221	232	19	8.2
	10	153	178	157	163	14	8.4
	5	120	124	118	121	3	2.6
	1	79	77	86	81	4	5.5
	0.5	56	59	57	57	1	2.3
	0.1	40	38	40	40	1	2.2

TABLE 45 Summary of Phase Angle Values Based on the Average of Three Replicates for (0 P, 2 A)

Phase Angle, Φ							
40	25	16.9	13.9	13.5	14.7	1.9	12.6
	10	19.0	18.9	18.6	18.8	0.2	1.2
	5	23.2	20.1	22.4	21.9	1.6	7.3
	1	24.6	23.6	26.8	25.0	1.6	6.5
	0.5	25.9	25.1	27.9	26.3	1.4	5.4
	0.1	29.7	30.5	40.4	33.5	6.0	17.8
70	25	26.9	31.0	22.7	26.9	4.1	15.4
	10	28.2	35.0	26.1	29.8	4.7	15.7
	5	29.9	36.3	28.7	31.6	4.1	13.1
	1	35.0	39.1	33.3	35.8	3.0	8.3
	0.5	37.4	39.4	34.7	37.2	2.4	6.4
	0.1	41.2	42.5	36.7	40.1	3.1	7.6
100	25	38.7	39.7	35.1	37.8	2.4	6.4
	10	38.4	38.1	32.6	36.3	3.2	8.9
	5	37.0	37.6	31.6	35.4	3.3	9.4
	1	33.6	32.4	31.9	32.6	0.9	2.6
	0.5	30.4	28.3	29.8	29.5	1.1	3.7
	0.1	24.3	22.7	27.8	24.9	2.6	10.4

TABLE 46 Summary of E* Values Based on the Average of Three Replicates for (0 P, 3 A)

Temp. (°F)	Frequency (Hz)	Dynamic Modulus E*					
		Rep. 1 (ksi)	Rep. 2 (ksi)	Rep. 3 (ksi)	Avg. (ksi)	Std. Dev.	Coeff. of Var.
40	25	2297	1868	1804	1990	268	13.5
	10	2040	1704	1602	1782	229	12.9
	5	1868	1573	1461	1634	210	12.9
	1	1440	1211	1102	1251	172	13.8
	0.5	1274	1079	974	1109	152	13.7
	0.1	931	792	712	811	111	13.6
70	25	920	852	735	836	94	11.2
	10	757	701	588	682	86	12.6
	5	471	608	499	526	72	13.7
	1	329	366	322	339	24	7.0
	0.5	251	305	270	276	27	9.9
	0.1	173	196	177	182	12	6.8
100	25	192	252	207	217	31	14.3
	10	134	186	144	155	27	17.7
	5	101	145	109	118	23	19.9
	1	77	73	69	73	4	5.7
	0.5	54	57	63	58	5	8.0
	0.1	37	41	41	39	3	6.5

TABLE 47 Summary of Phase Angle Values Based on the Average of Three Replicates for (0 P, 3 A)

Phase Angle, Φ							
40	25	14.9	12.1	12.4	13.1	1.5	11.6
	10	20.1	16.0	15.8	17.3	2.5	14.2
	5	22.6	17.9	18.2	19.6	2.6	13.4
	1	27.0	22.4	22.1	23.8	2.8	11.6
	0.5	29.2	25.5	24.5	26.4	2.5	9.4
	0.1	33.9	30.4	30.6	31.6	2.0	6.3
70	25	24.1	24.2	29.0	25.8	2.8	10.9
	10	26.8	29.1	32.3	29.4	2.8	9.4
	5	28.5	30.2	32.7	30.4	2.1	6.9
	1	34.3	38.3	37.8	36.8	2.2	5.9
	0.5	35.4	39.1	40.2	38.2	2.5	6.6
	0.1	37.9	40.0	43.9	40.6	3.1	7.5
100	25	35.1	37.3	37.1	36.5	1.2	3.3
	10	33.6	38.0	37.4	36.3	2.4	6.5
	5	34.9	37.8	35.5	36.0	1.5	4.2
	1	32.4	34.8	34.1	33.8	1.2	3.7
	0.5	31.6	33.7	34.9	33.4	1.7	5.0
	0.1	26.3	28.4	27.4	27.4	1.0	3.8

TABLE 48 Summary of E* Values Based on the Average of Three Replicates for (1 P, 0 A)

Temp. (°F)	Frequency (Hz)	Dynamic Modulus E*					
		Rep. 1 (ksi)	Rep. 2 (ksi)	Rep. 3 (ksi)	Avg. (ksi)	Std. Dev.	Coeff. of Var.
40	25	1875	2041	2295	2070	211	10.2
	10	1646	1882	2127	1885	240	12.8
	5	1497	1719	1957	1724	230	13.3
	1	1156	1312	1608	1359	230	16.9
	0.5	1033	1155	1413	1200	194	16.2
	0.1	865	855	1152	957	169	17.6
70	25	856	775	842	824	43	5.3
	10	690	600	684	658	50	7.6
	5	532	503	581	539	39	7.3
	1	353	307	357	339	28	8.2
	0.5	291	249	292	277	25	8.9
	0.1	221	155	182	186	33	17.8
100	25	234	206	239	226	18	7.8
	10	150	150	169	157	11	7.0
	5	122	118	130	123	6	5.0
	1	85	79	71	78	7	9.1
	0.5	66	64	55	62	6	10.0
	0.1	51	50	36	45	8	18.0

TABLE 49 Summary of Phase Angle Values Based on the Average of Three Replicates for (1 P, 0 A)

Phase Angle, Φ							
40	25	12.6	15.0	11.0	12.9	2.0	15.7
	10	15.4	18.0	12.2	15.2	2.9	18.9
	5	17.9	19.2	13.5	16.9	3.0	17.7
	1	20.7	23.1	17.7	20.5	2.7	13.2
	0.5	21.9	25.5	19.4	22.3	3.1	13.8
	0.1	24.9	34.0	24.5	27.8	5.4	19.3
70	25	24.3	28.3	30.6	27.7	3.2	11.5
	10	26.2	30.5	32.9	29.9	3.4	11.4
	5	27.8	32.5	33.1	31.2	2.9	9.3
	1	33.5	36.6	37.5	35.9	2.1	5.9
	0.5	34.8	36.7	38.6	36.7	1.9	5.2
	0.1	40.5	36.9	38.6	38.7	1.8	4.7
100	25	36.1	40.5	38.8	38.5	2.2	5.7
	10	35.6	40.1	36.1	37.3	2.4	6.5
	5	36.7	39.4	33.6	36.6	2.9	8.0
	1	32.7	33.9	32.0	32.9	0.9	2.9
	0.5	31.9	33.2	29.8	31.6	1.7	5.4
	0.1	25.1	26.0	24.9	25.3	0.6	2.3

TABLE 50 Summary of E* Values Based on the Average of Three Replicates for (1 P, 1 A)

Temp. (°F)	Frequency (Hz)	Dynamic Modulus E*					
		Rep. 1 (ksi)	Rep. 2 (ksi)	Rep. 3 (ksi)	Average (ksi)	Std. Dev.	Coeff. of Var.
40	25	1841	1978	2242	2021	204	10.1
	10	1671	1691	2023	1795	198	11.0
	5	1520	1540	1837	1632	178	10.9
	1	1129	1096	1418	1214	177	14.6
	0.5	1015	988	1233	1079	135	12.5
	0.1	732	735	901	789	97	12.3
70	25	741	804	908	818	84	10.3
	10	618	682	709	670	47	7.0
	5	530	585	588	567	32	5.7
	1	328	363	387	359	29	8.1
	0.5	270	320	318	303	28	9.4
	0.1	174	224	208	202	25	12.5
100	25	308	316	247	291	38	13.0
	10	209	227	180	205	24	11.6
	5	160	179	144	161	18	11.0
	1	109	112	84	101	15	15.3
	0.5	81	88	65	78	12	15.3
	0.1	60	57	39	52	12	22.3

TABLE 51 Summary of Phase Angle Values Based on the Average of Three Replicates for (1 P, 1 A)

Phase Angle, Φ							
40	25	12.5	12.0	9.5	11.3	1.6	14.1
	10	19.6	16.7	13.8	16.7	2.9	17.5
	5	22.5	17.9	16.4	18.9	3.2	16.8
	1	25.8	25.0	21.1	24.0	2.5	10.4
	0.5	28.1	26.6	22.3	25.6	3.0	11.7
	0.1	29.8	30.4	32.4	30.9	1.4	4.5
70	25	23.0	25.3	26.2	24.8	1.7	6.7
	10	27.0	30.2	27.5	28.2	1.7	6.1
	5	31.0	30.7	28.5	30.1	1.4	4.6
	1	36.9	38.2	34.5	36.5	1.9	5.2
	0.5	37.9	40.4	35.1	37.8	2.6	7.0
	0.1	39.4	41.7	40.0	40.4	1.2	2.9
100	25	38.1	31.1	36.9	35.4	3.7	10.5
	10	36.3	30.7	32.8	33.3	2.8	8.4
	5	38.3	30.8	34.9	34.7	3.7	10.8
	1	34.1	28.7	33.2	32.0	2.9	8.9
	0.5	32.7	25.8	32.4	30.3	3.9	12.9
	0.1	27.3	23.4	30.2	27.0	3.4	12.6

TABLE 52 Summary of E* Values Based on the Average of Three Replicates for (1 P, 2 A)

Temp. (°F)	Frequency (Hz)	Dynamic Modulus E*					
		Rep. 1 (ksi)	Rep. 2 (ksi)	Rep. 3 (ksi)	Avg. (ksi)	Std. Dev.	Coeff. of Var.
40	25	2131	2325	2161	2206	104	4.7
	10	1919	2139	1887	1982	137	6.9
	5	1777	1873	1674	1775	99	5.6
	1	1428	1694	1340	1487	184	12.4
	0.5	1276	1471	1202	1316	139	10.6
	0.1	950	1009	897	952	56	5.9
70	25	985	902	888	925	52	5.7
	10	782	730	727	746	31	4.2
	5	677	621	631	643	30	4.6
	1	429	372	425	409	32	7.9
	0.5	362	297	358	339	36	10.8
	0.1	231	252	241	241	11	4.4
100	25	325	317	309	317	8	2.6
	10	215	246	220	227	17	7.3
	5	167	213	174	185	25	13.6
	1	87	101	96	95	7	7.5
	0.5	79	80	82	81	2	1.9
	0.1	61	59	55	58	3	5.1

TABLE 53 Summary of Phase Angle Values Based on the Average of Three Replicates for (1 P, 2 A)

Phase Angle, Φ							
40	25	10.7	13.2	10.9	11.6	1.4	12.2
	10	15.6	17.7	13.9	15.7	1.9	12.1
	5	16.8	20.1	15.2	17.4	2.5	14.2
	1	19.7	24.1	18.7	20.9	2.9	13.8
	0.5	22.1	25.8	20.6	22.8	2.7	11.7
	0.1	26.9	30.0	23.8	26.9	3.1	11.6
70	25	26.7	25.4	21.3	24.5	2.8	11.5
	10	30.7	29.3	24.5	28.2	3.3	11.6
	5	31.6	30.8	27.9	30.1	2.0	6.5
	1	38.2	34.8	33.7	35.6	2.4	6.6
	0.5	38.5	34.8	35.5	36.3	2.0	5.4
	0.1	42.8	35.3	39.6	39.2	3.8	9.6
100	25	41.5	37.8	30.9	36.7	5.4	14.7
	10	40.0	35.5	33.3	36.3	3.4	9.4
	5	37.8	31.1	31.0	33.3	3.9	11.7
	1	35.0	25.5	36.5	32.3	5.9	18.3
	0.5	32.0	24.5	35.5	30.7	5.6	18.2
	0.1	27.8	22.5	34.2	28.2	5.9	20.8

TABLE 54 Summary of E* Values Based on the Average of Three Replicates for (1 P, 3 A)

Temp. (°F)	Frequency (Hz)	Dynamic Modulus E*					
		Rep. 1 (ksi)	Rep. 2 (ksi)	Rep. 3 (ksi)	Average (ksi)	Std. Dev.	Coeff. of Var.
40	25	2336	2062	2032	2144	167	7.8
	10	2199	1791	1865	1952	217	11.1
	5	1976	1602	1756	1778	188	10.6
	1	1498	1183	1325	1335	157	11.8
	0.5	1321	1032	1140	1164	146	12.5
	0.1	957	725	857	846	116	13.7
70	25	1159	1415	1081	1218	175	14.3
	10	910	1126	984	1007	110	10.9
	5	779	930	822	843	78	9.2
	1	494	587	509	530	50	9.4
	0.5	408	479	433	440	36	8.1
	0.1	255	284	253	264	17	6.6
100	25	309	324	304	312	10	3.2
	10	250	222	240	237	14	5.8
	5	201	166	193	187	19	10.0
	1	110	90	108	103	11	10.9
	0.5	78	71	72	74	4	5.1
	0.1	57	56	55	56	1	1.9

TABLE 55 Summary of Phase Angle Values Based on the Average of Three Replicates for (1 P, 3 A)

Phase Angle, Φ							
40	25	11.4	13.5	11.8	12.3	1.1	9.2
	10	16.1	18.0	18.8	17.6	1.4	7.8
	5	17.8	20.6	19.8	19.4	1.4	7.5
	1	21.2	24.5	23.9	23.2	1.7	7.5
	0.5	22.8	25.5	25.9	24.8	1.7	6.8
	0.1	27.7	30.0	30.0	29.2	1.4	4.6
70	25	25.9	21.1	19.2	22.0	3.4	15.7
	10	28.4	25.7	26.7	26.9	1.4	5.0
	5	30.0	27.7	29.4	29.0	1.2	4.2
	1	32.4	32.3	32.4	32.4	0.1	0.3
	0.5	33.7	33.1	36.2	34.3	1.6	4.7
	0.1	34.8	35.1	39.1	36.3	2.4	6.6
100	25	39.1	39.0	32.9	37.0	3.5	9.5
	10	37.3	35.8	31.9	35.0	2.8	8.0
	5	33.9	33.2	32.2	33.1	0.9	2.6
	1	28.4	29.4	28.4	28.7	0.5	1.8
	0.5	25.2	27.7	25.8	26.2	1.3	4.9
	0.1	24.8	20.7	19.7	21.7	2.7	12.5

TABLE 56 Summary of E* Values Based on the Average of Three Replicates for (2 P, 0 A)

Temp. (°F)	Frequency (Hz)	Dynamic Modulus E*					
		Rep. 1 (ksi)	Rep. 2 (ksi)	Rep. 3 (ksi)	Average (ksi)	Std. Dev.	Coeff. of Var.
40	25	2518	2856	2015	2463	423	17.2
	10	2377	2544	1796	2239	393	17.5
	5	2163	2328	1647	2046	355	17.3
	1	1721	1794	1430	1648	193	11.7
	0.5	1563	1603	1231	1466	205	14.0
	0.1	1199	1199	964	1121	135	12.1
70	25	1054	1203	1007	1088	103	9.4
	10	888	955	799	881	79	8.9
	5	765	779	657	734	67	9.1
	1	504	473	398	458	55	11.9
	0.5	422	372	328	374	47	12.6
	0.1	278	222	215	238	35	14.6
100	25	397	314	277	329	62	18.8
	10	285	246	189	240	48	20.2
	5	215	184	141	180	37	20.7
	1	103	90	77	90	13	14.7
	0.5	74	68	57	66	8	12.8
	0.1	48	51	47	49	2	5.0

TABLE 57 Summary of Phase Angle Values Based on the Average of Three Replicates for (2 P, 0 A)

Phase Angle, Φ							
40	25	9.6	10.0	11.2	10.3	0.8	8.0
	10	14.6	15.6	14.1	14.8	0.7	5.0
	5	16.9	17.2	16.0	16.7	0.6	3.6
	1	20.2	21.8	21.9	21.3	1.0	4.5
	0.5	21.9	22.7	24.3	23.0	1.2	5.3
	0.1	26.9	28.8	29.7	28.5	1.5	5.1
70	25	19.8	25.6	26.3	23.9	3.6	14.9
	10	24.0	29.2	28.6	27.2	2.8	10.4
	5	26.2	28.9	31.0	28.7	2.4	8.4
	1	30.9	33.9	34.7	33.2	2.0	6.0
	0.5	32.5	34.1	34.7	33.8	1.1	3.3
	0.1	36.4	33.3	32.1	33.9	2.2	6.4
100	25	33.4	40.0	39.7	37.7	3.7	9.9
	10	33.9	38.9	36.5	36.5	2.5	6.9
	5	30.3	35.9	34.9	33.7	3.0	8.8
	1	28.5	32.2	30.7	30.5	1.9	6.1
	0.5	28.6	30.8	30.7	30.0	1.2	4.0
	0.1	24.4	23.0	25.7	24.3	1.4	5.6

TABLE 58 Summary of E* Values Based on the Average of Three Replicates for (2 P, 1 A)

Temp. (°F)	Frequency (Hz)	Dynamic Modulus E*					
		Rep. 1 (ksi)	Rep. 2 (ksi)	Rep. 3 (ksi)	Average (ksi)	Std. Dev.	Coeff. Of Var.
40	25	2150	2394	1772	2105	314	14.9
	10	1826	2244	1531	1867	358	19.2
	5	1615	1989	1366	1656	314	18.9
	1	1220	1443	1022	1228	211	17.1
	0.5	1068	1267	897	1078	185	17.2
	0.1	753	817	644	738	87	11.8
70	25	846	752	678	759	84	11.1
	10	662	607	583	618	40	6.5
	5	546	505	502	518	25	4.8
	1	346	324	323	331	13	4.0
	0.5	284	266	272	274	9	3.4
	0.1	177	175	184	179	5	2.6
100	25	277	254	220	250	29	11.5
	10	211	161	181	185	25	13.6
	5	158	131	146	145	14	9.6
	1	93	87	97	92	5	5.1
	0.5	73	75	77	75	2	2.9
	0.1	52	50	59	54	4	8.3

TABLE 59 Summary of Phase Angle Values Based on the Average of Three Replicates for (2 P, 1 A)

Phase Angle, Φ							
40	25	11.5	10.7	11.4	11.2	0.4	4.0
	10	14.8	14.7	15.5	15.0	0.4	2.7
	5	16.9	16.0	19.5	17.5	1.8	10.5
	1	20.5	22.7	22.8	22.0	1.3	6.0
	0.5	22.5	24.5	23.2	23.4	1.0	4.4
	0.1	26.5	29.2	28.0	27.9	1.3	4.7
70	25	26.0	23.2	26.2	25.1	1.7	6.7
	10	27.7	26.2	31.1	28.4	2.5	8.9
	5	29.1	27.1	32.9	29.7	2.9	9.8
	1	35.1	32.3	37.8	35.1	2.8	7.9
	0.5	36.4	32.6	40.1	36.3	3.7	10.3
	0.1	39.7	34.9	45.0	39.9	5.1	12.7
100	25	38.6	35.4	45.7	39.9	5.3	13.2
	10	37.5	34.8	43.5	38.6	4.5	11.6
	5	36.9	34.0	43.3	38.1	4.8	12.5
	1	34.9	33.4	41.6	36.6	4.4	12.0
	0.5	33.7	30.1	41.7	35.2	5.9	16.9
	0.1	29.7	26.1	34.8	30.2	4.4	14.6

TABLE 60 Summary of E* Values Based on the Average of Three Replicates for (2 P, 2 A)

Temp. (°F)	Frequency (Hz)	Dynamic Modulus E*					
		Rep. 1 (ksi)	Rep. 2 (ksi)	Rep.3 (ksi)	Average (ksi)	Std. Dev.	Coeff. of Var.
40	25	2528	2276	2131	2312	201	8.7
	10	2158	1954	1752	1955	203	10.4
	5	1969	1773	1593	1778	188	10.6
	1	1472	1339	1249	1353	112	8.3
	0.5	1307	1173	1134	1205	91	7.6
	0.1	943	826	872	880	59	6.7
70	25	1009	1090	1039	1046	41	3.9
	10	923	878	905	902	23	2.5
	5	697	756	784	746	44	5.9
	1	511	488	535	511	24	4.7
	0.5	387	391	454	411	38	9.2
	0.1	297	310	284	297	13	4.5
100	25	288	324	349	320	31	9.5
	10	216	233	258	236	21	8.9
	5	168	177	198	181	15	8.3
	1	115	109	113	113	3	2.7
	0.5	87	91	88	89	2	2.6
	0.1	62	62	56	60	3	5.6

TABLE 61 Summary of Phase Angle Values Based on the Average of Three Replicates for (2 P, 2 A)

Phase Angle, Φ							
40	25	13.2	12.3	11.3	12.3	0.9	7.5
	10	18.3	16.2	13.5	16.0	2.4	15.0
	5	19.7	18.2	16.0	18.0	1.8	10.2
	1	23.1	21.8	19.2	21.4	2.0	9.2
	0.5	24.5	24.1	20.2	22.9	2.4	10.4
	0.1	27.1	28.6	24.8	26.8	1.9	7.0
70	25	27.5	30.6	18.9	25.7	6.0	23.5
	10	30.9	31.0	22.5	28.1	4.9	17.5
	5	31.8	31.7	25.2	29.5	3.8	12.8
	1	36.3	33.7	33.0	34.3	1.8	5.1
	0.5	35.9	33.5	33.1	34.2	1.5	4.5
	0.1	36.8	32.6	36.7	35.4	2.4	6.8
100	25	37.9	34.3	31.1	34.5	3.4	9.9
	10	34.6	33.0	31.4	33.0	1.6	5.0
	5	33.1	32.3	31.3	32.2	0.9	2.8
	1	29.4	27.4	31.0	29.3	1.8	6.1
	0.5	28.1	26.6	28.7	27.8	1.1	3.8
	0.1	22.9	22.8	24.4	23.4	0.9	3.7

TABLE 62 Summary of E* Values Based on the Average of Three Replicates for (2 P, 3 A)

Temp. (°F)	Frequency (Hz)	Dynamic Modulus E*					
		Rep. 1 (ksi)	Rep. 2 (ksi)	Rep .3 (ksi)	Average (ksi)	Std. Dev.	Coeff. of Var.
40	25	2578	3460	2507	2848	531	18.6
	10	2353	3012	2264	2543	409	16.1
	5	2176	2746	2053	2325	370	15.9
	1	1868	2122	1578	1856	272	14.7
	0.5	1489	1887	1372	1583	270	17.1
	0.1	1100	1392	978	1157	213	18.4
70	25	1222	1099	1277	1199	91	7.6
	10	1126	922	998	1015	103	10.2
	5	949	780	885	871	85	9.8
	1	672	549	631	617	62	10.1
	0.5	534	417	486	479	59	12.3
	0.1	376	312	333	340	33	9.6
100	25	361	285	299	315	40	12.8
	10	267	201	203	224	37	16.6
	5	204	153	148	168	31	18.2
	1	123	93	95	104	17	15.9
	0.5	101	73	78	84	15	17.7
	0.1	71	43	69	61	15	25.3

TABLE 63 Summary of Phase Angle Values Based on the Average of Three Replicates for (2 P, 3 A)

Phase Angle, Φ							
40	25	13.8	9.8	12.5	12.0	2.1	17.1
	10	17.8	14.6	15.7	16.0	1.6	10.0
	5	19.9	16.0	17.9	17.9	1.9	10.8
	1	22.6	21.2	22.2	22.0	0.8	3.5
	0.5	24.2	24.0	24.4	24.2	0.2	0.8
	0.1	29.1	30.5	31.8	30.5	1.4	4.5
70	25	25.7	25.2	25.0	25.3	0.4	1.5
	10	32.1	28.5	29.8	30.1	1.8	6.0
	5	33.1	29.6	30.6	31.1	1.8	5.8
	1	38.0	35.0	36.5	36.5	1.5	4.2
	0.5	38.8	36.6	37.5	37.6	1.1	2.9
	0.1	41.1	41.2	39.6	40.7	0.9	2.2
100	25	36.5	36.5	42.2	38.4	3.3	8.5
	10	36.9	35.1	44.4	38.8	4.9	12.7
	5	36.1	34.5	40.6	37.1	3.2	8.5
	1	32.4	31.2	37.0	33.5	3.1	9.2
	0.5	29.9	29.5	35.5	31.7	3.4	10.7
	0.1	26.0	26.1	27.8	26.6	1.0	3.8

TABLE 64 Summary of E* Values Based on the Average of Three Replicates for (3 P, 0 A)

Temp. (°F)	Frequency (Hz)	Dynamic Modulus E*					
		Rep. 1 (ksi)	Rep. 2 (ksi)	Rep.3 (ksi)	Average (ksi)	Std. Dev.	Coeff. of Var.
40	25	2518	2770	3362	2884	434	15.0
	10	2377	2222	2665	2421	225	9.3
	5	2163	2010	2314	2163	152	7.0
	1	1721	1572	1682	1658	77	4.7
	0.5	1563	1406	1432	1467	84	5.7
	0.1	1199	1028	999	1075	108	10.1
70	25	1054	1157	807	1006	180	17.9
	10	845	790	657	764	97	12.7
	5	725	636	540	634	92	14.6
	1	515	390	325	410	96	23.5
	0.5	385	309	259	318	63	20.0
	0.1	266	198	161	209	53	25.5
100	25	367	442	241	350	102	29.0
	10	242	307	198	249	55	21.9
	5	195	219	148	187	36	19.4
	1	123	111	98	111	12	11.1
	0.5	86	76	76	79	5	6.8
	0.1	67	58	58	61	5	8.6

TABLE 65 Summary of Phase Angle Values Based on the Average of Three Replicates for (3 P, 0 A)

Phase Angle, Φ							
40	25	9.6	11.3	17.9	12.9	4.4	34.0
	10	14.6	13.9	21.5	16.7	4.2	25.3
	5	16.9	15.9	22.9	18.5	3.8	20.2
	1	20.2	20.5	25.6	22.1	3.0	13.7
	0.5	21.9	23.2	26.9	24.0	2.6	10.7
	0.1	26.9	29.2	31.4	29.2	2.3	7.8
70	25	19.8	26.7	27.3	24.6	4.1	16.9
	10	24.0	29.3	31.8	28.4	4.0	14.1
	5	26.2	30.4	32.3	29.6	3.1	10.6
	1	30.9	36.3	35.0	34.1	2.8	8.3
	0.5	32.5	38.6	36.0	35.7	3.1	8.6
	0.1	36.4	39.3	35.3	37.0	2.1	5.6
100	25	33.4	39.3	46.0	39.6	6.3	15.9
	10	33.9	36.4	38.2	36.2	2.1	5.9
	5	30.3	36.9	37.6	34.9	4.0	11.6
	1	28.5	32.8	34.5	31.9	3.1	9.8
	0.5	28.6	31.0	33.9	31.2	2.7	8.5
	0.1	24.4	24.0	28.7	25.7	2.6	10.2

TABLE 66 Summary of E* Values Based on the Average of Three Replicates for (3 P, 1 A)

Temp. (°F)	Frequency (Hz)	Dynamic Modulus E*					
		Rep. 1 (ksi)	Rep. 2 (ksi)	Rep. 3 (ksi)	Average (ksi)	Std. Dev.	Coeff. of Var.
40	25	3059	2594	3126	2926	290	9.9
	10	2654	2344	2742	2580	209	8.1
	5	2447	2139	2480	2355	188	8.0
	1	2018	1643	1924	1861	195	10.5
	0.5	1709	1417	1712	1613	169	10.5
	0.1	1265	1217	1376	1286	82	6.4
70	25	1147	1074	1235	1152	81	7.0
	10	956	867	956	927	51	5.5
	5	776	731	751	752	22	3.0
	1	580	530	537	549	27	5.0
	0.5	465	426	420	437	25	5.6
	0.1	347	325	338	337	11	3.2
100	25	337	331	339	335	4	1.2
	10	234	235	239	236	3	1.1
	5	159	162	160	160	1	0.8
	1	100	99	99	99	1	0.7
	0.5	82	83	82	82	0	0.5
	0.1	72	66	67	68	4	5.1

TABLE 67 Summary of Phase Angle Values Based on the Average of Three Replicates for (3 P, 1 A)

Phase Angle, Φ							
40	25	13.7	10.7	12.4	12.2	1.5	12.3
	10	16.7	14.7	14.9	15.4	1.1	7.0
	5	18.7	16.0	17.9	17.5	1.4	8.1
	1	23.1	22.7	21.9	22.6	0.6	2.6
	0.5	26.1	24.5	24.2	24.9	1.0	4.0
	0.1	32.6	29.2	29.1	30.3	2.0	6.6
70	25	24.9	23.2	30.6	26.2	3.9	14.8
	10	27.2	26.2	31.2	28.2	2.6	9.4
	5	29.9	27.1	33.6	30.2	3.3	10.8
	1	33.7	32.3	39.4	35.1	3.7	10.7
	0.5	33.6	32.6	40.9	35.7	4.6	12.8
	0.1	32.1	34.9	41.1	36.0	4.6	12.7
100	25	43.9	46.9	40.2	43.7	3.4	7.7
	10	40.8	41.0	37.9	39.9	1.8	4.4
	5	39.0	37.8	36.5	37.8	1.2	3.3
	1	31.4	32.8	33.0	32.4	0.9	2.7
	0.5	28.1	30.7	29.9	29.6	1.4	4.6
	0.1	22.1	24.3	24.4	23.6	1.3	5.5

TABLE 68 Summary of E* Values Based on the Average of Three Replicates for (3 P, 2 A)

Temp. (°F)	Frequency (Hz)	Dynamic Modulus E*					
		Rep. 1 (ksi)	Rep. 2 (ksi)	Rep.3 (ksi)	Average (ksi)	Std. Dev.	Coeff. of Var.
40	25	3193	2891	2501	2862	347	12.1
	10	2989	2489	2337	2605	341	13.1
	5	2704	2260	2136	2367	298	12.6
	1	2272	1627	1614	1838	376	20.5
	0.5	1944	1451	1435	1610	290	18.0
	0.1	1470	1030	995	1165	265	22.7
70	25	1097	1111	1091	1100	10	0.9
	10	920	960	939	939	20	2.1
	5	773	797	710	760	45	5.9
	1	446	569	469	495	66	13.2
	0.5	369	447	399	405	40	9.8
	0.1	226	290	231	249	36	14.4
100	25	251	309	244	268	36	13.4
	10	197	235	191	208	24	11.5
	5	159	186	138	161	24	14.9
	1	90	91	93	91	1	1.5
	0.5	69	75	72	72	3	4.2
	0.1	53	59	57	57	3	5.4

TABLE 69 Summary of Phase Angle Values Based on the Average of Three Replicates for (3 P, 2A)

Phase Angle, Φ							
40	25	10.8	11.2	16.3	12.8	3.1	24.0
	10	16.3	15.9	19.3	17.2	1.9	10.9
	5	17.7	18.3	20.8	18.9	1.6	8.7
	1	19.5	24.1	24.5	22.7	2.8	12.4
	0.5	21.2	24.8	26.8	24.3	2.8	11.7
	0.1	26.8	31.2	31.7	29.9	2.7	9.0
70	25	30.5	22.8	28.9	27.4	4.0	14.7
	10	33.3	25.2	30.7	29.7	4.1	13.9
	5	35.5	27.1	32.1	31.6	4.3	13.5
	1	38.0	33.6	36.9	36.1	2.3	6.4
	0.5	39.0	35.4	37.9	37.4	1.8	4.9
	0.1	38.6	38.8	38.8	38.7	0.1	0.3
100	25	38.8	30.8	38.3	36.0	4.5	12.5
	10	35.7	31.1	37.4	34.7	3.3	9.5
	5	35.6	28.4	37.3	33.7	4.7	14.0
	1	30.9	25.2	34.8	30.3	4.8	16.0
	0.5	28.6	20.2	32.9	27.2	6.5	23.8
	0.1	23.7	18.6	30.5	24.3	6.0	24.6

TABLE 70 Summary of E* Values Based on the Average of Three Replicates for (3 P, 3 A)

Temp. (°F)	Frequency (Hz)	Dynamic Modulus E*					
		Rep. 1 (ksi)	Rep. 2 (ksi)	Rep. 3 (ksi)	Average (ksi)	Std. Dev.	Coeff. of Var.
40	25	3303	3254	2721	3093	323	10.4
	10	3188	2848	2480	2839	354	12.5
	5	2951	2565	2290	2602	332	12.7
	1	2363	1971	1789	2041	293	14.4
	0.5	2135	1747	1593	1825	279	15.3
	0.1	1595	1253	1074	1307	265	20.3
70	25	1242	1124	1166	1177	60	5.1
	10	1122	955	841	973	141	14.5
	5	922	814	704	813	109	13.4
	1	496	525	433	485	47	9.7
	0.5	418	427	356	400	39	9.7
	0.1	276	272	217	255	33	13.0
100	25	328	304	272	301	28	9.3
	10	270	224	218	237	28	11.9
	5	198	170	173	180	16	8.6
	1	115	101	102	106	8	7.2
	0.5	81	80	74	78	4	5.1
	0.1	61	61	59	60	1	2.0

TABLE 71 Summary of Phase Angle Values Based on the Average of Three Replicates for (3 P, 3 A)

Phase Angle, Φ							
40	25	10.8	11.0	11.0	10.9	0.1	0.9
	10	16.3	15.1	13.3	14.9	1.5	10.3
	5	17.7	16.2	15.1	16.3	1.3	7.8
	1	19.5	20.9	20.4	20.2	0.7	3.5
	0.5	21.2	23.7	22.5	22.5	1.2	5.4
	0.1	26.8	29.7	29.3	28.6	1.6	5.5
70	25	30.5	25.5	24.1	26.7	3.3	12.5
	10	33.3	28.8	28.5	30.2	2.7	8.8
	5	35.5	30.5	30.2	32.1	3.0	9.4
	1	38.0	36.9	34.4	36.4	1.8	5.1
	0.5	39.0	37.9	35.3	37.4	1.9	5.1
	0.1	38.6	40.5	36.2	38.4	2.1	5.6
100	25	38.8	34.9	32.4	35.4	3.2	9.1
	10	35.7	35.0	36.4	35.7	0.7	2.0
	5	35.6	35.1	36.3	35.6	0.6	1.8
	1	30.9	31.4	35.5	32.6	2.5	7.8
	0.5	28.6	28.5	30.5	29.2	1.1	3.8
	0.1	23.7	24.6	30.0	26.1	3.4	12.9

TABLE 72 Summary of Maximum Tensile Strength Values Based on the Average of Three Replicates

Tensile Strength					
Mixture Type	**Temperature**	**Replicate 1**	**Replicate 2**	**Replicate 3**	**Average**
Control	40	1901.2	1937.9	1953.3	1930.8
	70	610.1	624.8	677.3	637.4
	100	876.4	917.3	918.6	904.1
0 P, 1 A	40	2309.8	2346	2295.4	2317.067
	70	770.8	701.2	756.6	742.8667
	100	1011	1047.8	987.5	1015.433
0 P, 2 A	40	2286.9	2318.8	2307.3	2304.333
	70	837.9	833.7	850.9	840.8333
	100	1025.7	1042.4	993.6	1020.567
0 P, 3 A	40	2488.7	2418.4	2415.7	2440.933
	70	847.3	838.2	803.2	829.5667
	100	1046.6	1073.2	1016.5	1045.433
1 P, 0 A	40	2066.9	2098.8	2057	2074.233
	70	717.9	735.8	741.8	731.8333
	100	948	976.3	924.3	949.5333
1 P, 1 A	40	2264.9	2281.6	2313.1	2286.533
	70	844.4	869.3	810.5	841.4
	100	1060.2	1035.4	1005.8	1033.8
1 P, 2 A	40	2390.1	2406.3	2444.6	2413.667
	70	867.2	851.8	834.1	851.0333
	100	1081.6	1073.6	1048.9	1068.033
1 P, 3 A	40	2423.9	2432.5	2413.3	2423.233
	70	837.8	820.5	864.1	840.8
	100	1099.1	1038.8	1045.6	1061.167
2 P, 0 A	40	2090.5	2127.1	2063.5	2093.7
	70	751.5	799.5	688.8	746.6
	100	982	929.6	971.1	960.9
2 P, 1 A	40	2329.9	2371.1	2363.5	2354.833
	70	825.7	791.7	814	810.4667
	100	1041.1	1097.9	1065.8	1068.267
2 P, 2 A	40	2395.9	2438.5	2387.5	2407.3
	70	734.5	753.2	897.3	795
	100	1148.3	1115.6	1100.7	1121.533
	100	1093.3	1062.5	1118	1091.267
3 P, 0 A	40	2123.4	2108.9	2139.2	2123.833

Tensile Strength					
Mixture Type	**Temperature**	**Replicate 1**	**Replicate 2**	**Replicate 3**	**Average**
3 P, 0 A	70	782.8	794	728	768.2667
	100	1016	997.9	1054.2	1022.7
3 P, 1 A	40	2339.6	2429.7	2409.6	2392.967
	70	891	887	939.6	905.8667
	100	1110.6	1190.6	1282.7	1194.633
3 P, 2 A	40	2472.9	2449.8	2441.6	2454.767
	70	808.8	894.3	834.1	845.7333
	100	1127.8	1175.3	1195.1	1166.067
3 P, 3 A	40	2585.2	2645.4	2523.8	2584.8
	70	936.9	944.9	1027.3	969.7
	100	1215	1180.7	1247.3	1214.333

TABLE 73 Summary of Pre- Energy Based on the Average of Three Replicates

Pre Energy					
Mixture Type	**Temperature**	**Replicate 1**	**Replicate 2**	**Replicate 3**	**Average**
Control	40	615.5774	626.39827	634.722	625.5659
	70	658.8293	663.794025	642.7781	655.1338
	100	1374.502	1368.95685	1339.215	1360.891
0 P, 1 A	40	725.7	742.22445	709.6843	725.8696
	70	666.3333	721.559695	680.8587	689.5839
	100	1430.063	1428.45307	1405.686	1421.401
0 P, 2 A	40	871.3025	865.917338	849.1384	862.1194
	70	734.4129	760.57704	716.6014	737.1971
	100	1387.035	1371.4191	1485.476	1414.643
0 P, 3 A	40	811.4832	909.765388	838.0918	853.1135
	70	732.7378	661.504195	755.5932	716.6117
	100	1535.911	1512.80487	1543.628	1530.782
1 P, 0 A	40	700.3006	716.718748	713.9332	710.3175
	70	643.0689	671.15976	690.0886	668.1058
	100	1383.396	1373.15845	1357.467	1371.34
1 P, 1 A	40	793.2029	779.289653	804.6317	792.3747
	70	748.4917	743.714715	717.1137	736.4401
	100	1451.134	1410.87427	1466.69	1442.899
1 P, 2 A	40	888.6893	913.190448	932.1086	911.3295
	70	692.9156	764.87327	788.5408	748.7766
	100	1491.777	1529.52468	1525.665	1515.656
1 P, 3 A	40	923.4233	834.116308	924.7982	894.1126
	70	675.5305	708.10298	769.3982	717.6772
	100	1435.228	1473.25003	1527.331	1478.603
2 P, 0 A	40	683.6294	717.647963	657.9587	686.412
	70	663.6644	713.993065	700.1909	692.6161
	100	1405.98	1398.39026	1434.502	1412.957
2 P, 1 A	40	824.4442	857.046885	803.0677	828.1863
	70	766.1909	773.41482	770.324	769.9766
	100	1449.95	1441.71702	1528.033	1473.233
2 P, 2 A	40	955.7734	927.213413	946.6771	943.2213
	70	749.5521	777.608305	742.9618	756.7074
	100	1546.682	1585.505	1514.138	1548.775
2 P, 3 A	40	1109.071	1115.83586	1056.865	1093.924
	70	828.2468	775.28791	814.8044	806.113

Pre Energy					
Mixture Type	**Temperature**	**Replicate 1**	**Replicate 2**	**Replicate 3**	**Average**
2 P, 3 A	100	1607.884	1612.38044	1600.445	1606.903
3 P, 0 A	40	787.4155	774.019505	767.4612	776.2988
	70	681.3239	711.45946	736.5913	709.7916
	100	1401.969	1534.87134	1413.519	1450.12
3 P, 1 A	40	822.8533	881.83141	883.6541	862.7796
	70	798.4559	793.023955	834.509	808.663
	100	1507.047	1524.95277	1535.283	1522.428
3 P, 2 A	40	804.3547	895.628308	890.513	863.4987
	70	828.9332	806.9963	829.3982	821.7759
	100	1580.778	1564.47797	1595.91	1580.389
3 P, 3 A	40	1165.295	1043.23863	1144.911	1117.815
	70	843.5428	844.35499	875.3498	854.4159
	100	1605.507	1570.9225	1614.896	1597.109

TABLE 74 Summary of Post Energy Based on the Average of Three Replicates

Post Energy					
Mixture Type	**Temperature**	**Replicate 1**	**Replicate 2**	**Replicate 3**	**Average**
Control	40	1632.892	1685.655	1690.939	1669.829
	70	1265.561	1241.853	1289.864	1265.759
	100	2970.408	3036.748	3035.414	3014.19
0 P, 1 A	40	1875.198	1796.069	1848.649	1839.972
	70	1506.372	1476.078	1418.428	1466.96
	100	3274.055	3244.512	3225.598	3248.055
0 P, 2 A	40	1834.411	1795.852	1822.127	1817.463
	70	1496.933	1485.286	1446.517	1476.245
	100	3270.172	3272.908	3243.717	3262.266
0 P, 3 A	40	1917.332	2036.757	2020.137	1991.409
	70	1519.638	1545.641	1562.237	1542.505
	100	3343.632	3283.481	3324.564	3317.225
1 P, 0 A	40	1731.205	1726.451	1677.583	1711.746
	70	1321.559	1297.362	1302.343	1307.088
	100	3063.089	3076.727	3115.064	3084.96
1 P, 1 A	40	1799.089	1762.202	1828.456	1796.582
	70	1395.019	1416.405	1421.144	1410.856
	100	3118.692	3094.384	3158.965	3124.014
1 P, 2 A	40	1925.356	1917.063	1878.349	1906.923
	70	1577.905	1529.097	1417.209	1508.07
	100	3361.247	3325.436	3246.201	3310.961
1 P, 3 A	40	2126.343	2154.465	2096.13	2125.646
	70	1682.407	1698.937	1605.432	1662.259
	100	3488.346	3358.09	3458.349	3434.928
2 P, 0 A	40	1766.65	1790.304	1785.859	1780.938
	70	1310.523	1321.67	1257.815	1296.669
	100	3120.35	3085.013	3070.408	3091.924
2 P, 1 A	40	1787.003	1768.466	1890.768	1815.412
	70	1477.815	1544.146	1519.963	1513.975
	100	3361.453	3347.592	3253.504	3320.85
2 P, 2 A	40	2180.365	2154.359	2122.636	2152.453
	70	1698.495	1625.746	1684.758	1669.666
	100	3411.11	3452.282	3425.265	3429.552
2 P, 3 A	40	2257.557	2211.988	2272.103	2247.216
	70	1662.411	1646.405	1588.024	1632.28

Post Energy					
Mixture Type	**Temperature**	**Replicate 1**	**Replicate 2**	**Replicate 3**	**Average**
2 P, 3 A	100	3467.845	3383.536	3408.263	3419.881
3 P, 0 A	40	1808.432	1778.083	1809.658	1798.724
	70	1651.216	1616.833	1560.835	1609.628
	100	3268.185	3291.556	3377.917	3312.552
3 P, 1 A	40	1934.851	1893.277	1827.822	1885.317
	70	1613.211	1543.134	1651.613	1602.653
	100	3397.394	3487.752	3325.724	3403.624
3 P, 2 A	40	2302.06	2434.595	2499.146	2411.934
	70	1741.85	1808.602	1885.432	1811.962
	100	3380.788	3422.289	3459.46	3420.846
3 P, 3 A	40	2464.607	2383.108	2374.782	2407.499
	70	1993.441	1919.204	1838.534	1917.06
	100	3639.425	3703.566	3737.419	3693.47

TABLE 75 Summary of Total Energy Based on the Average of Three Replicates

Total Energy					
Mixture Type	**Temperature**	**Replicate 1**	**Replicate 2**	**Replicate 3**	**Average**
Control	40	2248.47	2312.053	2325.661	2295.395
	70	1924.39	1905.647	1932.642	1920.893
	100	4344.91	4405.705	4374.629	4375.081
0 P, 1 A	40	2600.898	2538.293	2558.333	2565.841
	70	2172.706	2197.638	2099.287	2156.544
	100	4704.118	4672.965	4631.283	4669.455
0 P, 2 A	40	2705.713	2661.77	2671.265	2679.583
	70	2231.346	2245.863	2163.118	2213.442
	100	4657.207	4644.327	4729.193	4676.909
0 P, 3 A	40	2728.815	2946.522	2858.229	2844.522
	70	2252.376	2207.145	2317.83	2259.117
	100	4879.543	4796.286	4868.192	4848.007
1 P, 0 A	40	2431.506	2443.17	2391.516	2422.064
	70	1964.628	1968.522	1992.432	1975.194
	100	4446.485	4449.885	4472.531	4456.3
1 P, 1 A	40	2592.292	2541.491	2633.087	2588.957
	70	2143.511	2160.12	2138.257	2147.296
	100	4569.826	4505.258	4625.655	4566.913
1 P, 2 A	40	2814.046	2830.254	2810.458	2818.252
	70	2270.821	2293.97	2205.75	2256.847
	100	4853.024	4854.961	4771.866	4826.617
1 P, 3 A	40	3049.766	2988.581	3020.929	3019.759
	70	2357.938	2407.04	2374.831	2379.936
	100	4923.574	4831.34	4985.68	4913.531
2 P, 0 A	40	2450.279	2507.952	2443.818	2467.35
	70	1974.187	2035.663	1958.006	1989.285
	100	4526.33	4483.403	4504.91	4504.881
2 P, 1 A	40	2611.447	2625.513	2693.836	2643.599
	70	2244.006	2317.56	2290.287	2283.951
	100	4811.404	4789.309	4781.537	4794.083
2 P, 2 A	40	3136.139	3081.572	3069.313	3095.674
	70	2448.047	2403.354	2427.72	2426.374
	100	4957.792	5037.787	4939.403	4978.327
2 P, 3 A	40	3366.628	3327.824	3328.968	3341.14
	70	2490.658	2421.693	2402.828	2438.393

Total Energy					
Mixture Type	**Temperature**	**Replicate 1**	**Replicate 2**	**Replicate 3**	**Average**
2 P, 3 A	100	5075.729	4995.917	5008.709	5026.785
3 P, 0 A	40	2595.847	2552.103	2577.119	2575.023
	70	2332.539	2328.292	2297.426	2319.419
	100	4670.154	4826.427	4791.436	4762.67
3 P, 1 A	40	2757.704	2775.109	2711.476	2748.096
	70	2411.667	2336.158	2486.122	2411.316
	100	4904.441	5012.705	4861.007	4926.051
3 P, 2 A	40	3106.415	3330.223	3389.659	3275.432
	70	2570.784	2615.598	2714.831	2633.737
	100	4961.566	4986.767	5055.371	5001.234
3 P, 3 A	40	3629.902	3426.347	3519.693	3525.314
	70	2836.984	2763.559	2713.883	2771.475
	100	5244.932	5274.489	5352.315	5290.579

APPENDIX B

FIGURES – FORTA FIBER DATA

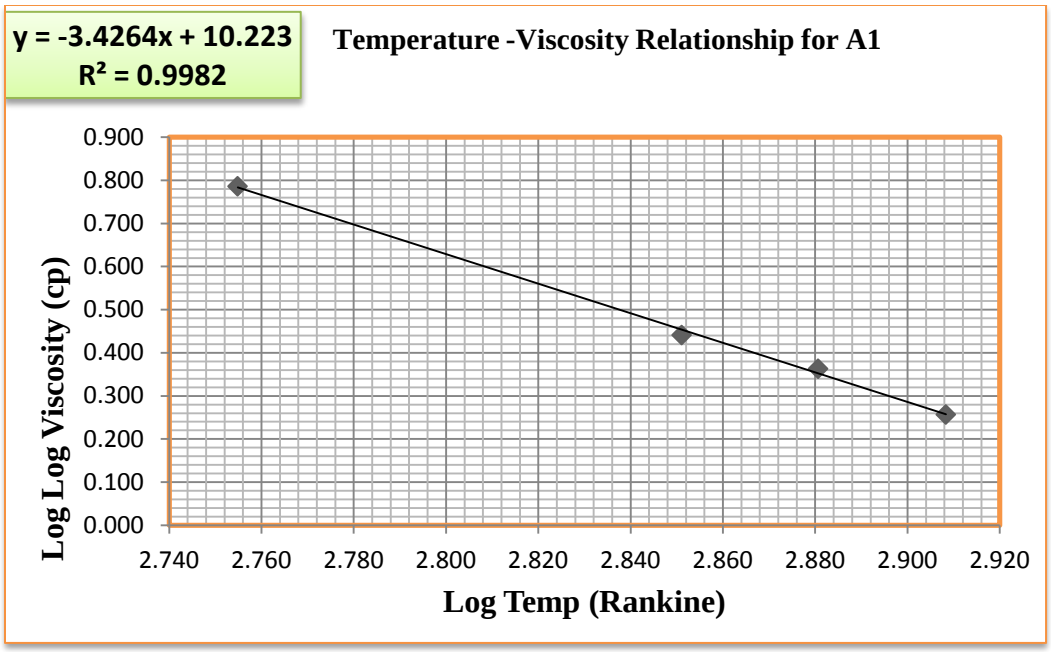

FIGURE 42 Temperature -viscosity relationship for A1.

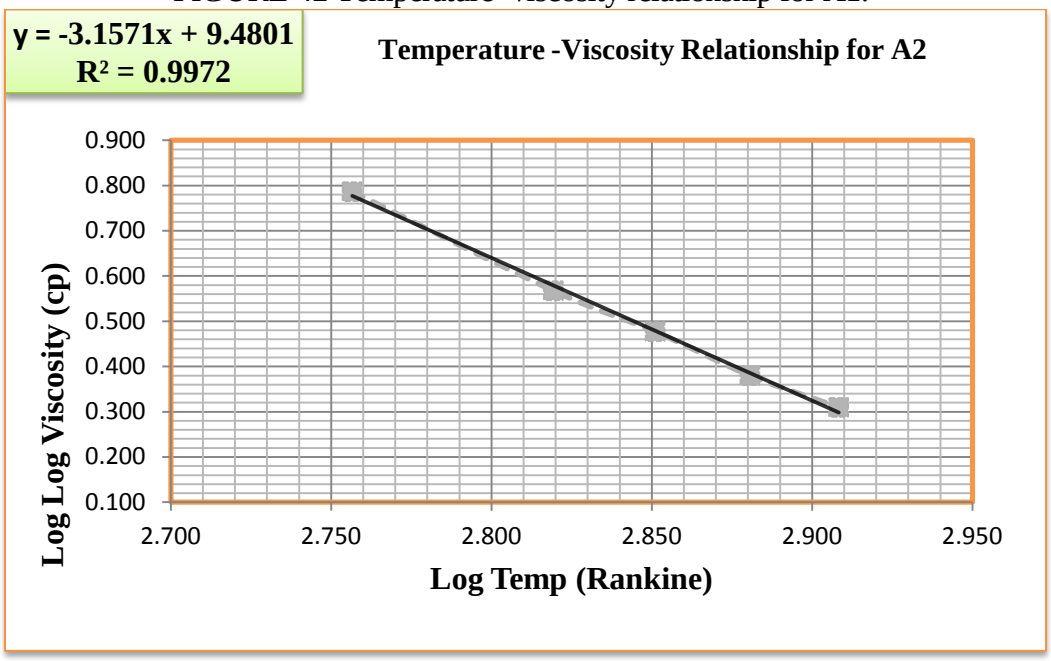

FIGURE 43 Temperature -viscosity relationship for A2.

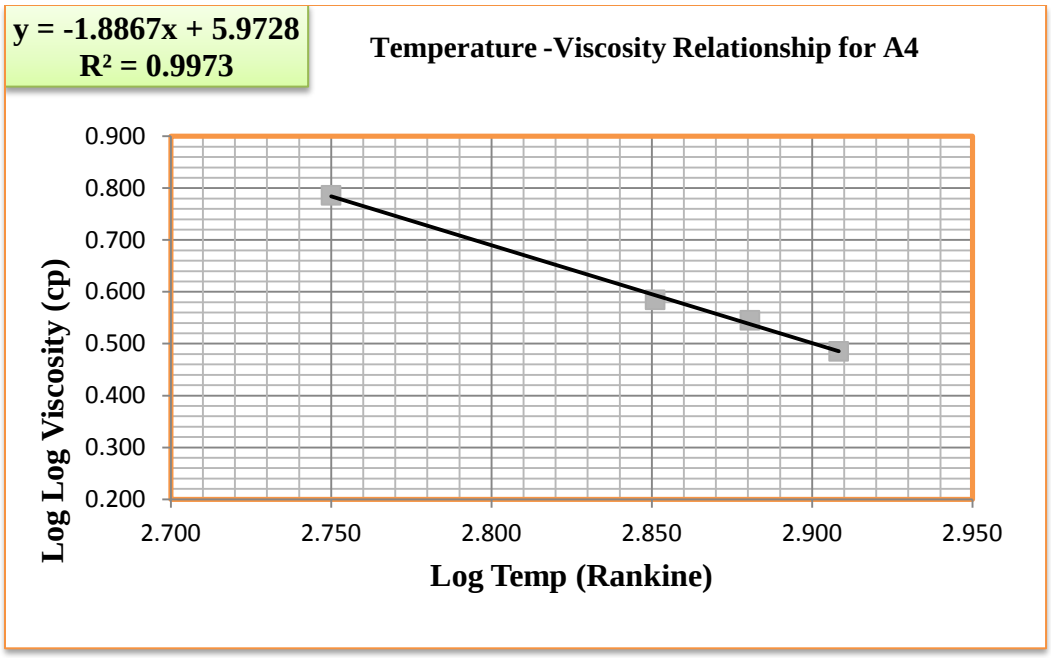

FIGURE 44 Temperature -viscosity relationship for A4.

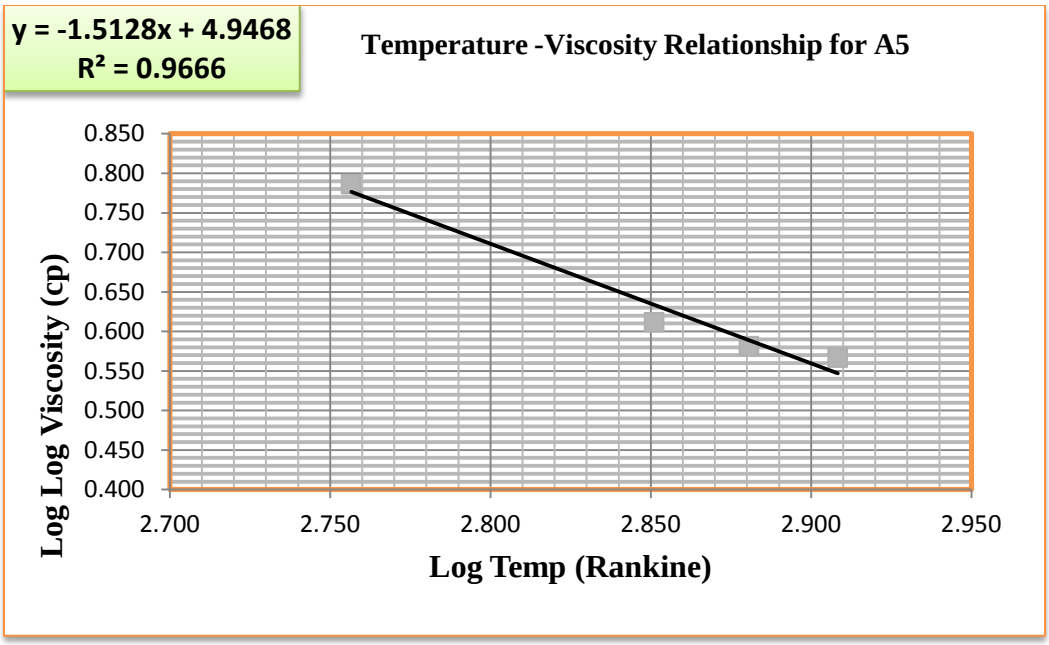

FIGURE 45 Temperature -viscosity relationship for A5.

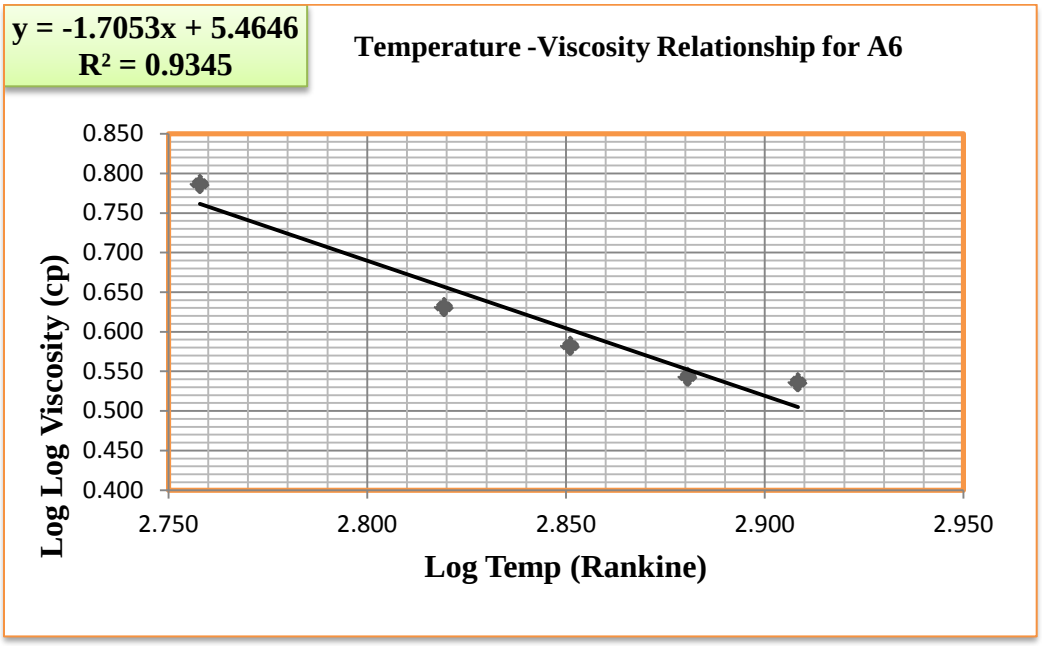

FIGURE 46 Temperature -viscosity relationship for A6.

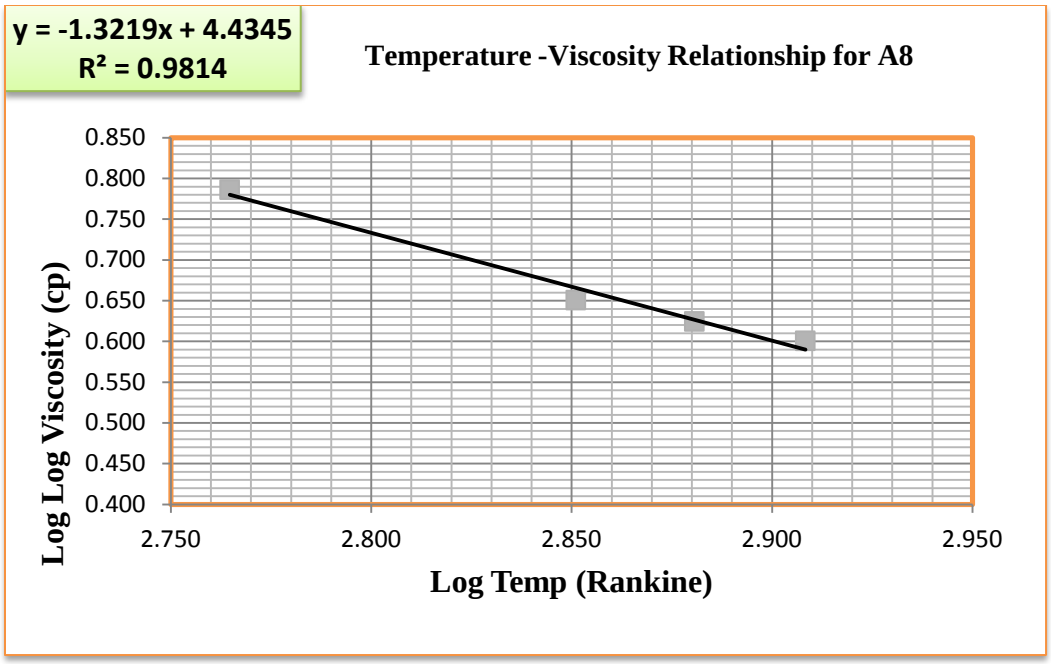

FIGURE 47 Temperature -viscosity relationship for A8.

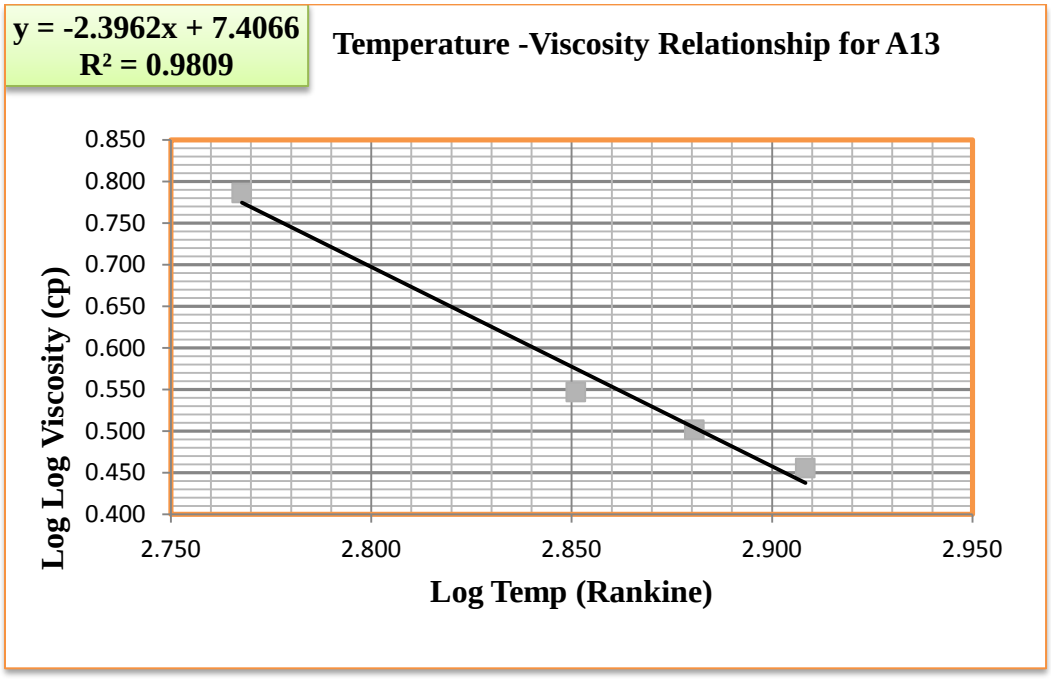

FIGURE 48 Temperature -viscosity relationship for A13.

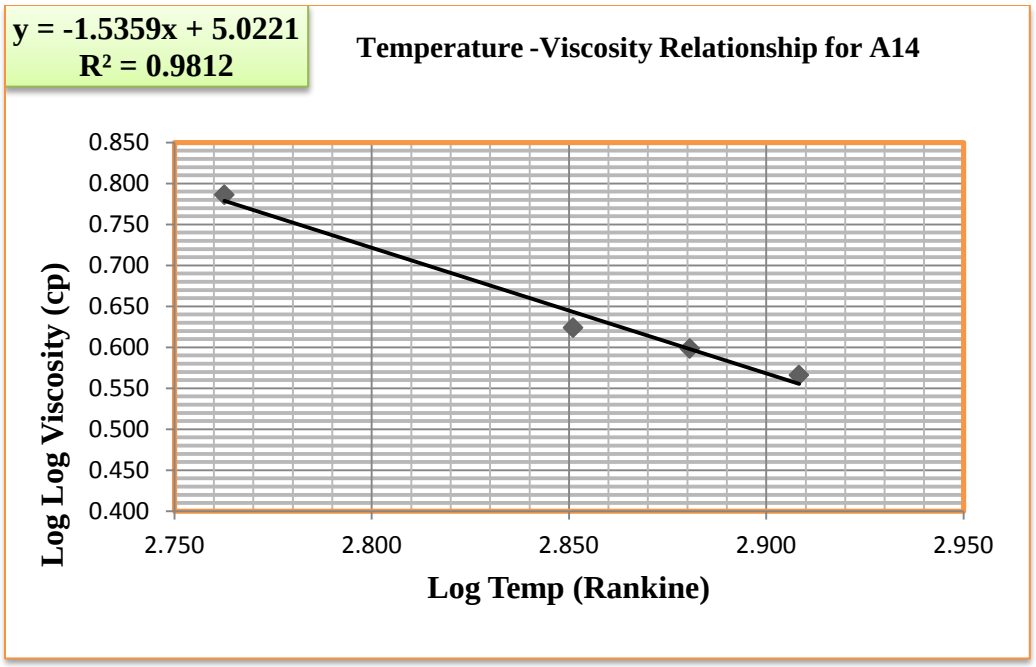

FIGURE 49 Temperature -viscosity relationship for A14.

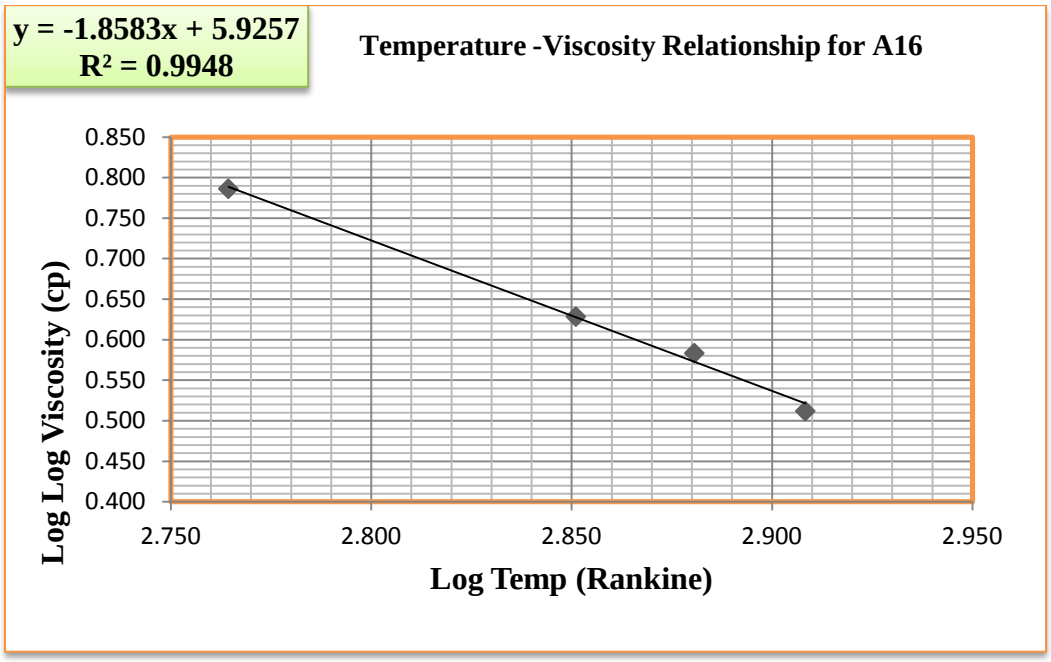

FIGURE 50 Temperature -viscosity relationship for A16.

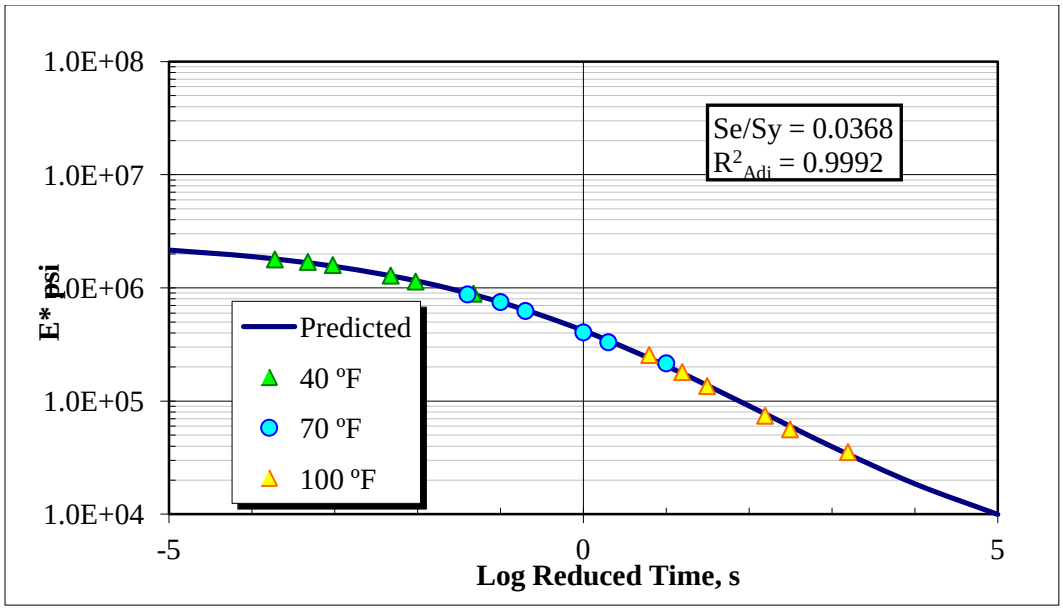

FIGURE 51 Master curves based on average of three replicates for control.

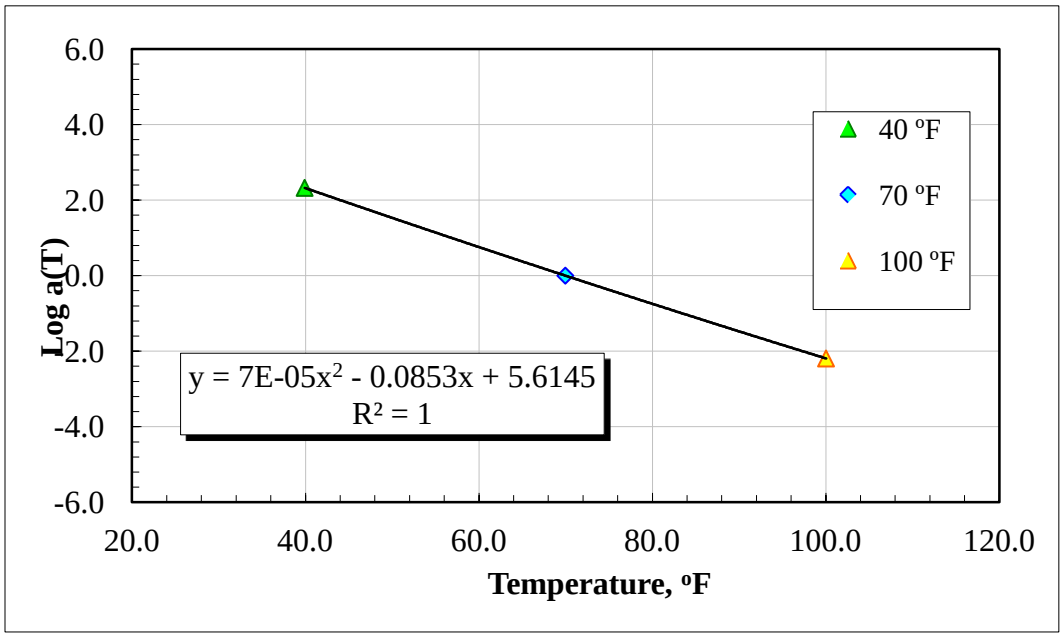

FIGURE 52 Shift factors based on average of three replicates for control.

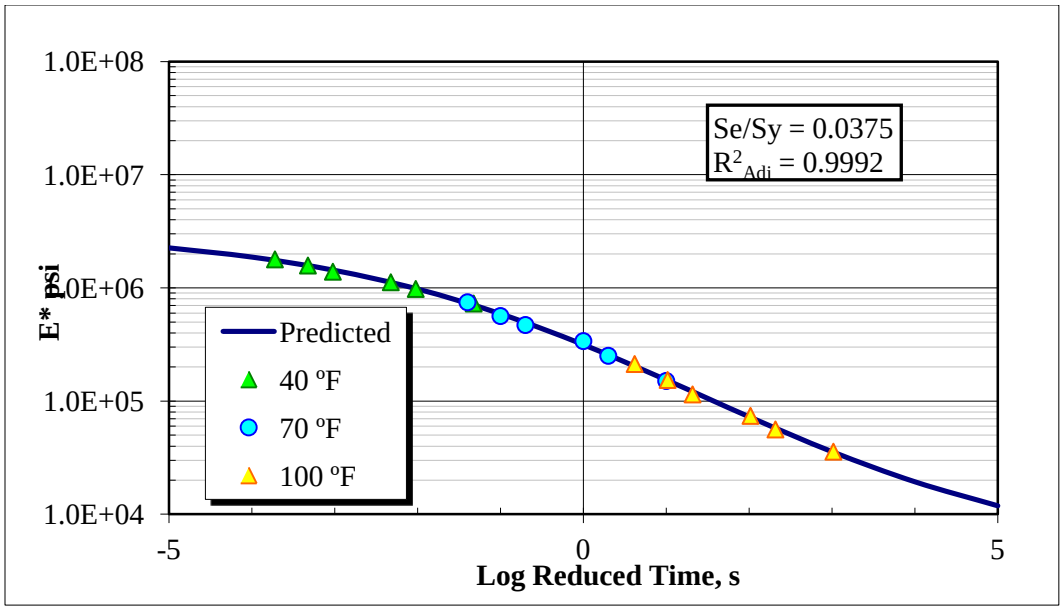

FIGURE 53 Master curves based on average of three replicates for (0 P, 1 A).

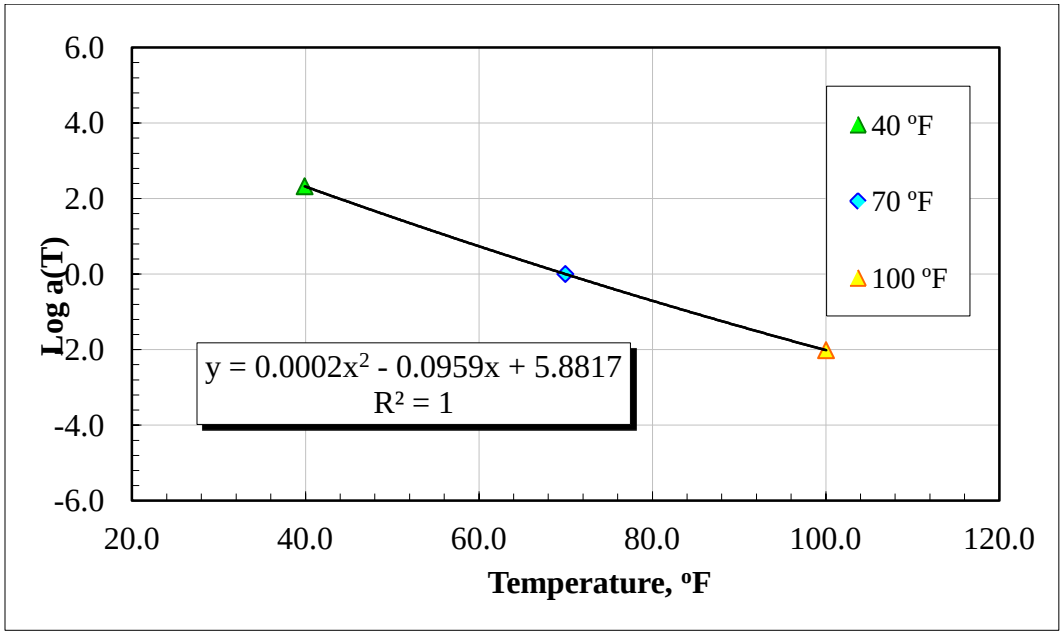

FIGURE 54 Shift factors based on average of three replicates for (0 P, 1 A).

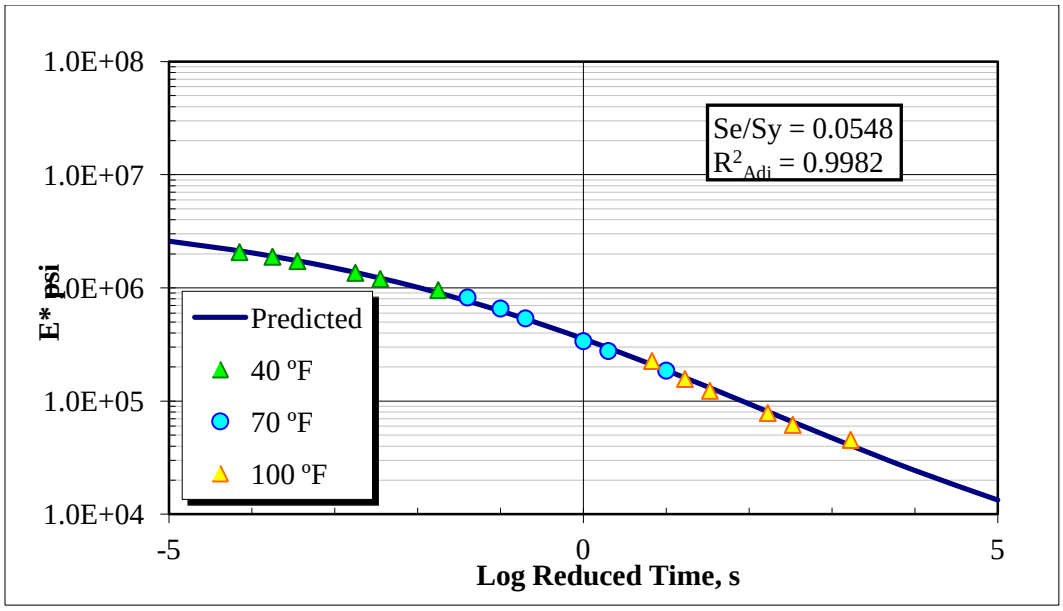

FIGURE 55 Master curves based on average of three replicates for (0 P, 2 A).

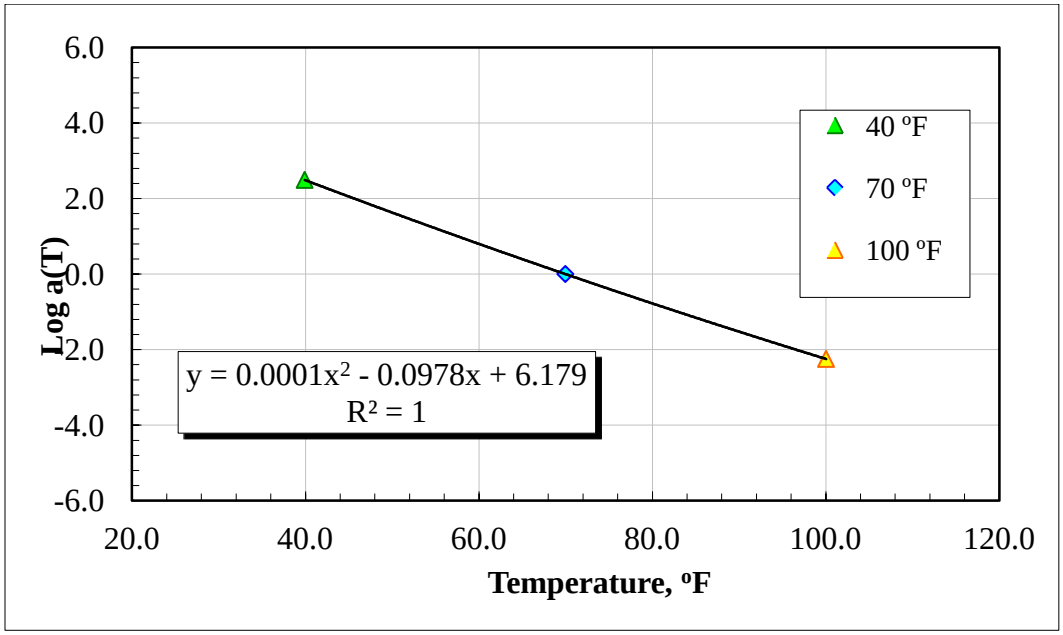

FIGURE 56 Shift factors based on average of three replicates for (0 P, 2 A).

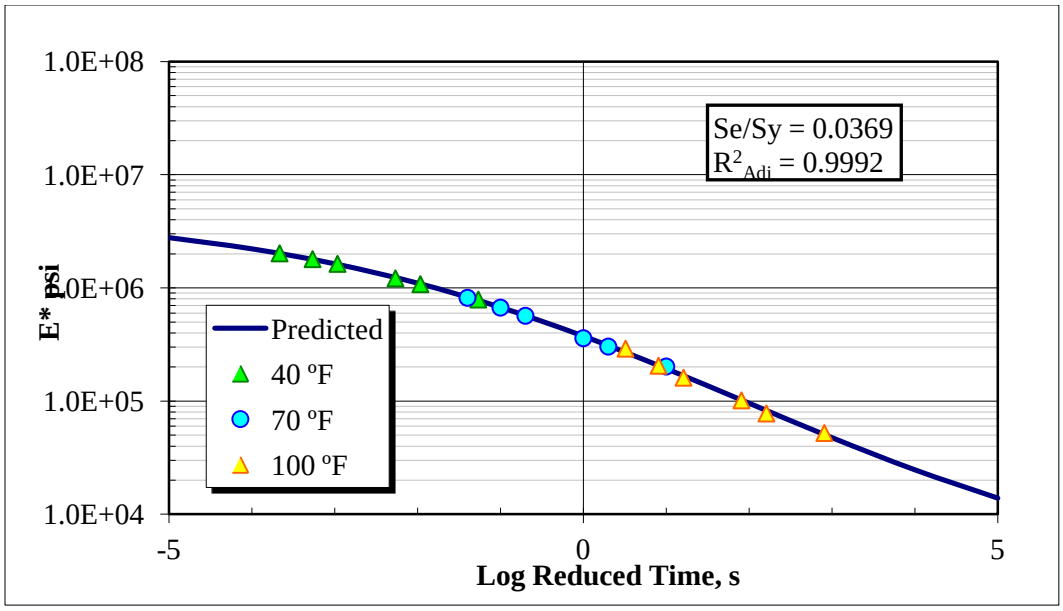

FIGURE 57 Master curves based on average of three replicates for (0 P, 3 A).

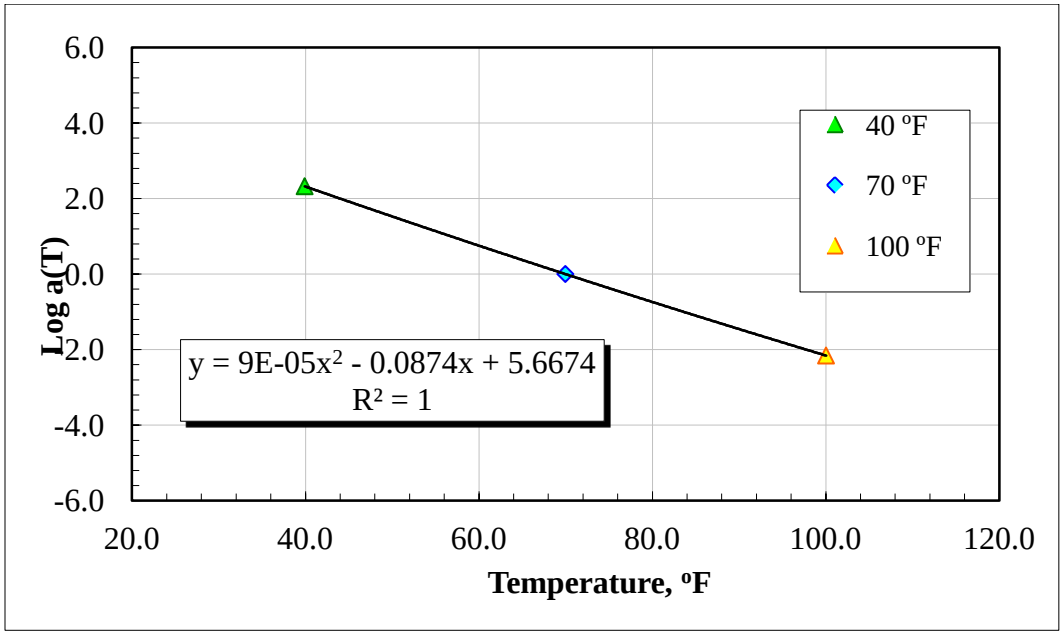

FIGURE 58 Shift factors based on average of three replicates for (0 P, 3 A).

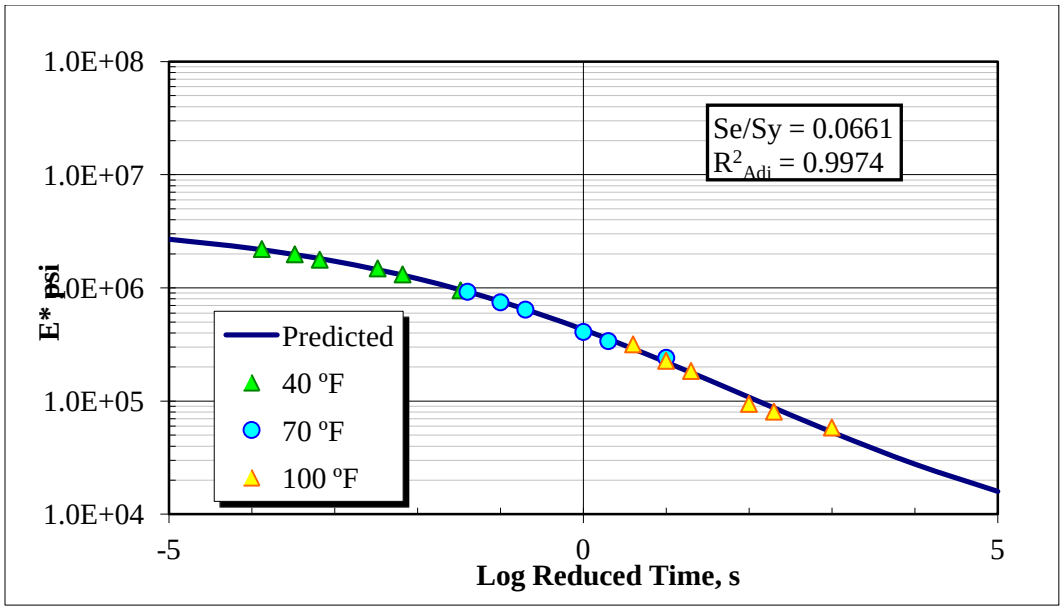

FIGURE 59 Master curves based on average of three replicates for (1 P, 0 A).

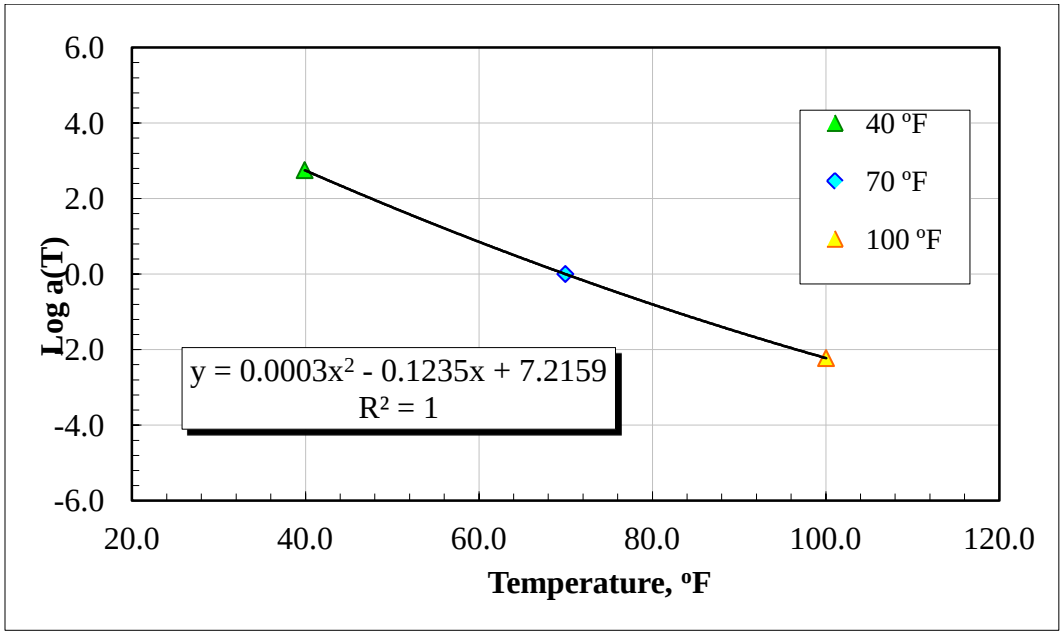

FIGURE 60 Shift factors based on average of three replicates for (1 P, 0 A).

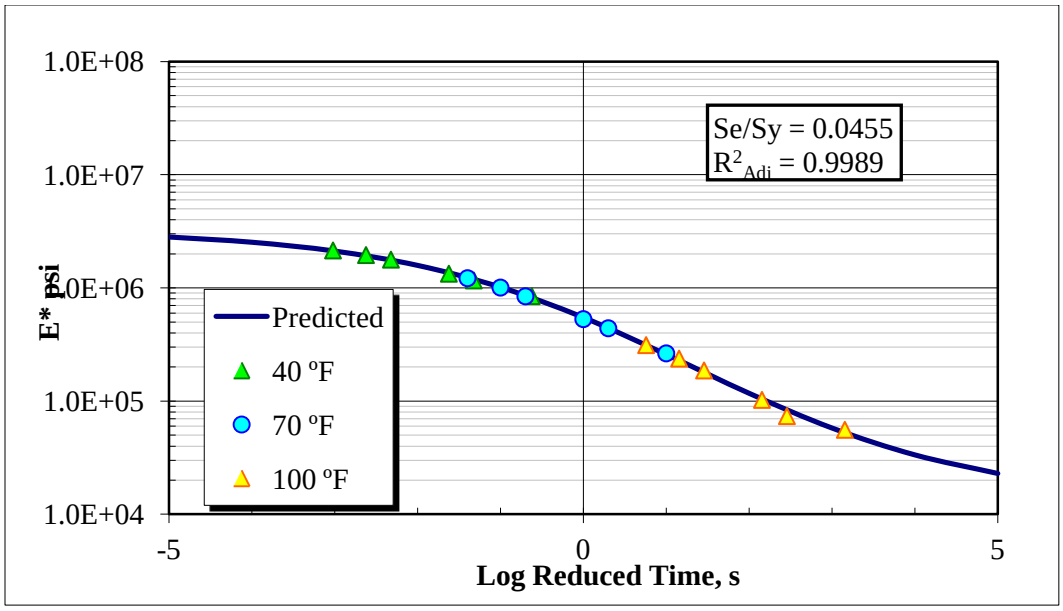

FIGURE 61 Master curves based on average of three replicates for (1 P, 1 A).

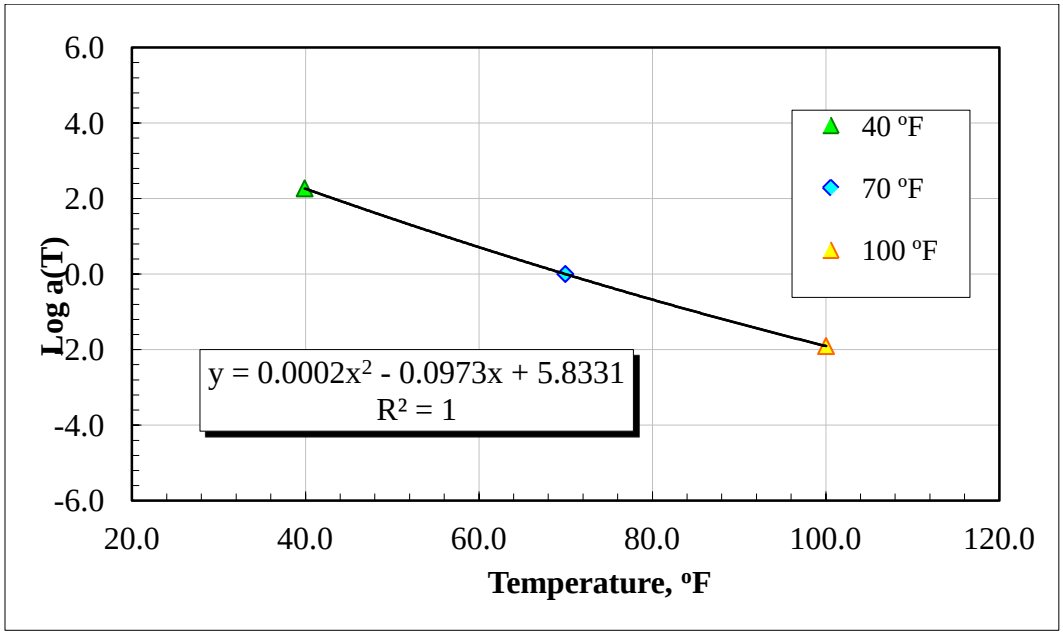

FIGURE 62 Shift factors based on average of three replicates for (1 P, 1 A).

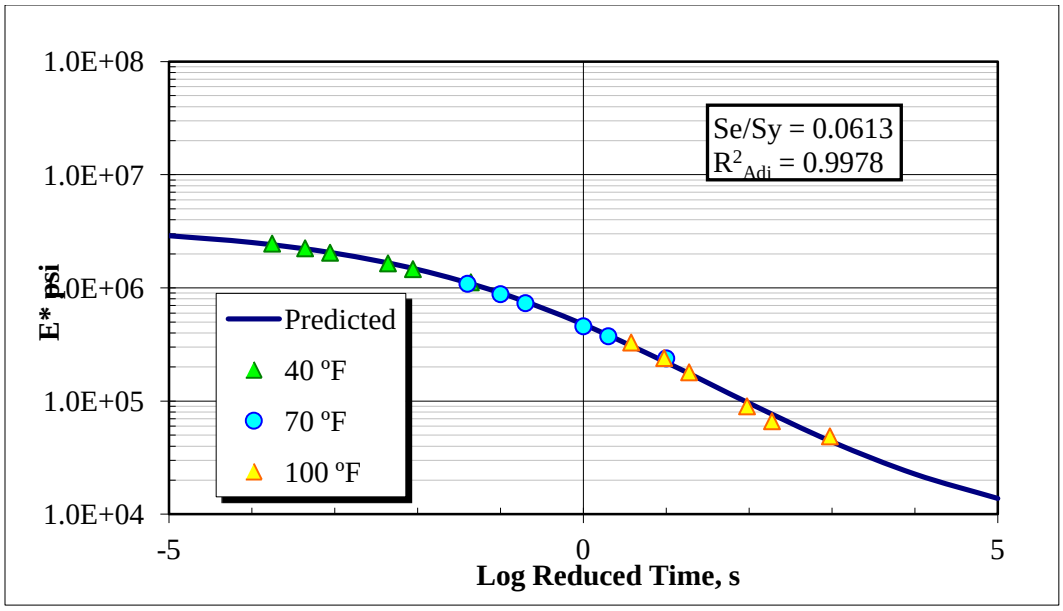

FIGURE 63 Master curves based on average of three replicates for (1 P, 2 A).

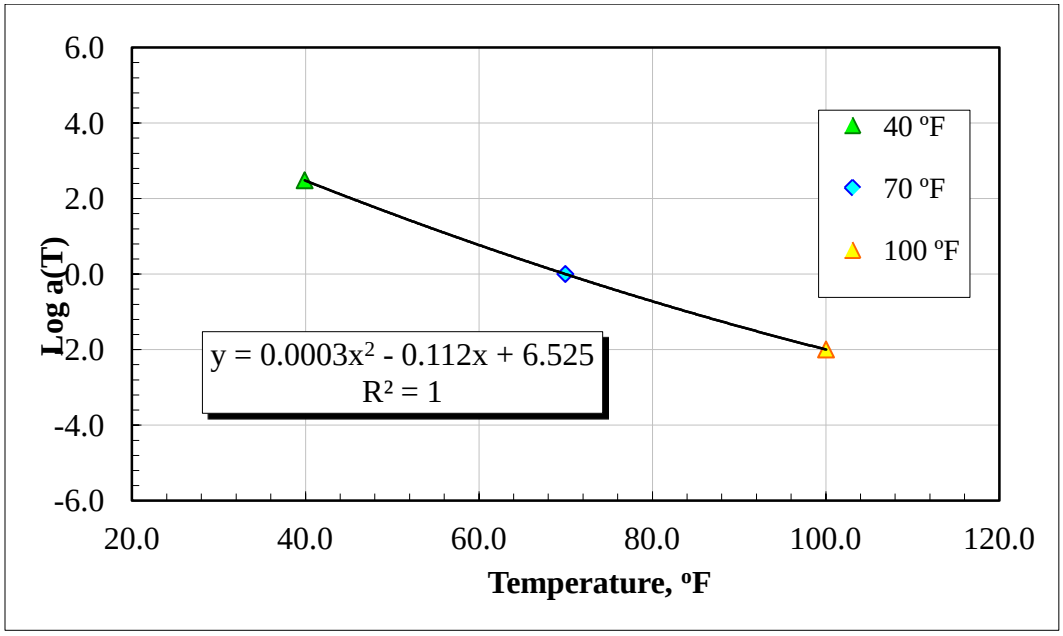

FIGURE 64 Shift factors based on average of three replicates for (1 P, 2 A).

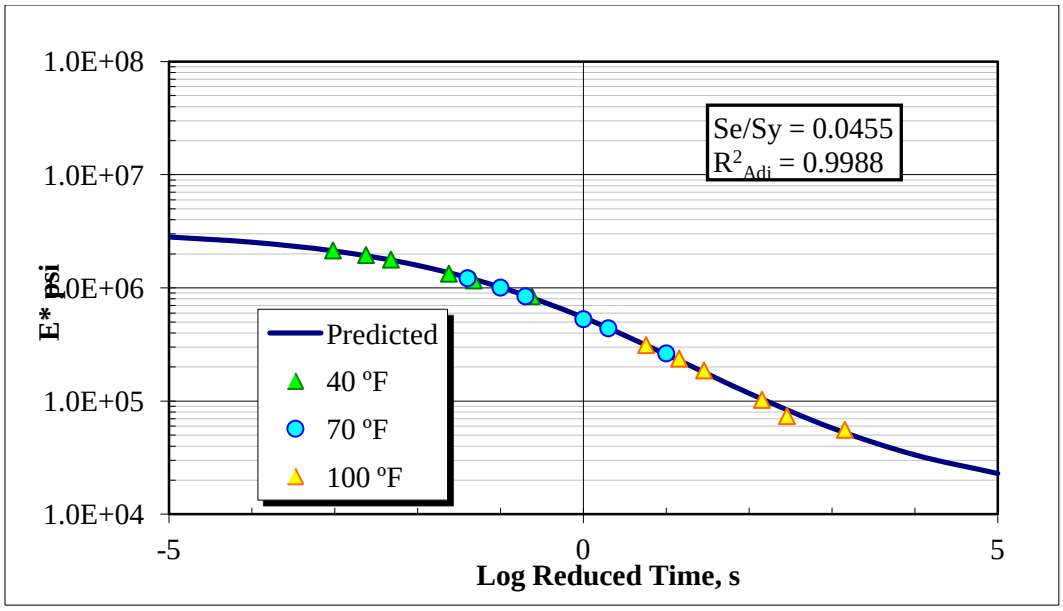

FIGURE 65 Master curves based on average of three replicates for (1 P, 3 A).

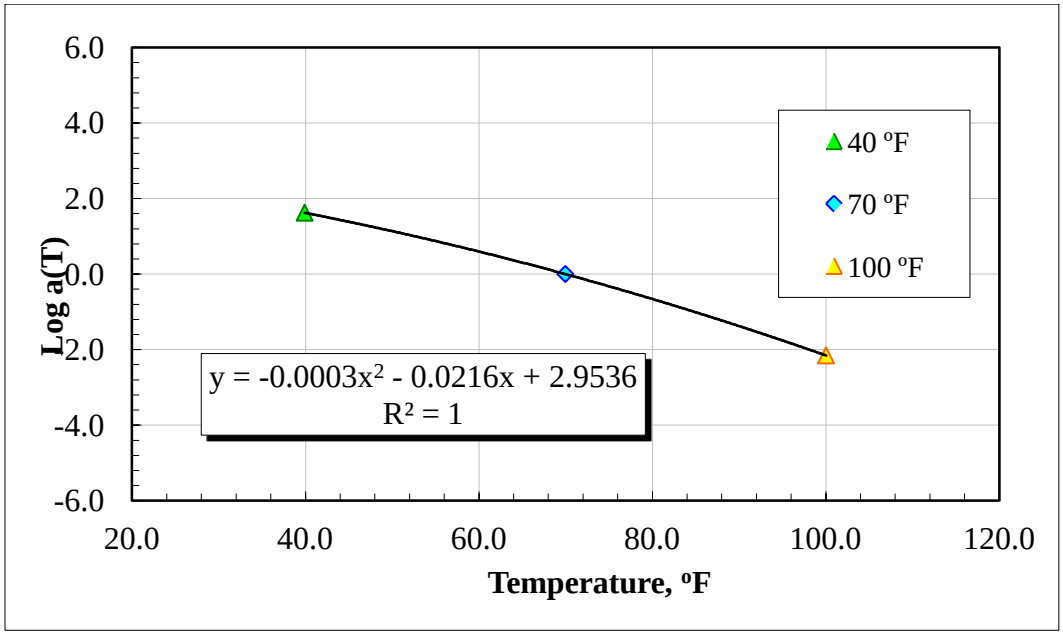

FIGURE 66 Shift factors based on average of three replicates for (1 P, 3 A).

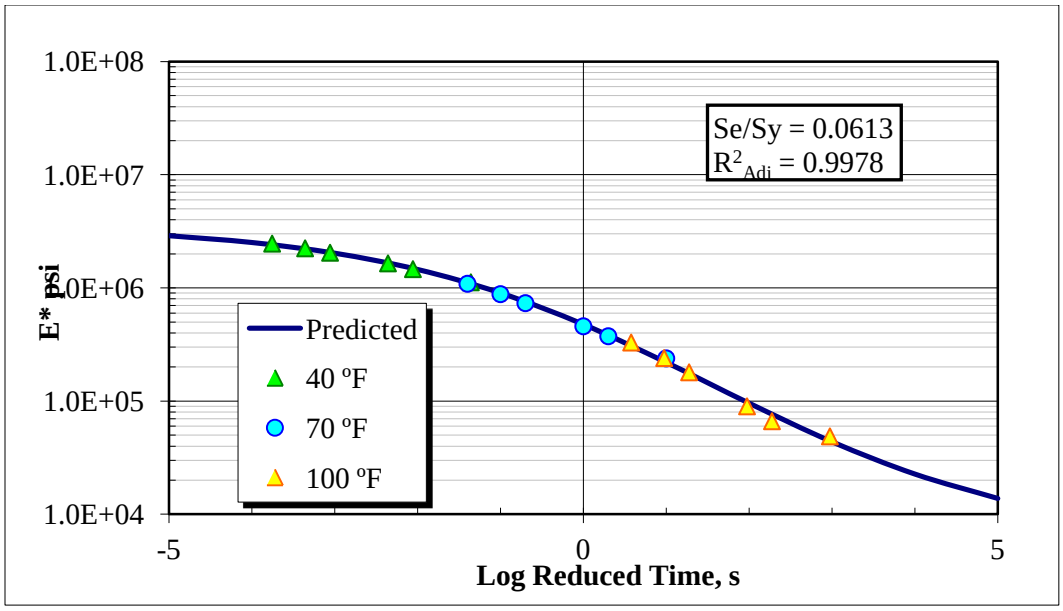

FIGURE 67 Master curves based on average of three replicates for (2 P, 0 A).

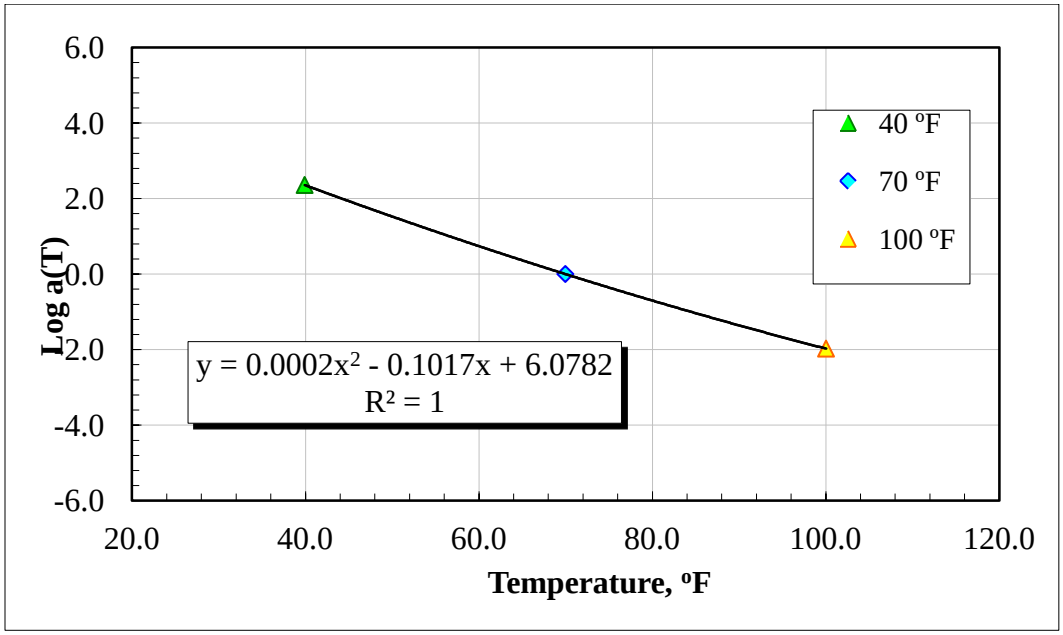

FIGURE 68 Shift factors based on average of three replicates for (2 P, 0 A).

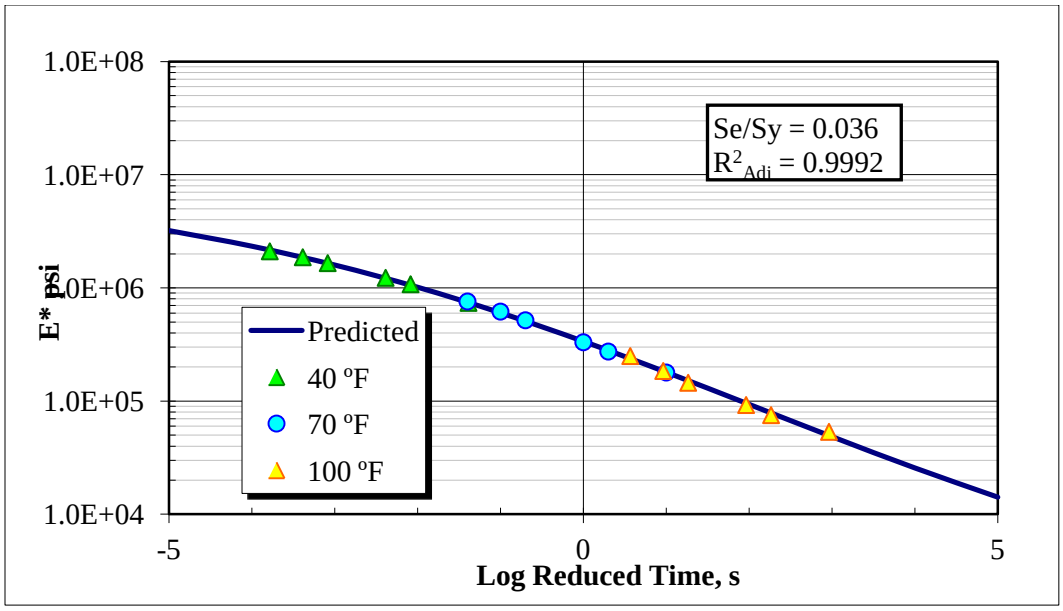

FIGURE 69 Master curves based on average of three replicates for (2 P, 1 A).

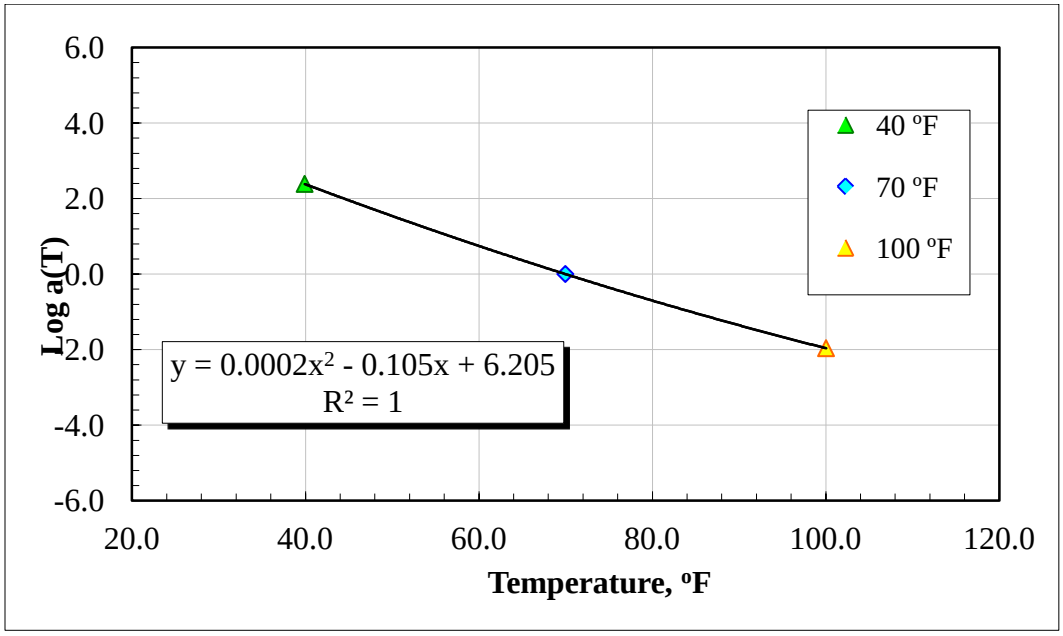

FIGURE 70 Shift factors based on average of three replicates for (2 P, 1 A).

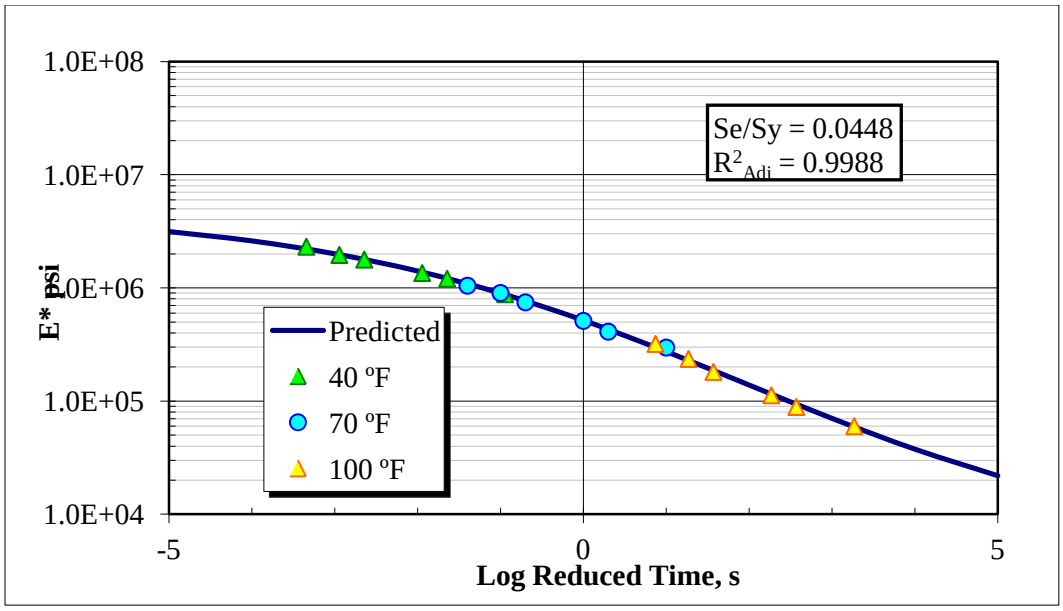

FIGURE 71 Master curves based on average of three replicates for (2 P, 2 A).

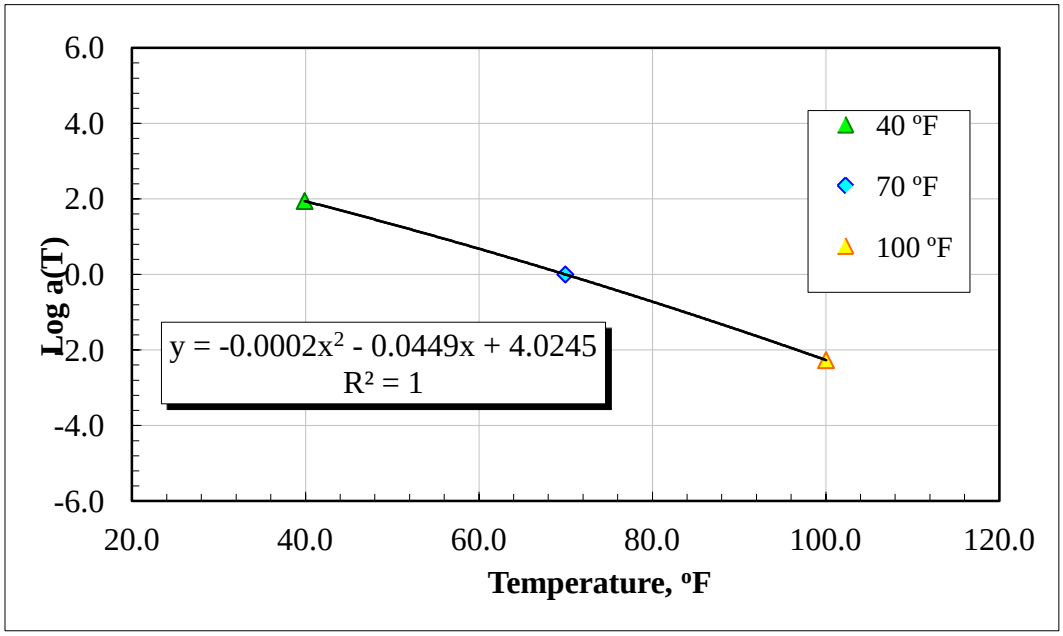

FIGURE 72 Shift factors based on average of three replicates for (2 P, 2 A).

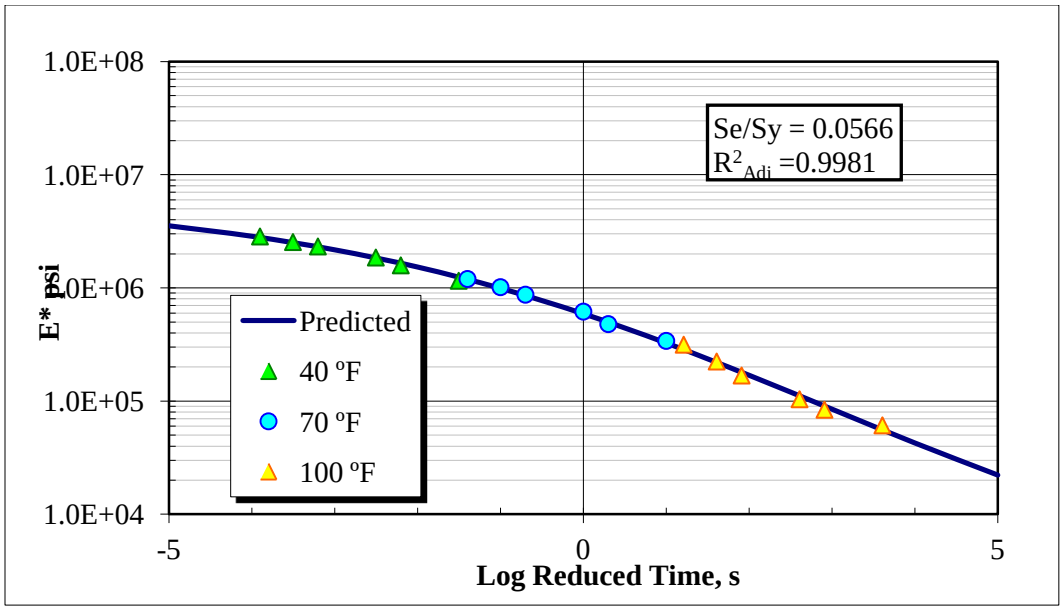

FIGURE 73 Master curves based on average of three replicates for (2 P, 3 A).

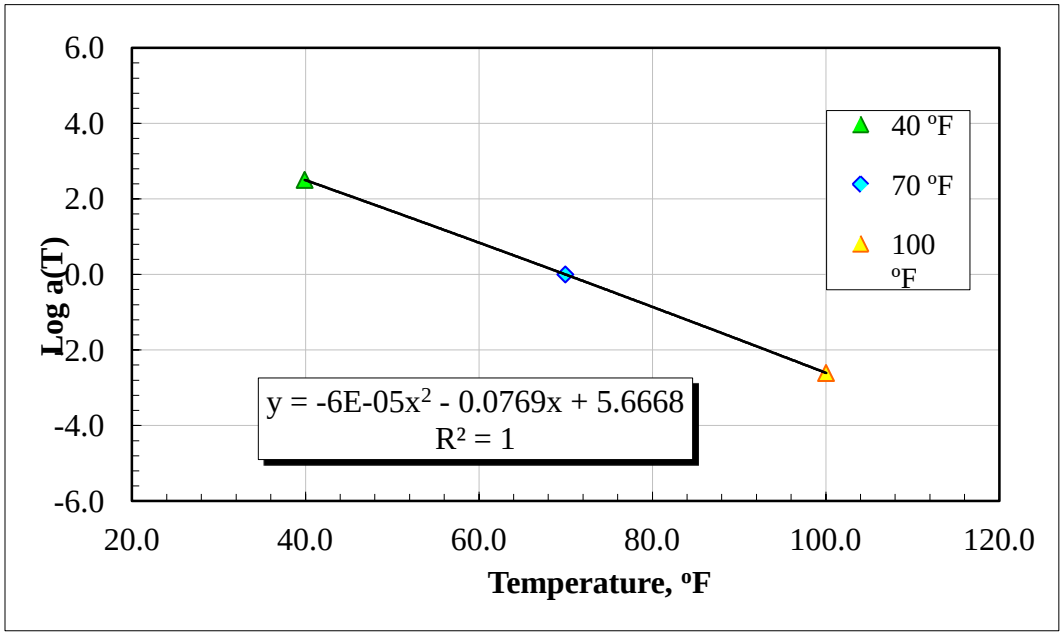

FIGURE 74 Shift factors based on average of three replicates for (2 P, 3 A).

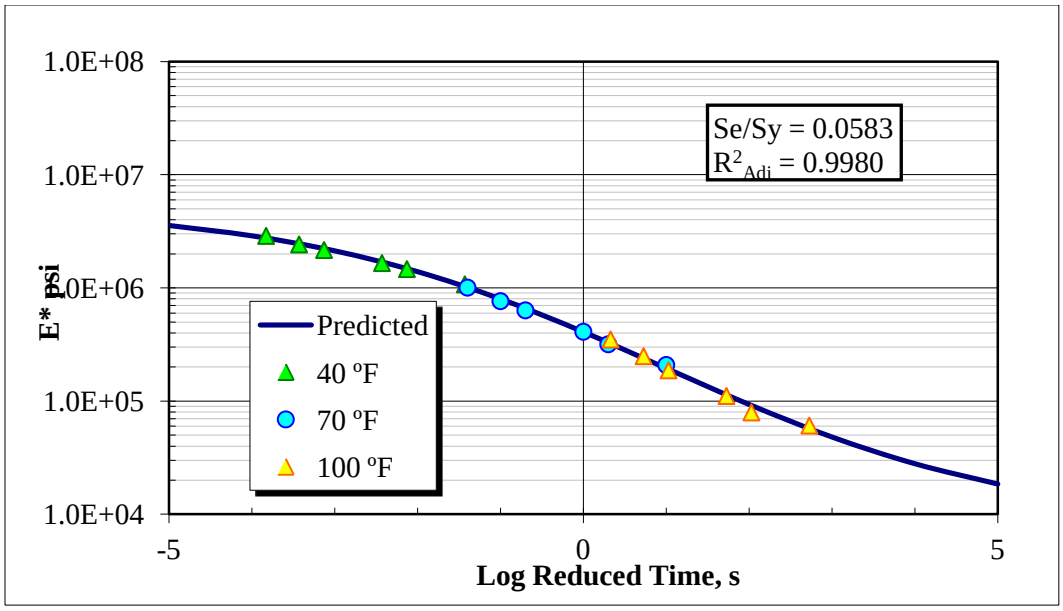

FIGURE 75 Master curves based on average of three replicates for (3 P, 0 A).

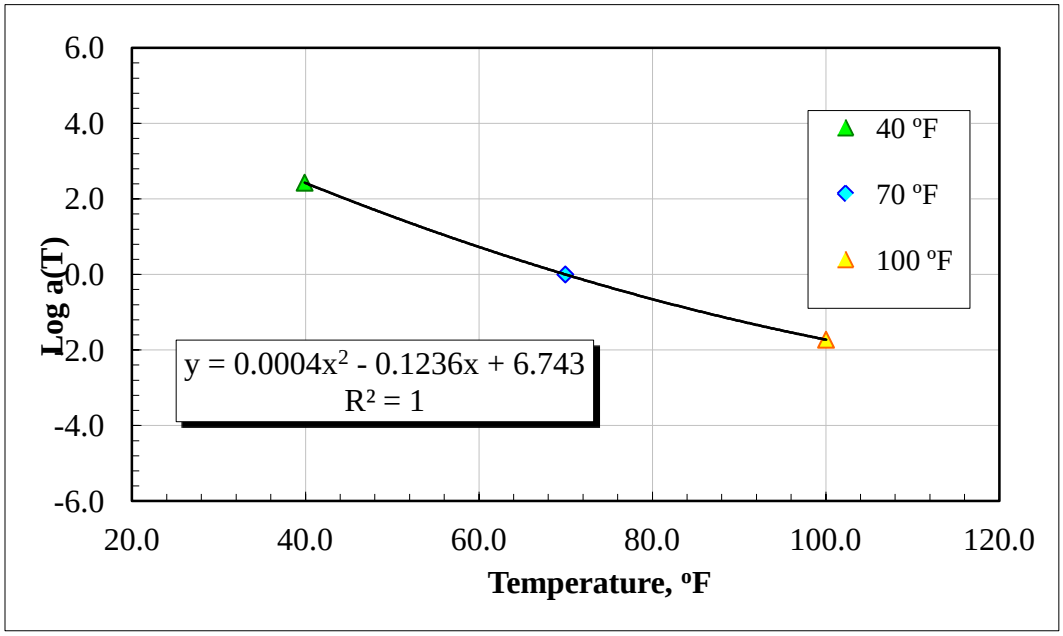

FIGURE 76 Shift factors based on average of three replicates for (3 P, 0 A).

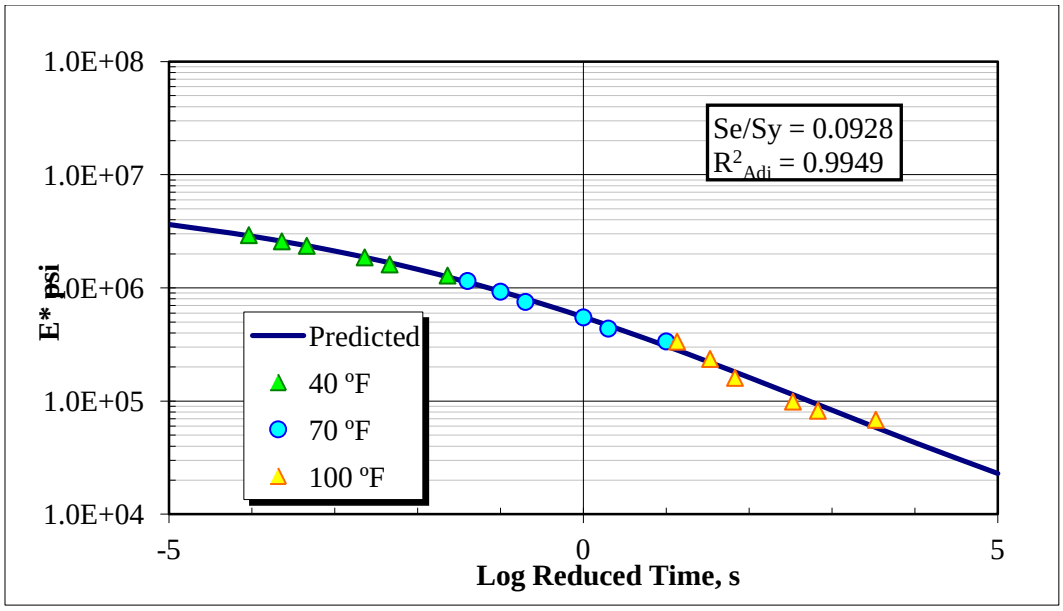

FIGURE 77 Master curves based on average of three replicates for (3 P, 1 A).

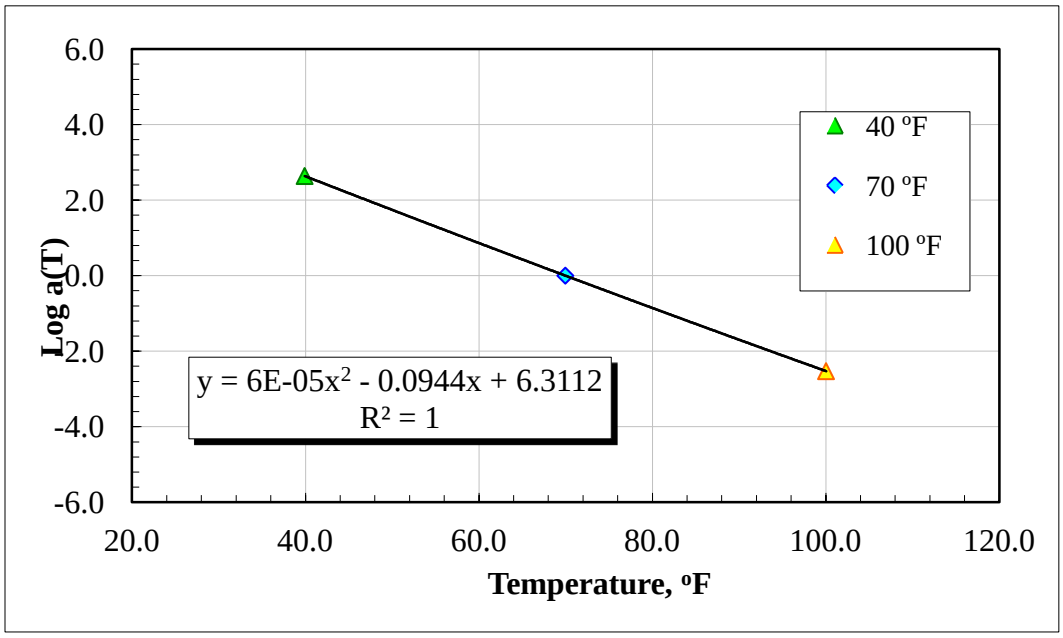

FIGURE 78 Shift factors based on average of three replicates for (3 P, 1 A).

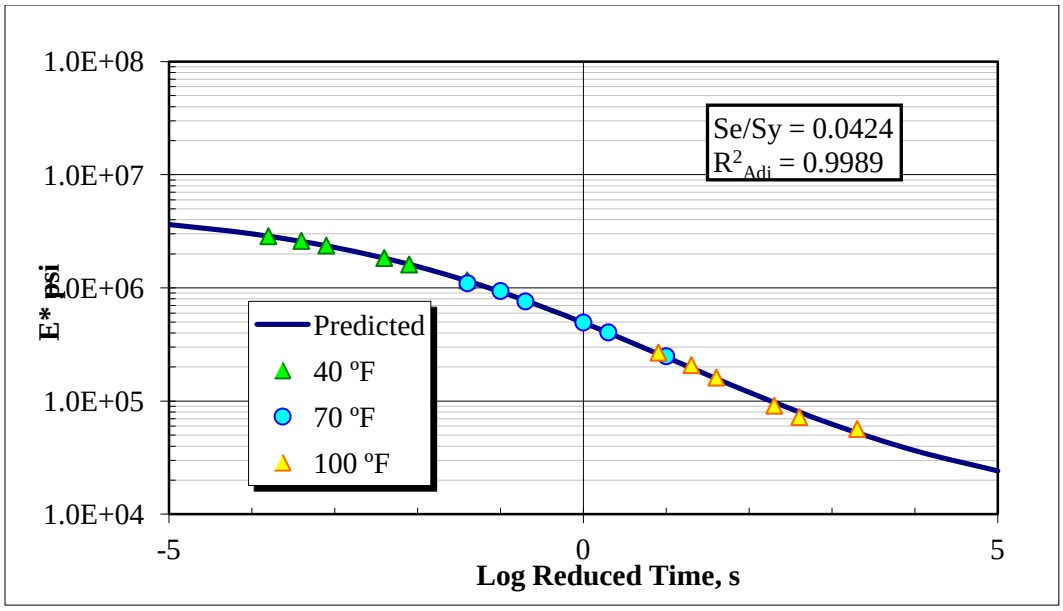

FIGURE 79 Master curves based on average of three replicates for (3 P, 2 A).

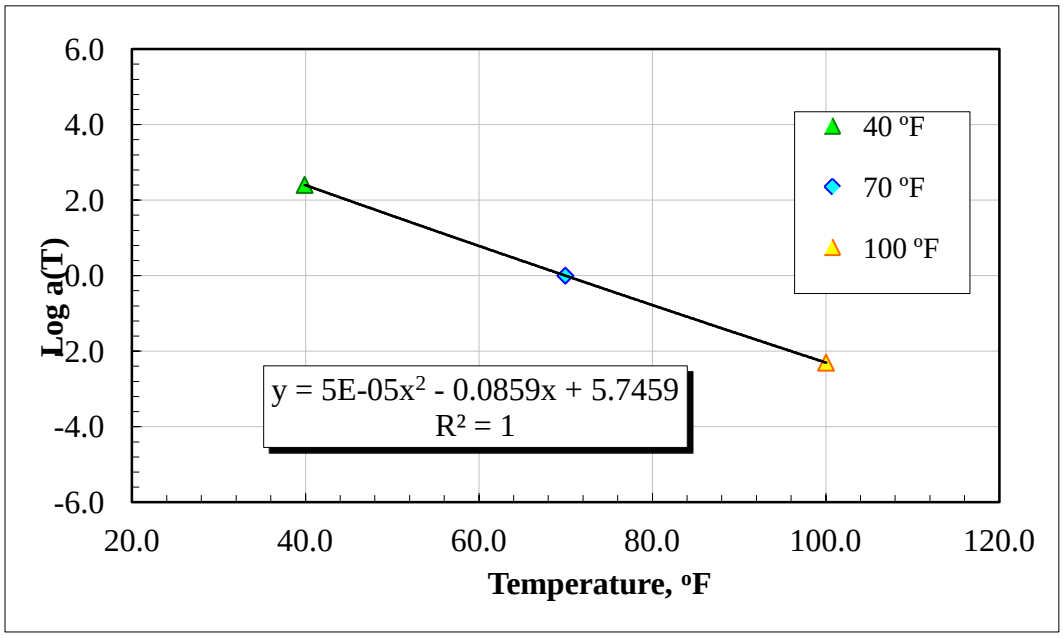

FIGURE 80 Shift factors based on average of three replicates for (3 P, 2 A).

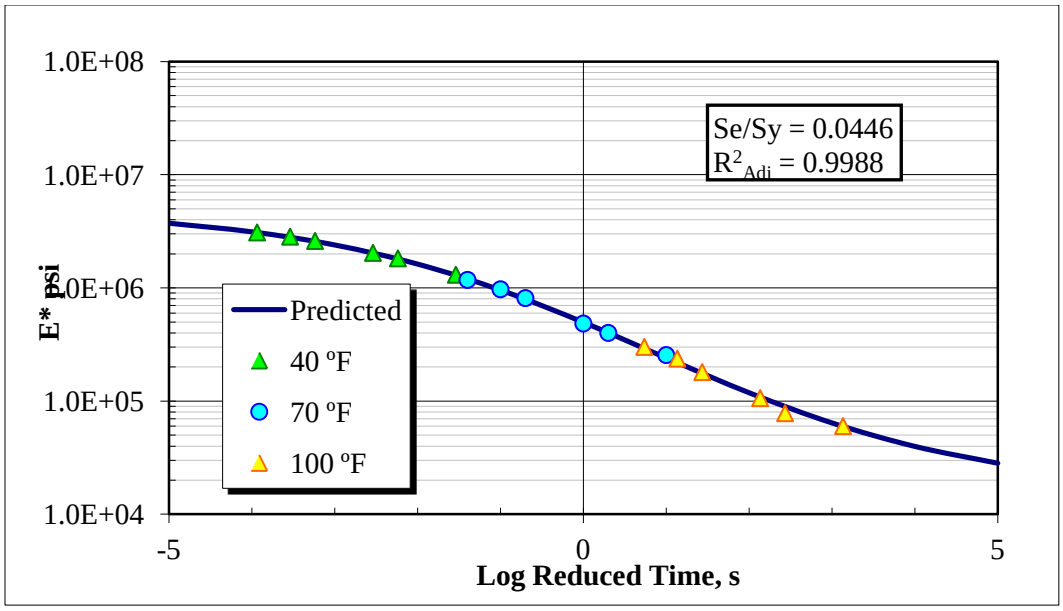

FIGURE 81 Master curves based on average of three replicates for (3 P, 3 A).

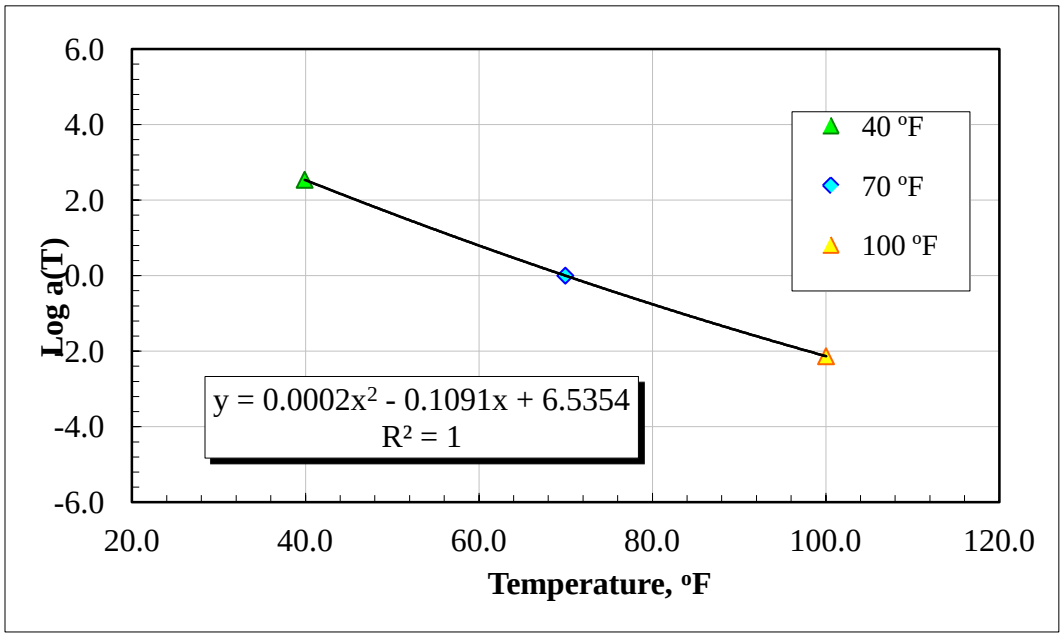

FIGURE 82 Shift factors based on average of three replicates for (3 P, 3 A).

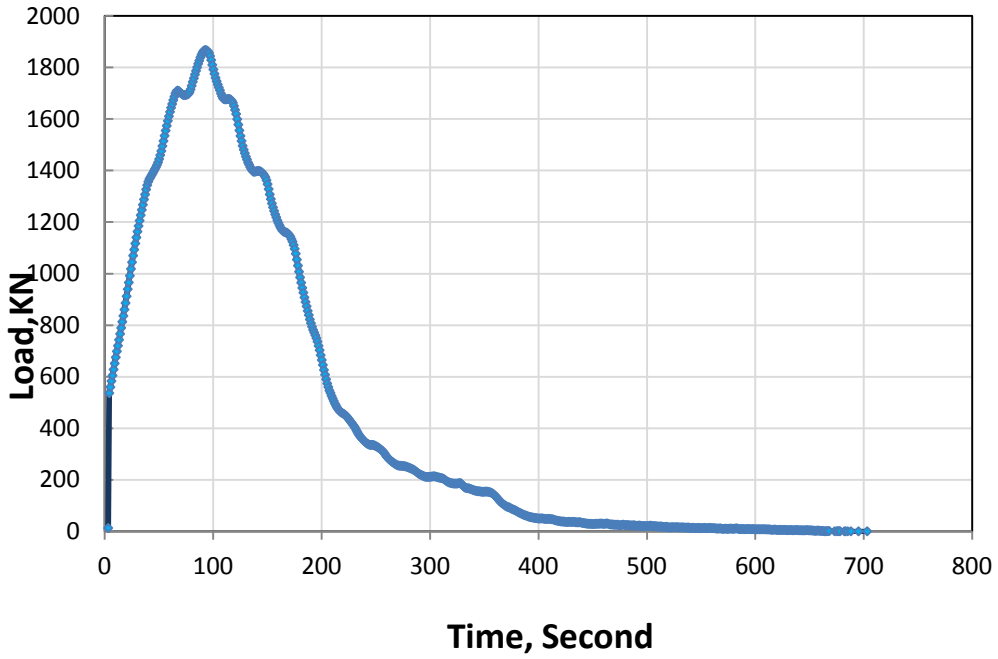

FIGURE 83 Indirect tensile strength for (0 P, 0 A) at 40 ºF.

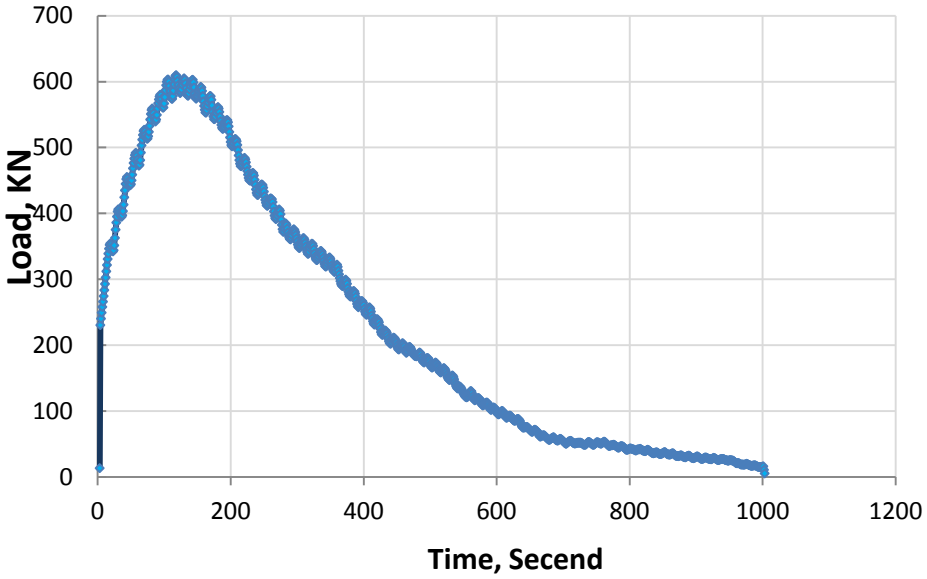

FIGURE 84 Indirect tensile strength for (0 P, 0 A) at 70 ºF.

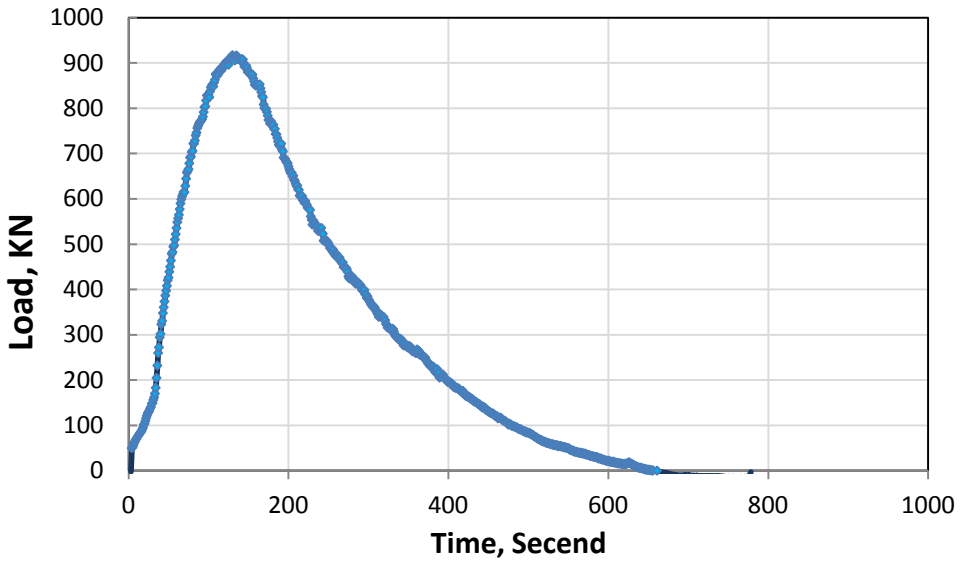

FIGURE 85 Indirect tensile strength for (0 P, 0 A) at 100 ºF.

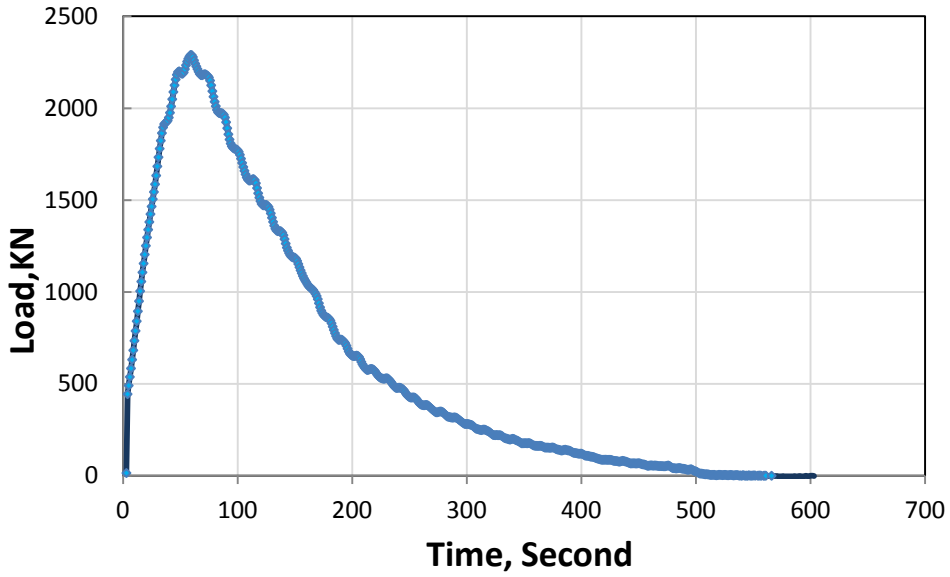

FIGURE 86 Indirect tensile strength for (0 P, 1 A) at 40 ºF.

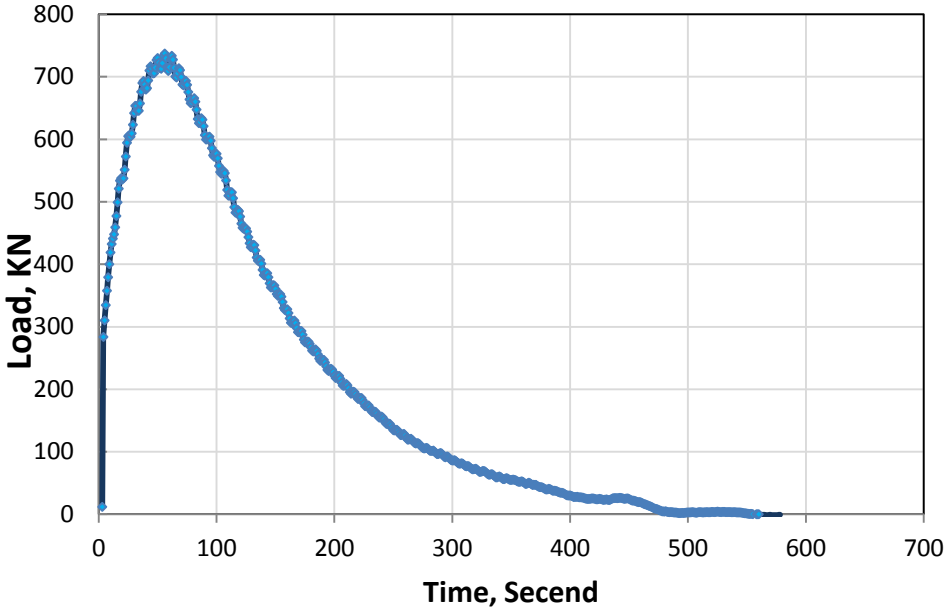

FIGURE 87 Indirect tensile strength for (0 P, 1 A) at 70 ºF.

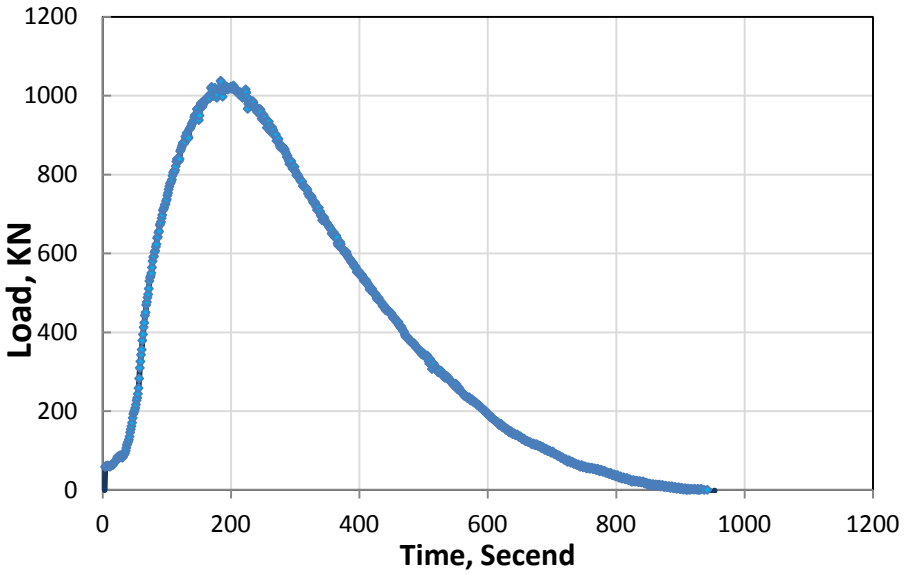

FIGURE 88 Indirect tensile strength for (0 P, 1 A) at 100 ºF.

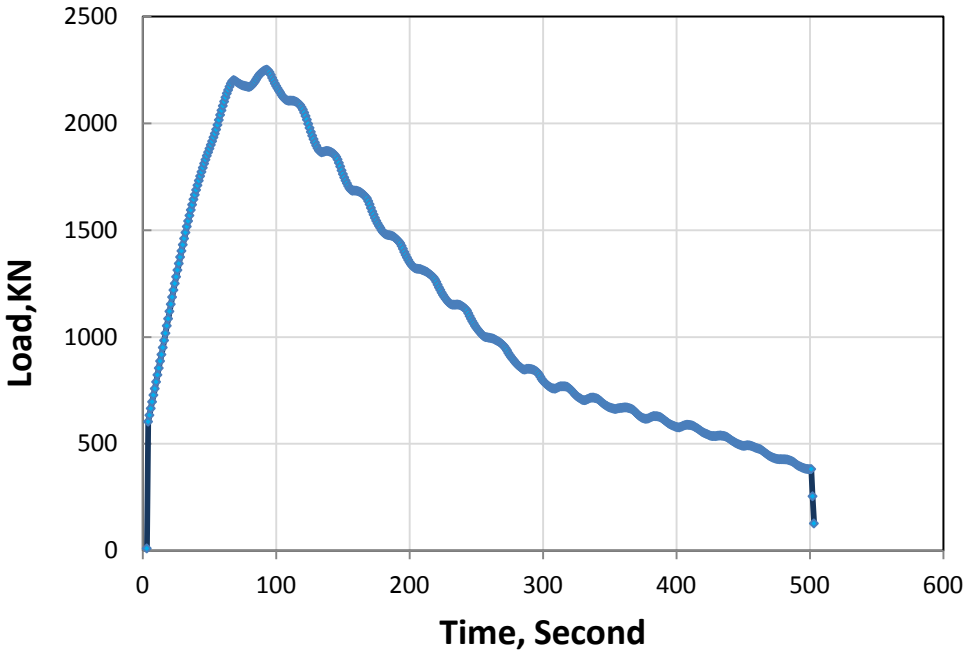

FIGURE 89 Indirect tensile strength for (0 P, 2 A) at 40 ºF.

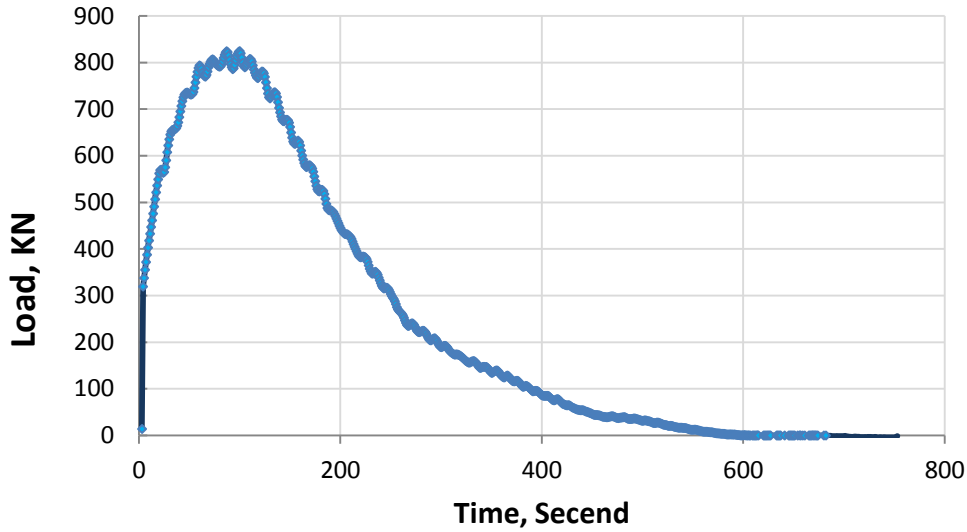

FIGURE 90 Indirect tensile strength for (0 P, 2 A) at 70 ºF

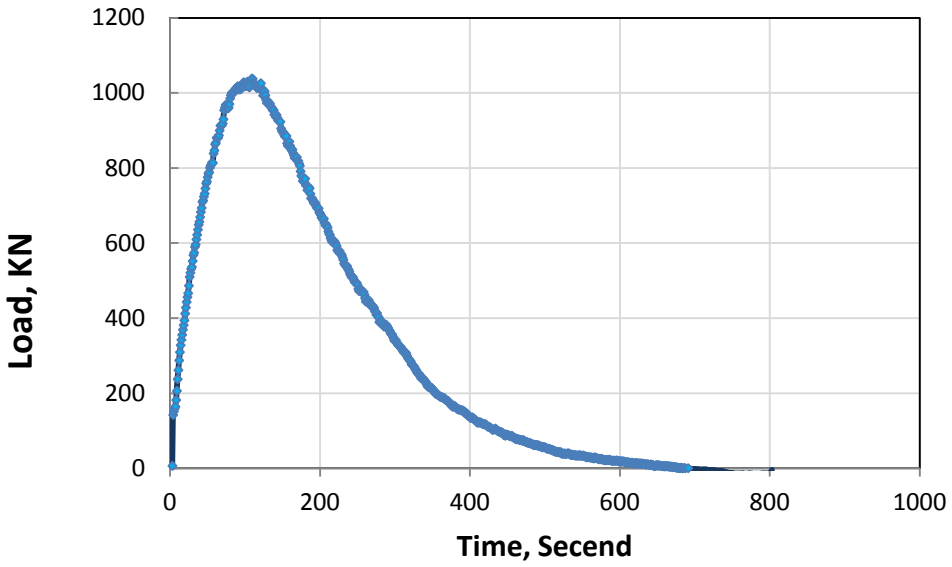

FIGURE 91 Indirect tensile strength for (0 P, 2 A) at 100 ºF.

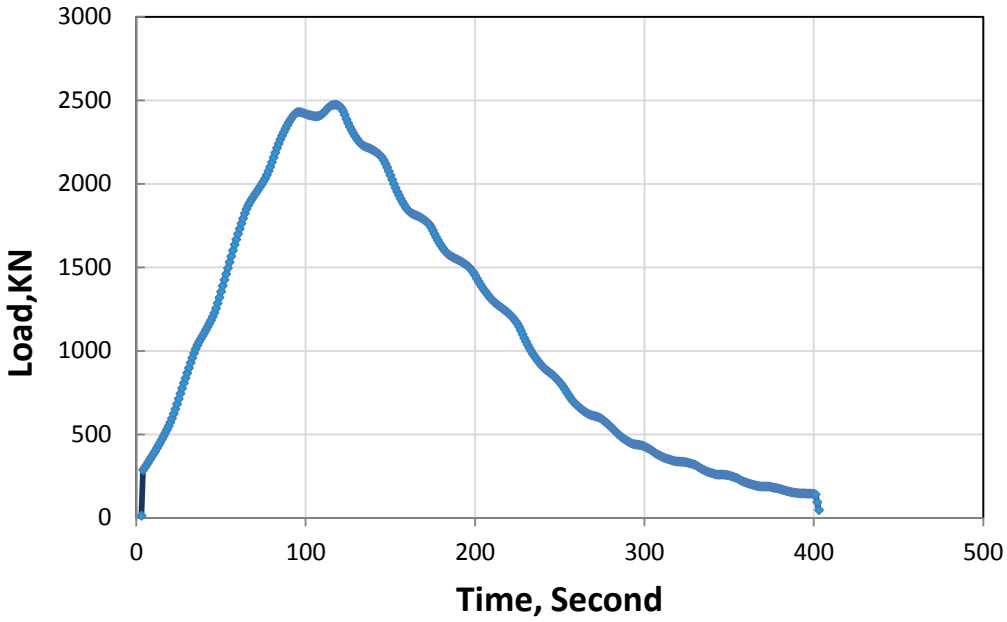

FIGURE 92 Indirect tensile strength for (0 P, 3 A) at 40 ºF

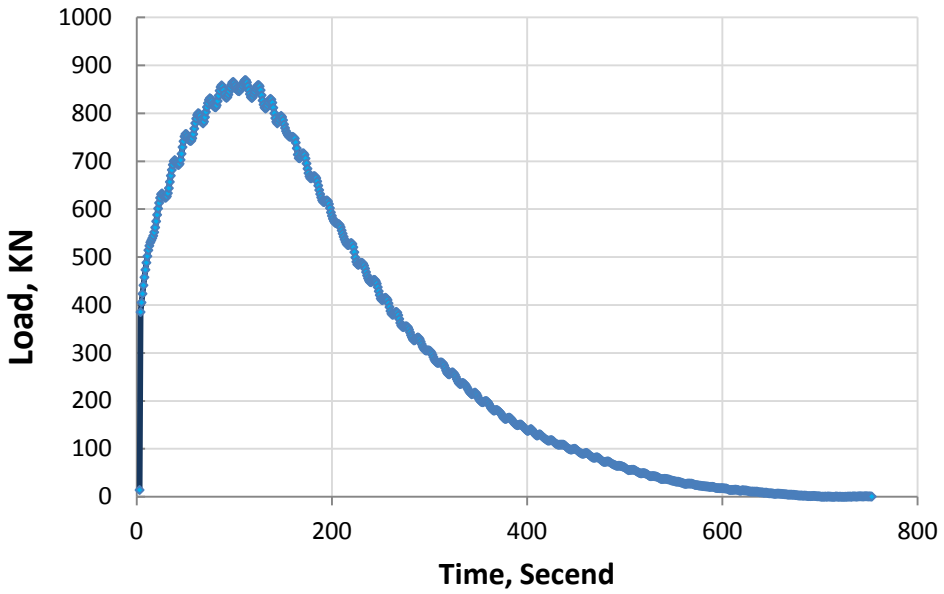

FIGURE 93 Indirect tensile strength for (0 P, 3 A) at 70 ºF

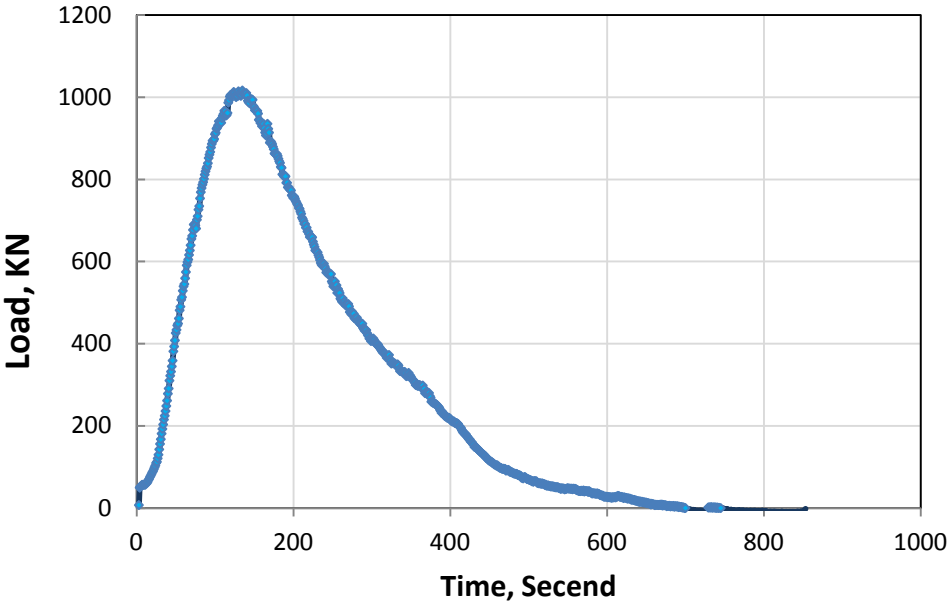

FIGURE 94 Indirect tensile strength for (0 P, 3 A) at 100 ºF

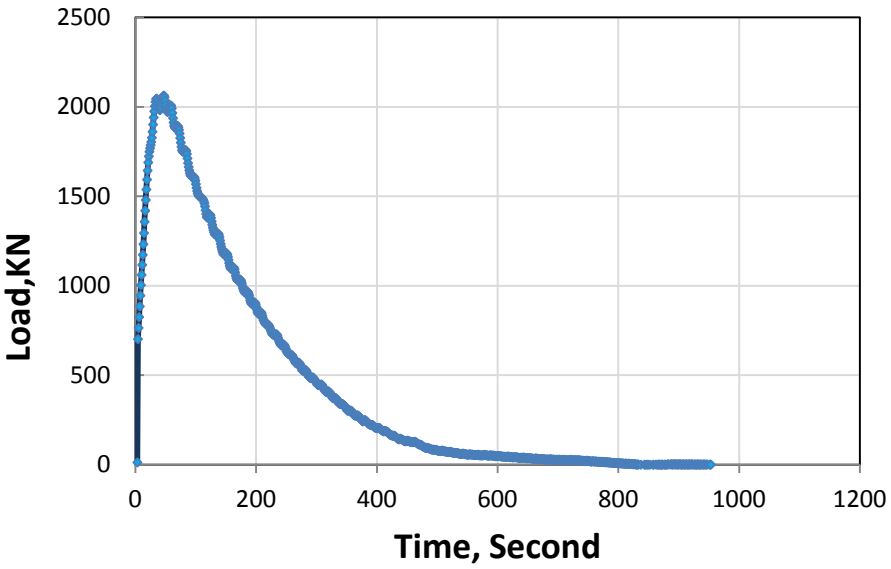

FIGURE 95 Indirect tensile strength for (1 P, 0 A) at 40 ºF.

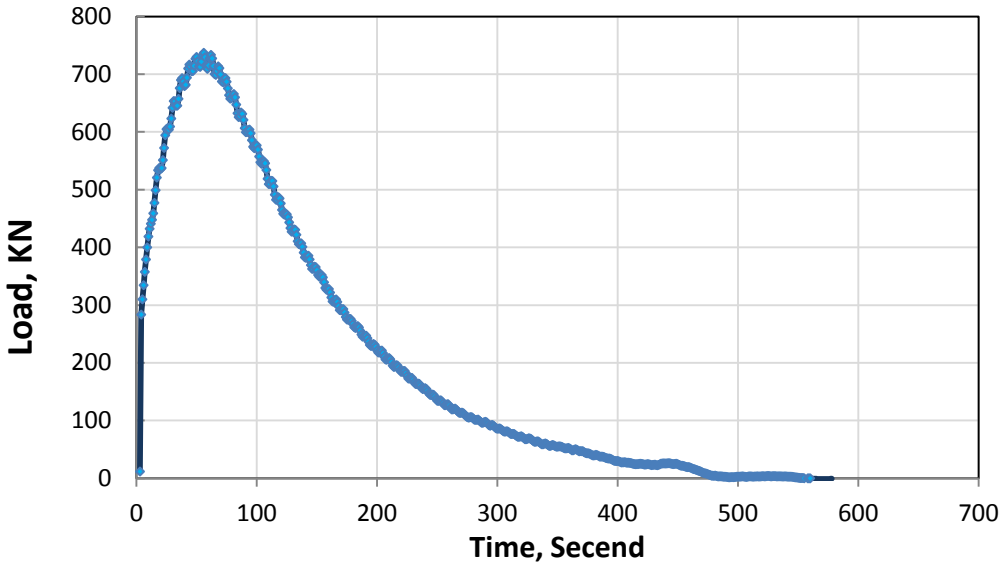

FIGURE 96 Indirect tensile strength for (1 P, 0 A) at 70 ºF.

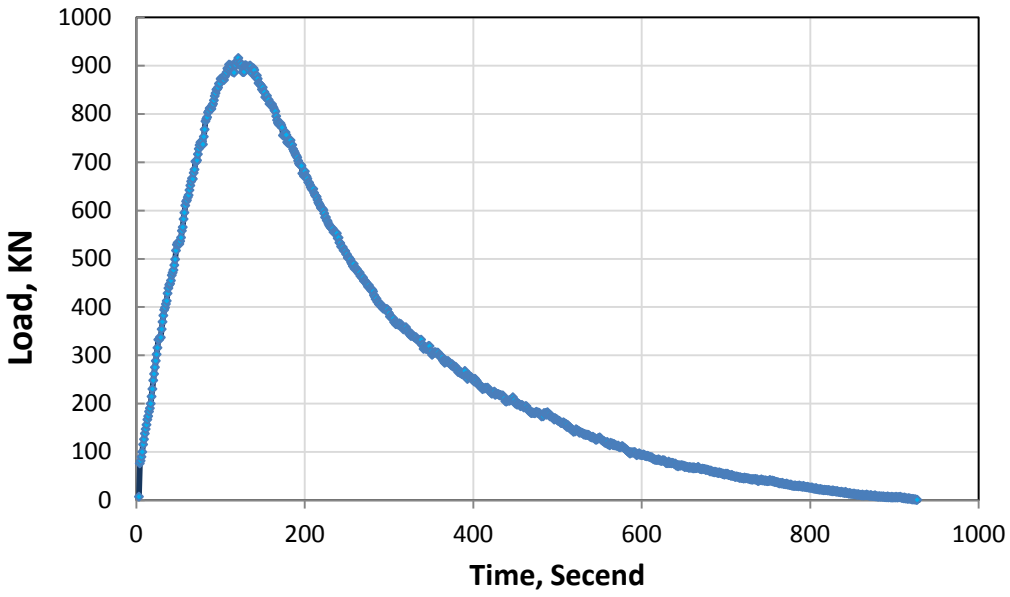

FIGURE 97 Indirect tensile strength for (1 P, 0 A) at 100 ºF.

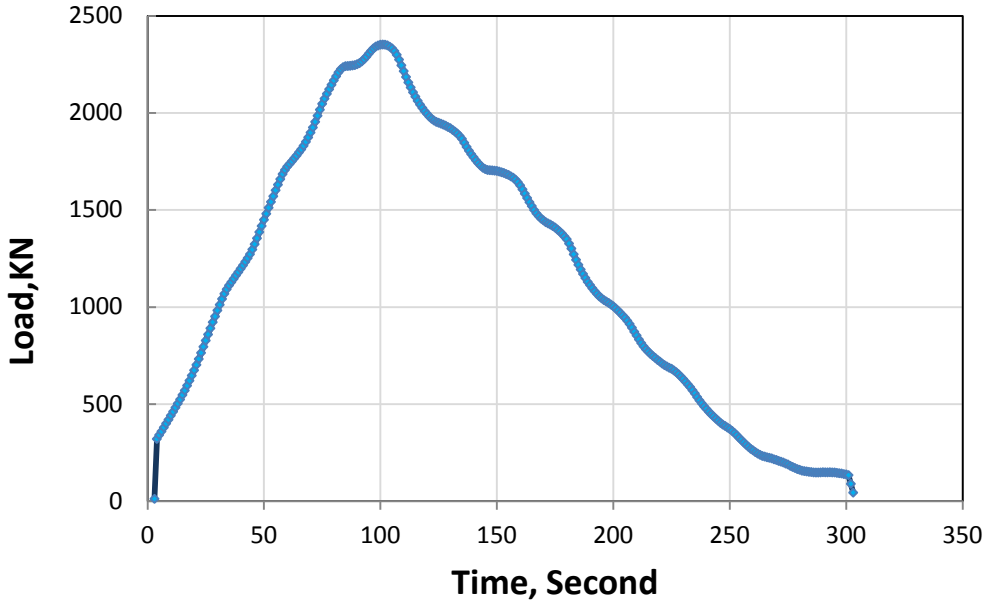

FIGURE 98 Indirect tensile strength for (1 P, 1 A) at 40 ºF.

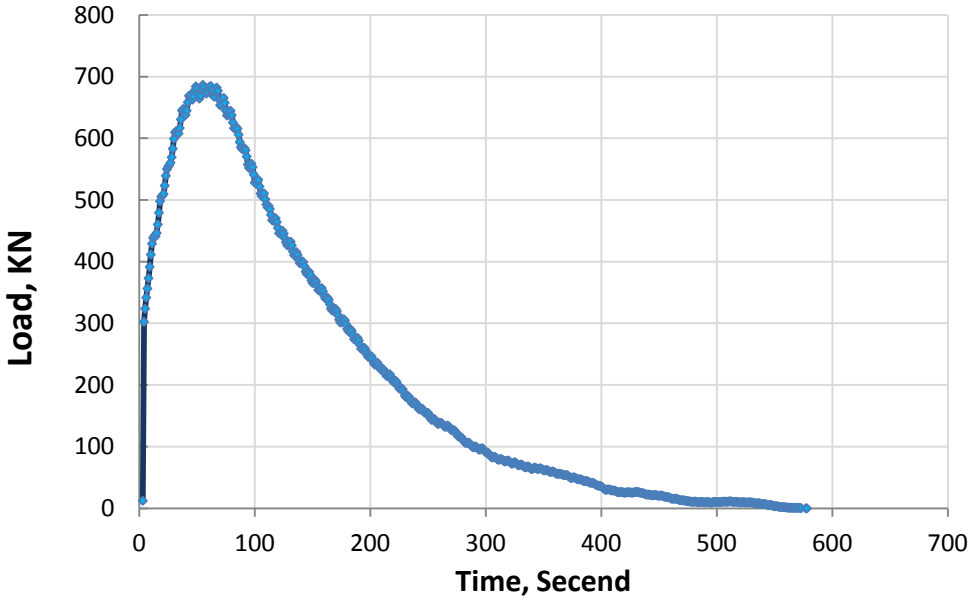

FIGURE 99 Indirect tensile strength for (1 P, 1 A) at 70 ºF.

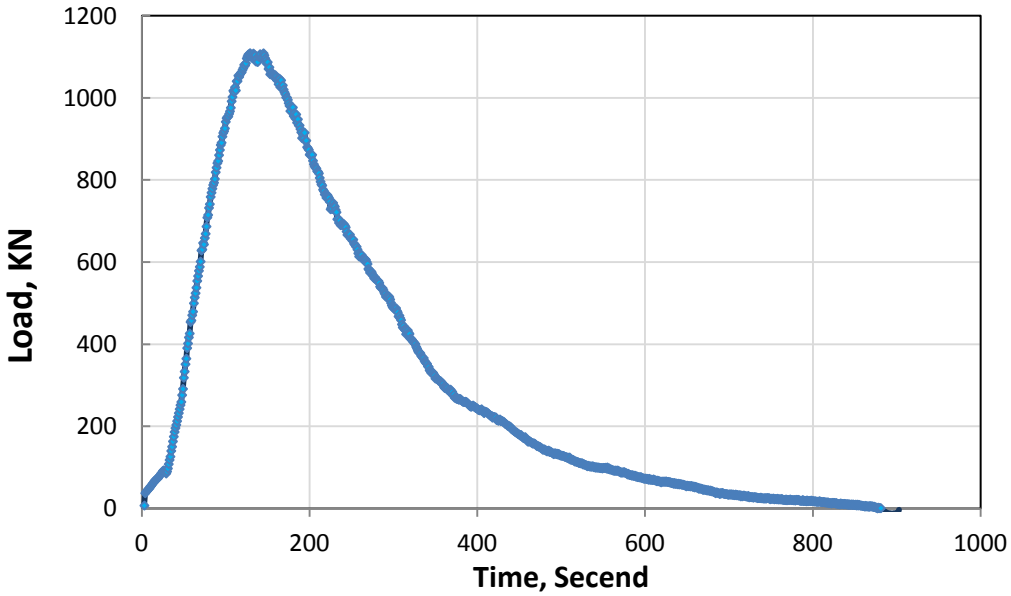

FIGURE 100 Indirect tensile strength for (1 P, 1 A) at 100 ºF.

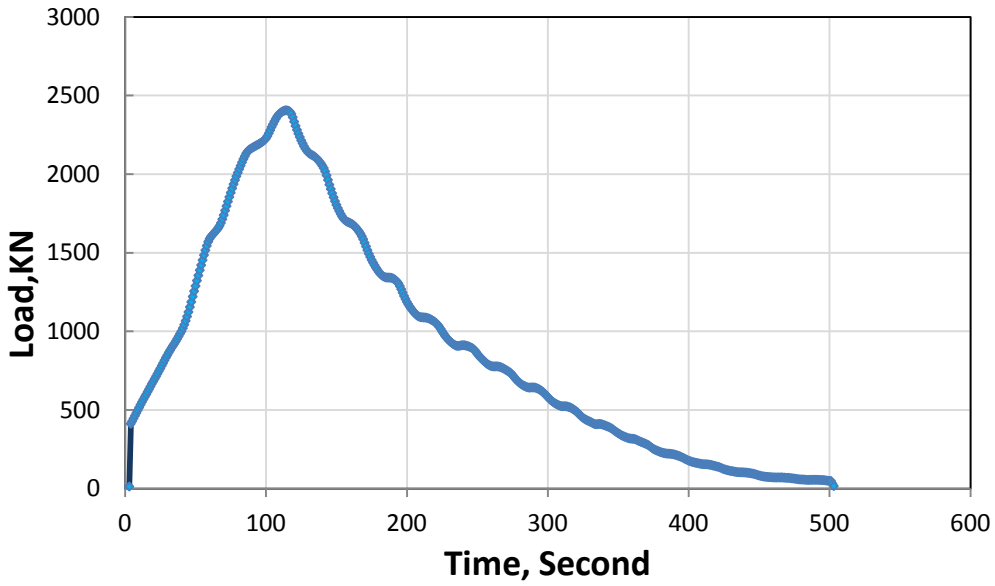

FIGURE 101 Indirect tensile strength for (1 P, 2 A) at 40 ºF.

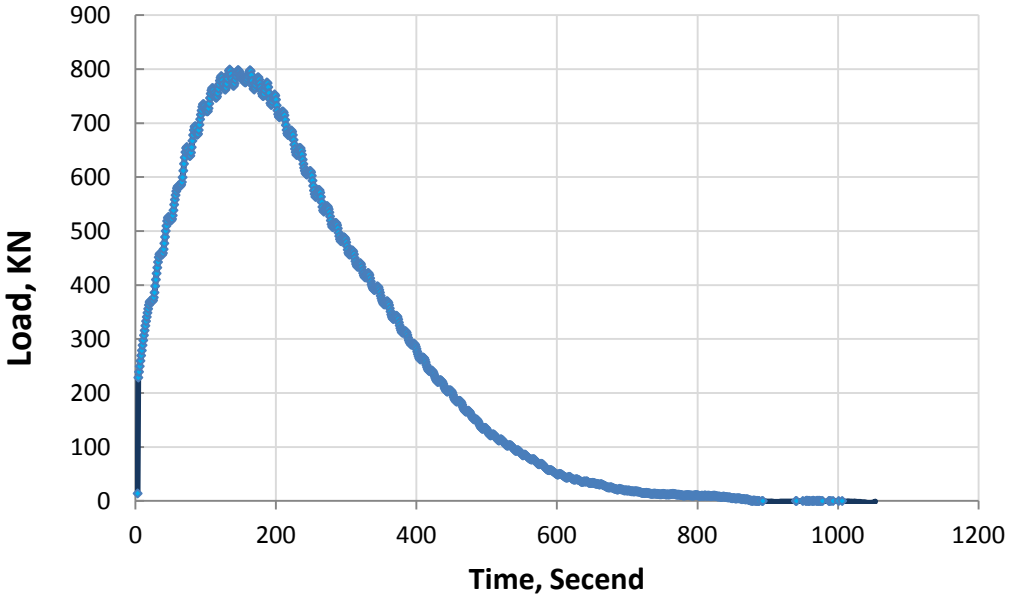

FIGURE 102 Indirect tensile strength for (1 P, 2 A) at 70 ºF.

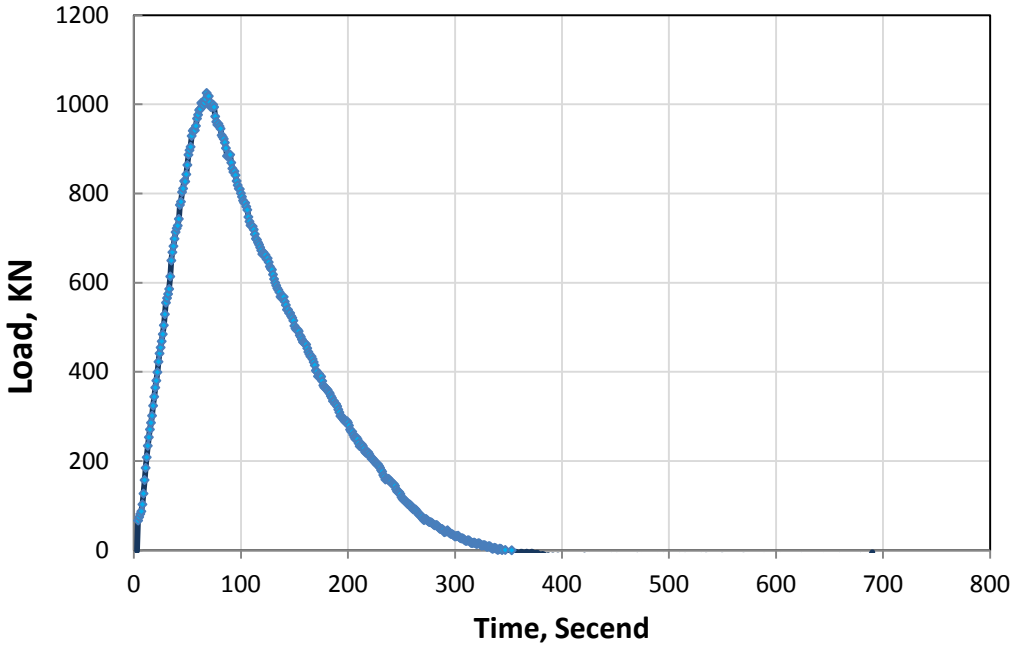

FIGURE 103 Indirect tensile strength for (1 P, 2 A) at 100 ºF.

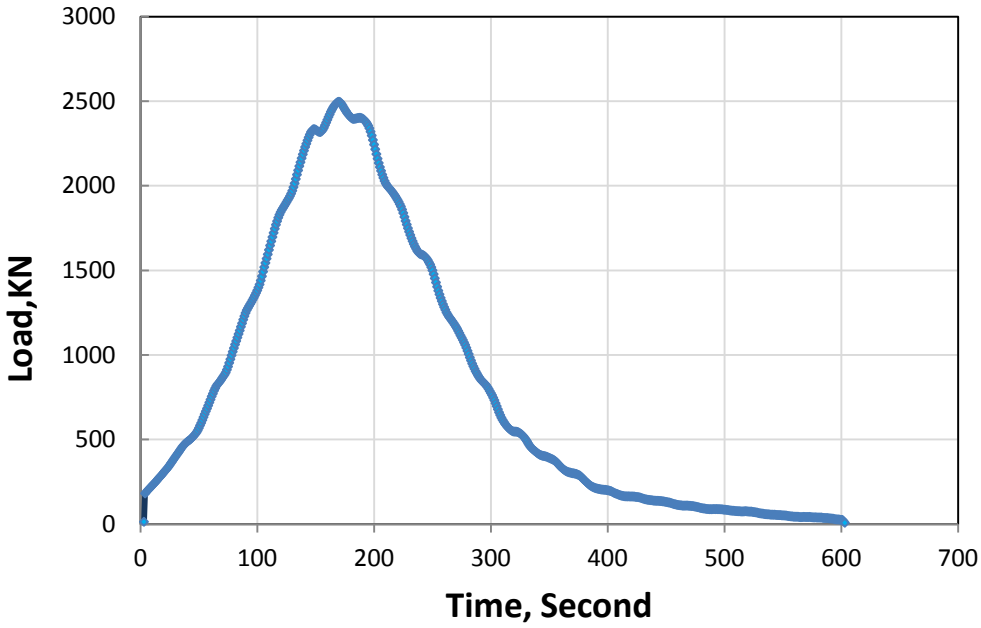

FIGURE 104 Indirect tensile strength for (1 P, 3 A) at 40 ºF.

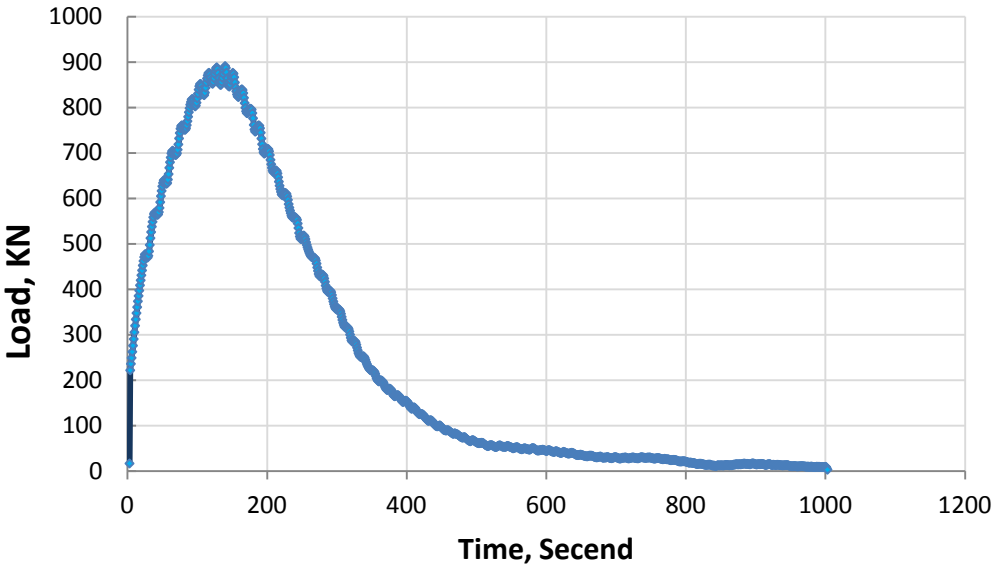

FIGURE 105 Indirect tensile strength for (1 P, 3 A) at 70 ºF.

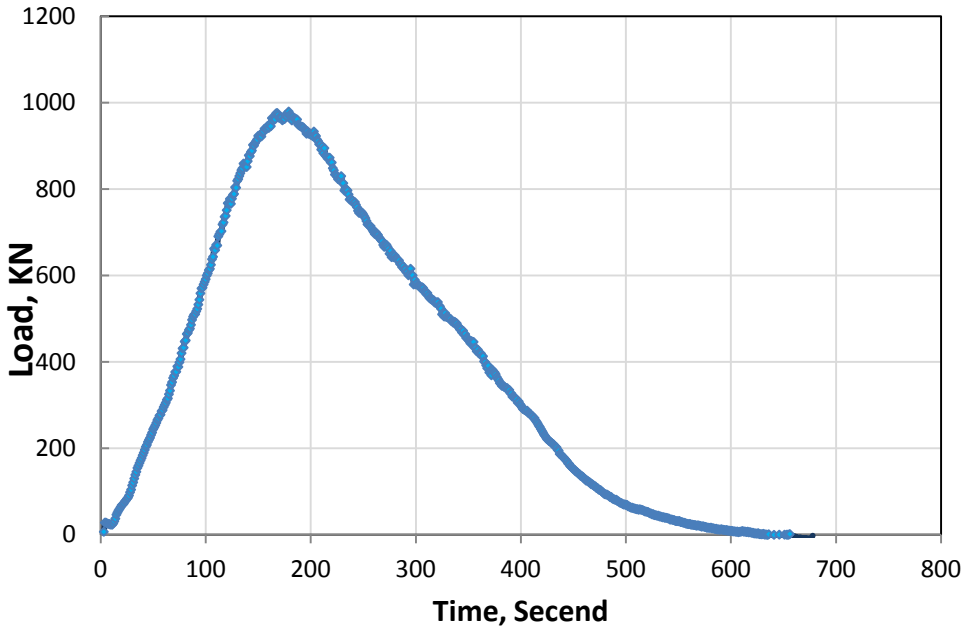

FIGURE 106 Indirect tensile strength for (1 P, 3 A) at 100 ºF.

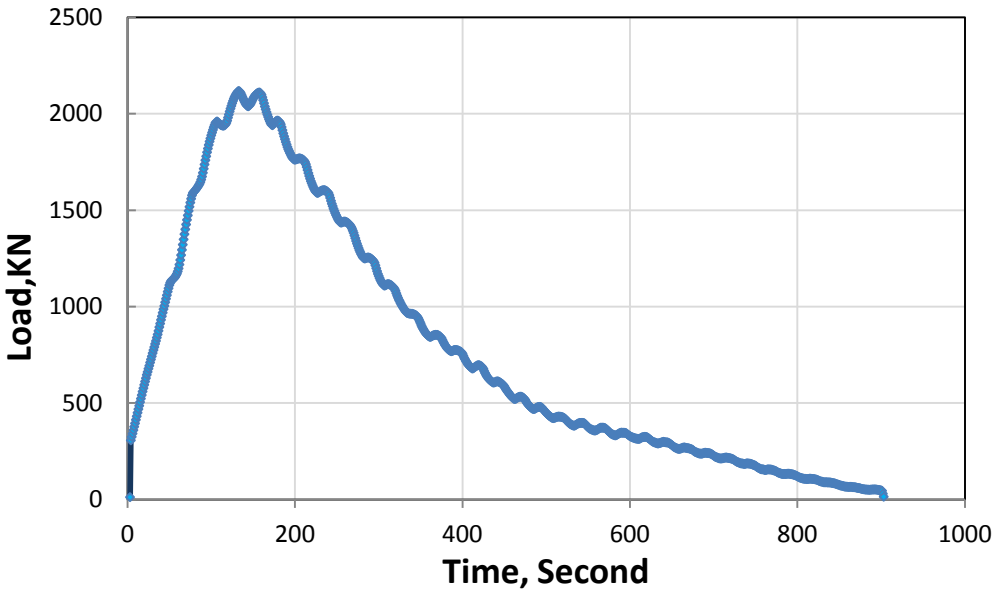

FIGURE 107 Indirect tensile strength for (2 P, 0 A) at 40 ºF.

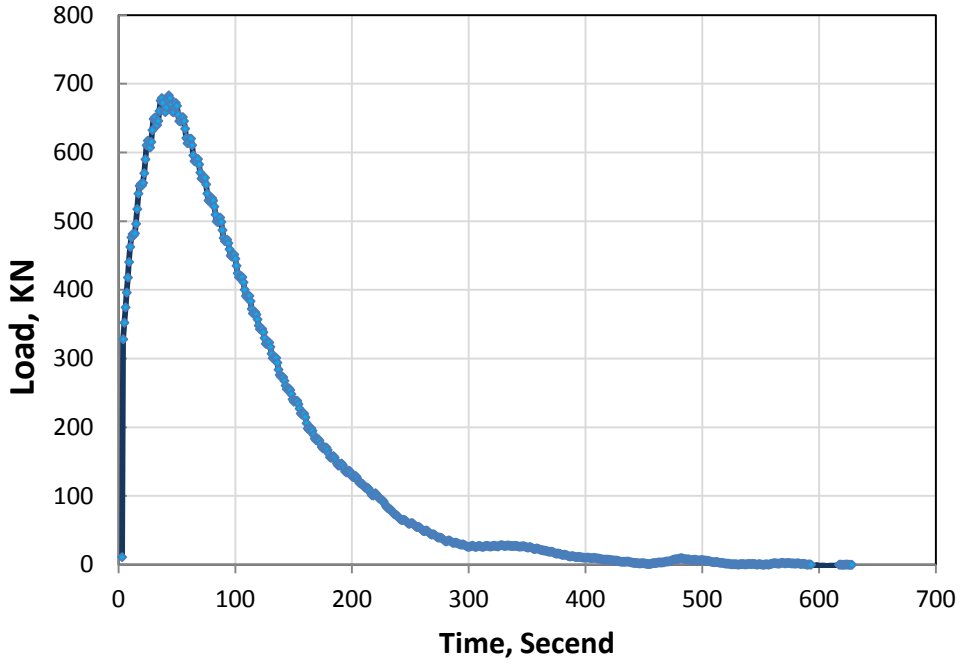

FIGURE 108 Indirect tensile strength for (2 P, 0 A) at 70 ºF.

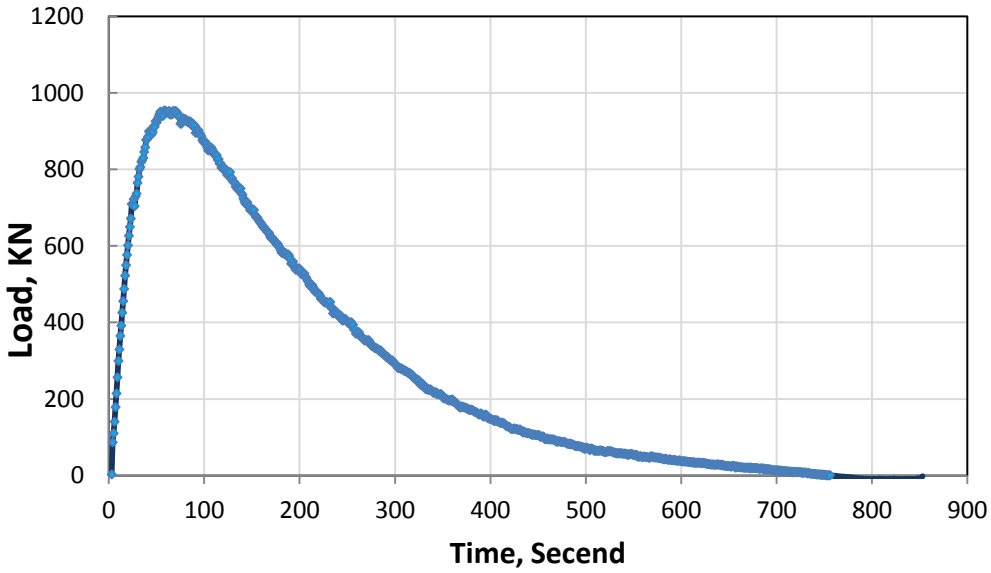

FIGURE 109 Indirect tensile strength for (2 P, 0 A) at 100 ºF.

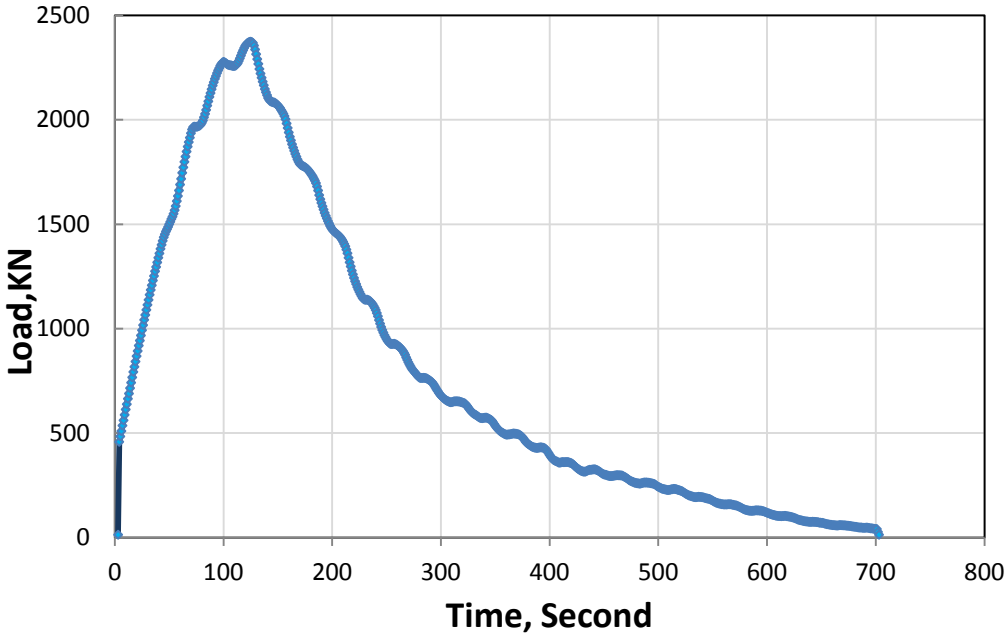

FIGURE 110 Indirect tensile strength for (2 P, 1 A) at 40 ºF.

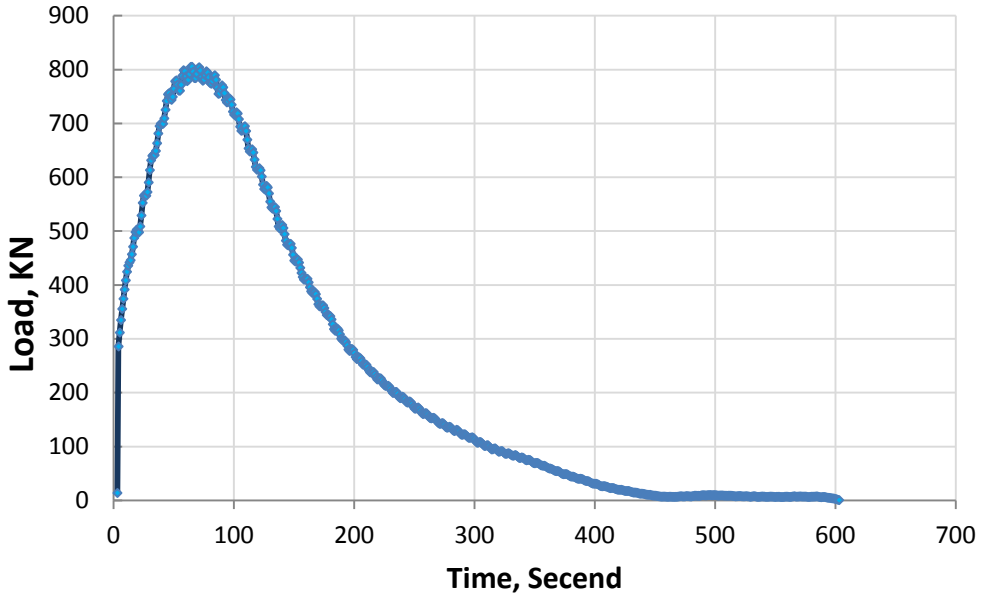

FIGURE 111 Indirect tensile strength for (2 P, 1 A) at 70 ºF.

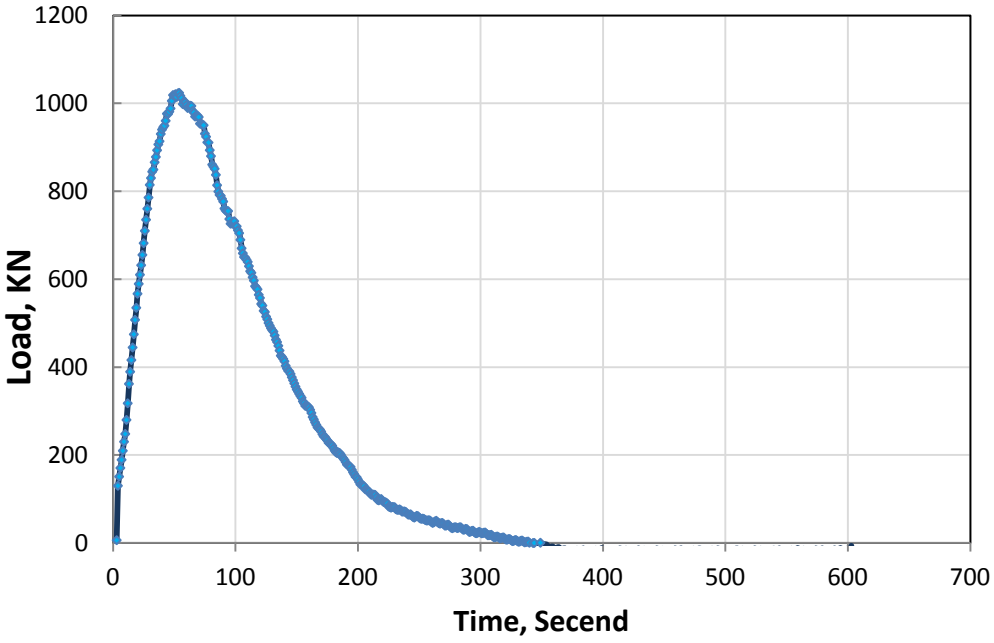

FIGURE 112 Indirect tensile strength for (2 P, 1 A) at 100 ºF.

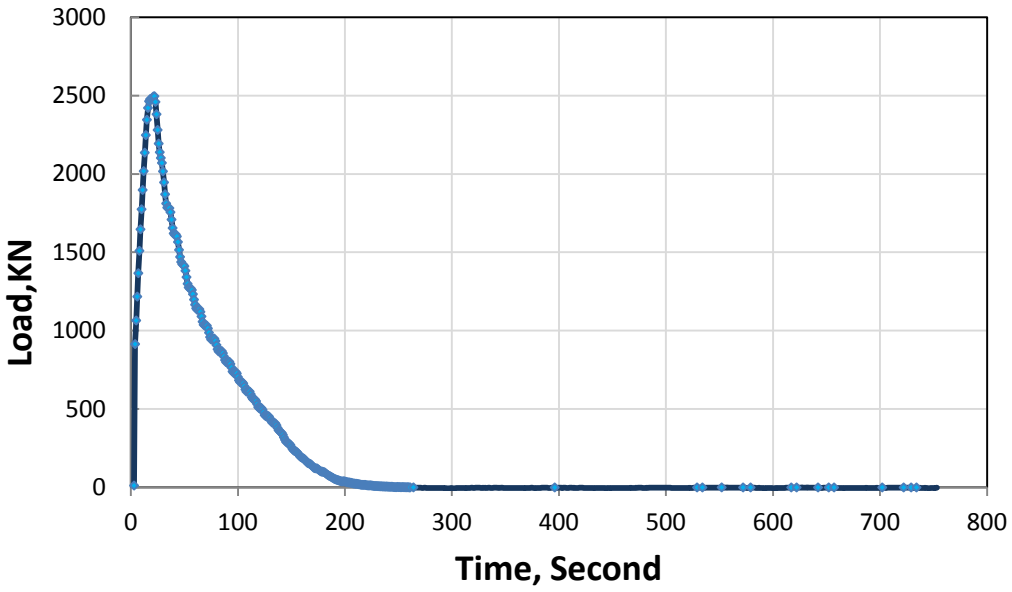

FIGURE 113 Indirect tensile strength for (2 P, 2 A) at 40 ºF.

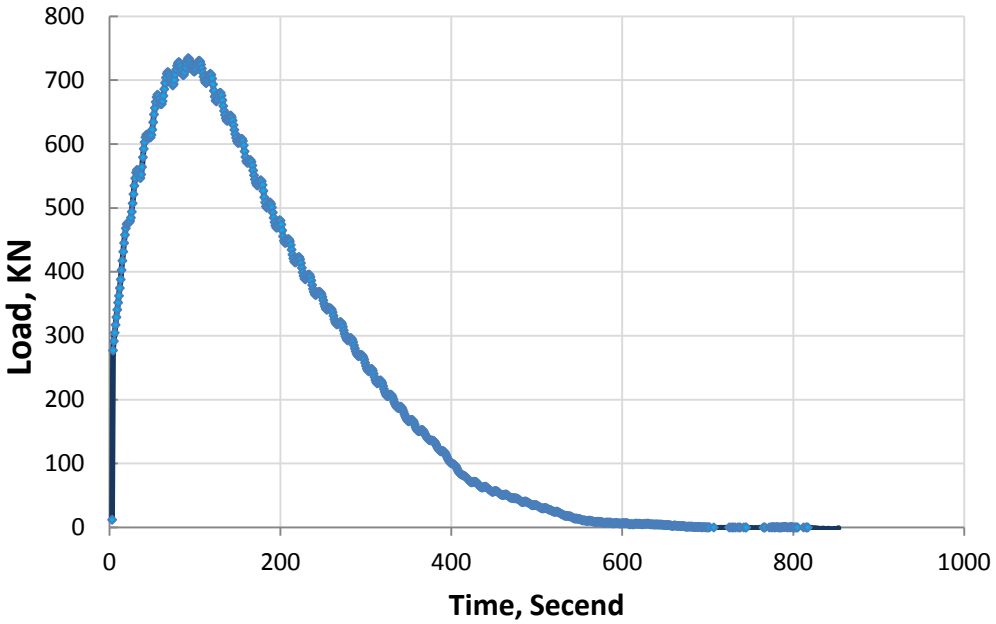

FIGURE 114 Indirect tensile strength for (2 P, 2 A) at 70 ºF.

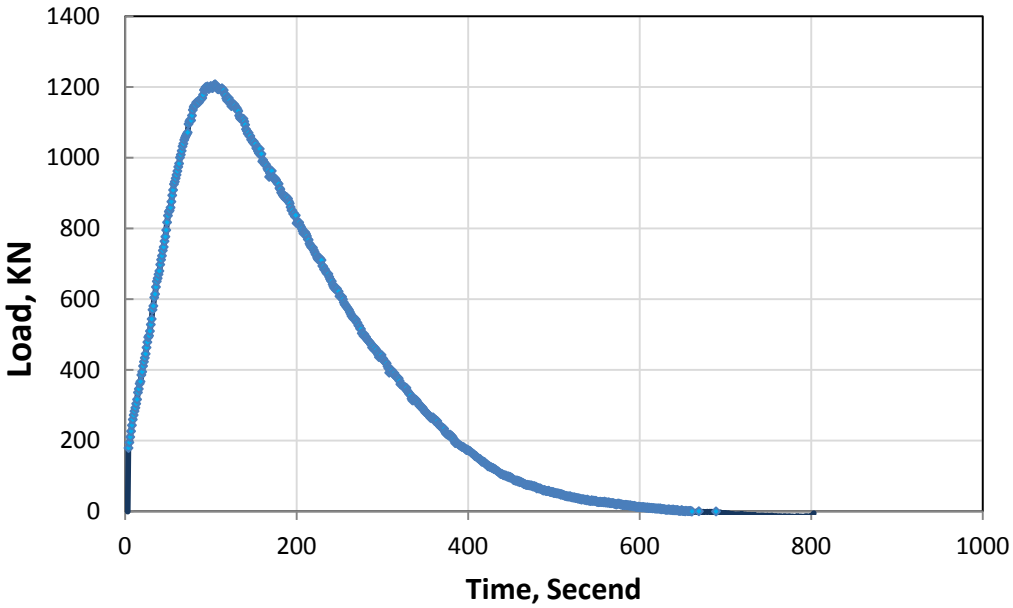

FIGURE 115 Indirect tensile strength for (2 P, 2 A) at 100 ºF.

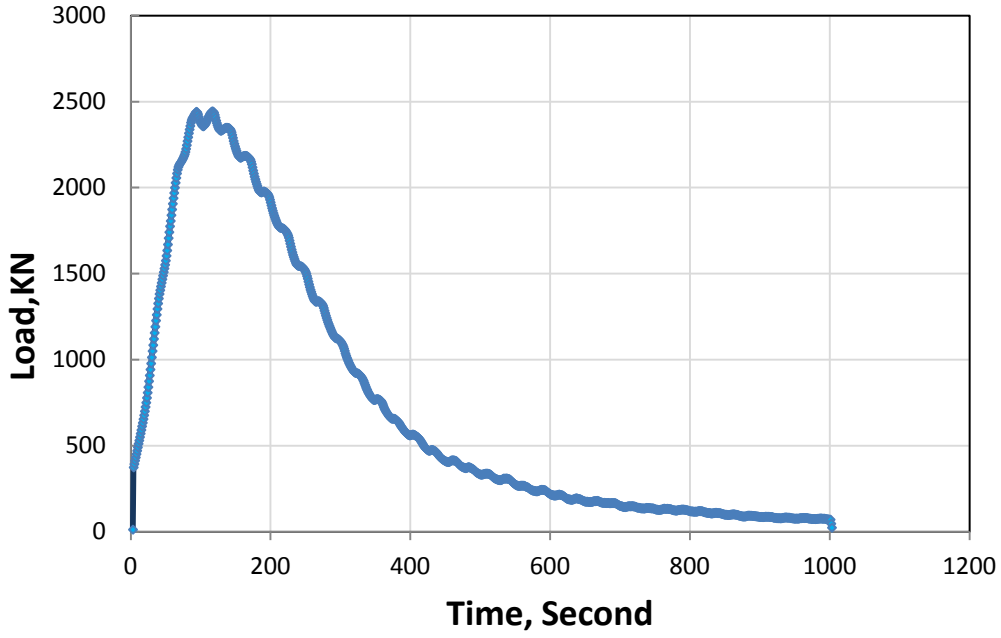

FIGURE 116 Indirect tensile strength for (2 P, 3 A) at 40 ºF.

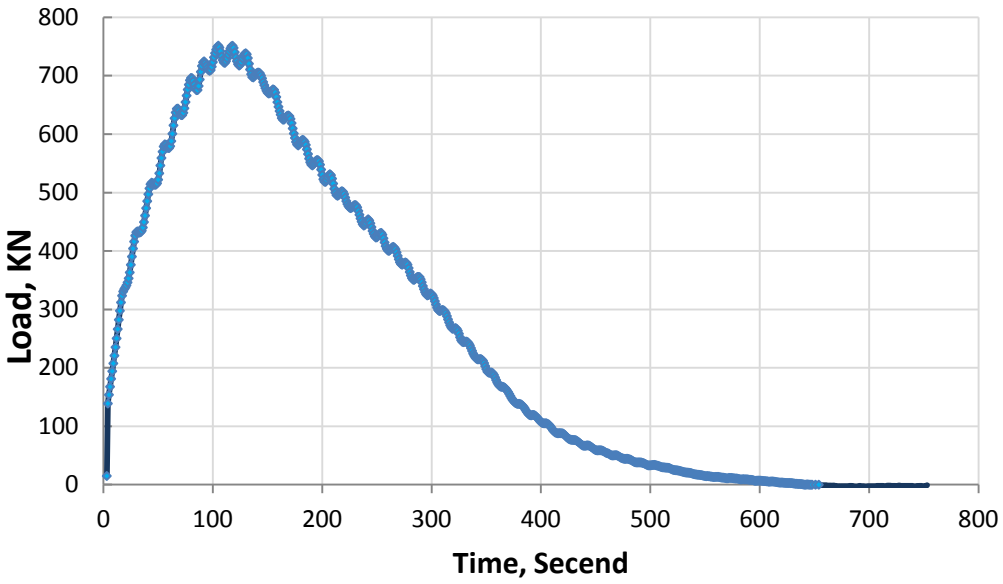

FIGURE 117 Indirect tensile strength for (2 P, 3 A) at 70 ºF.

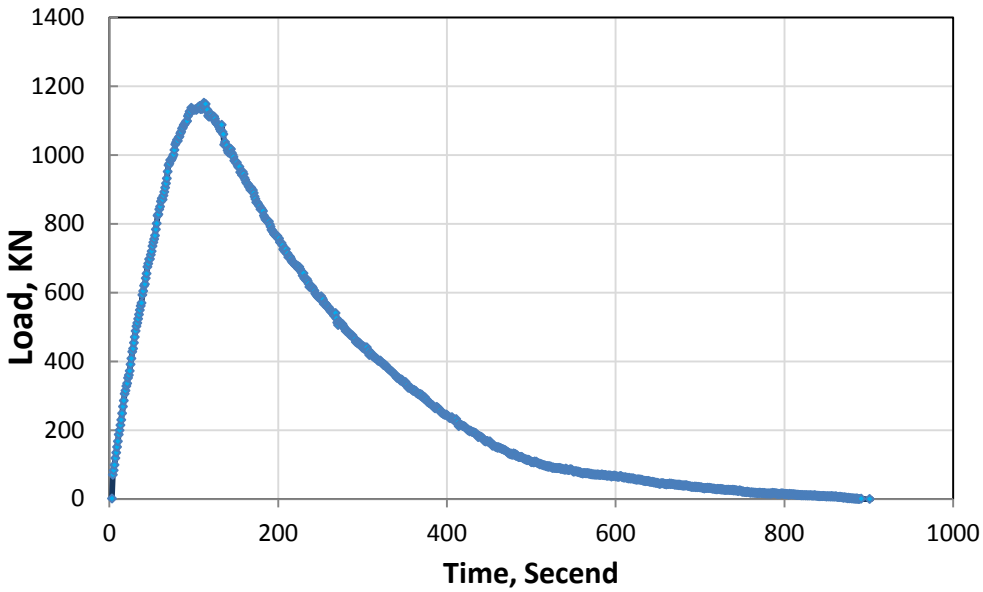

FIGURE 118 Indirect tensile strength for (2 P, 3 A) at 100 ºF.

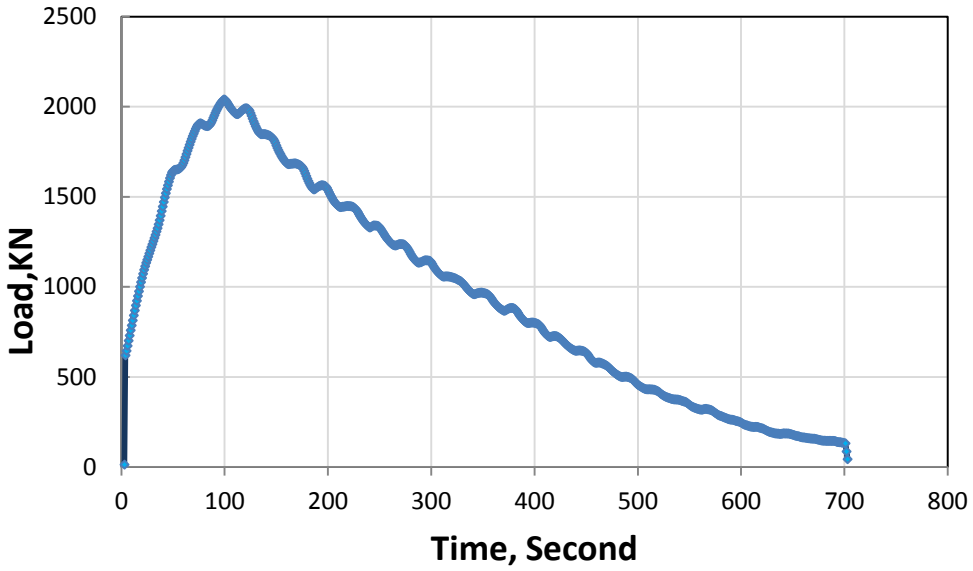

FIGURE 119 Indirect tensile strength for (3 P, 0 A) at 40 ºF.

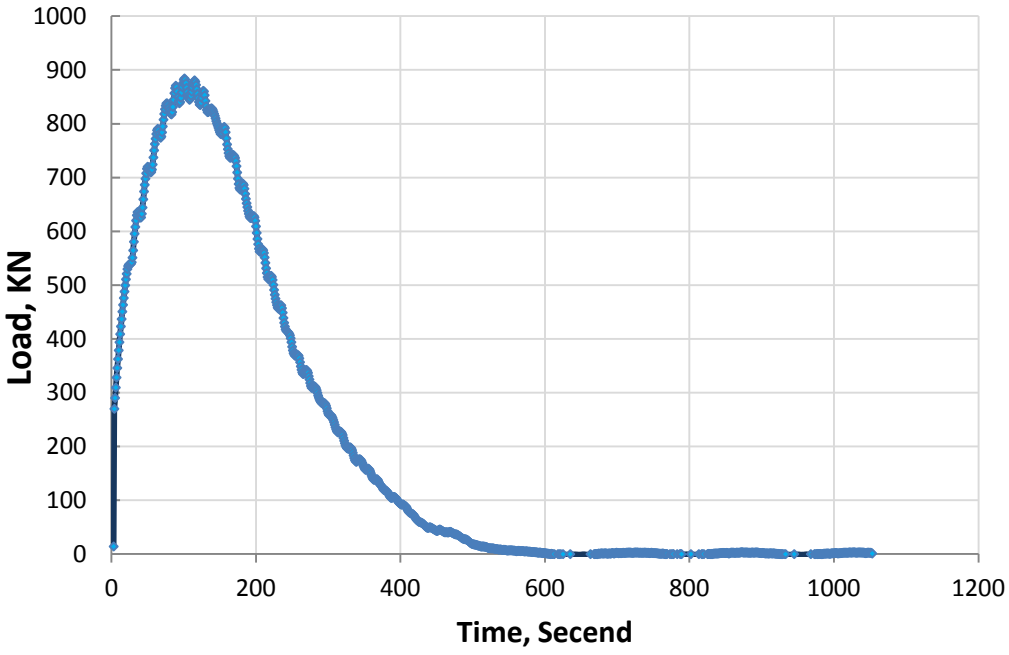

FIGURE 120 Indirect tensile strength for (3 P, 0 A) at 70 ºF.

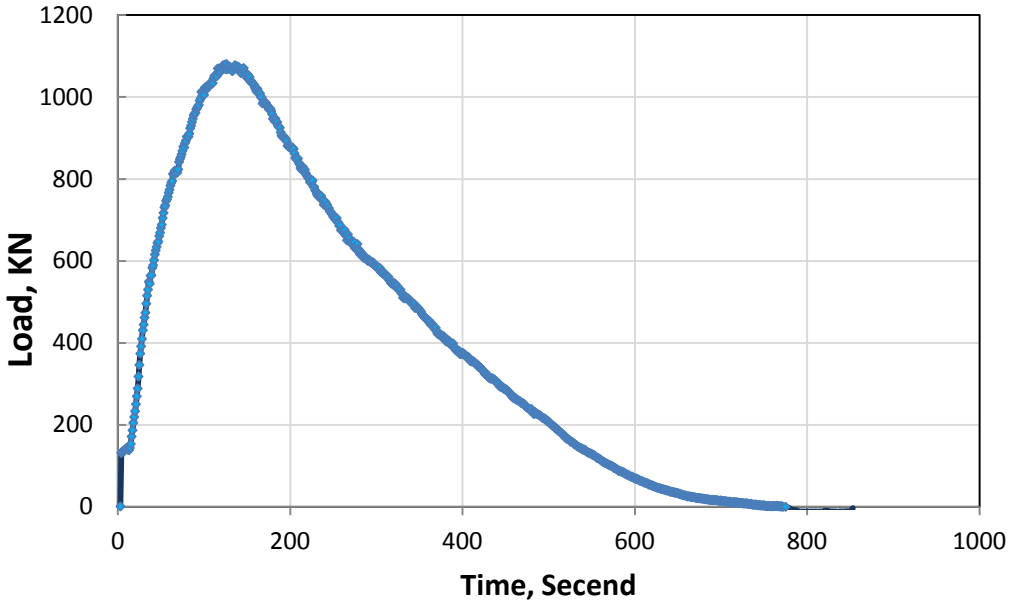

FIGURE 121 Indirect tensile strength for (3 P, 0 A) at 100 ºF.

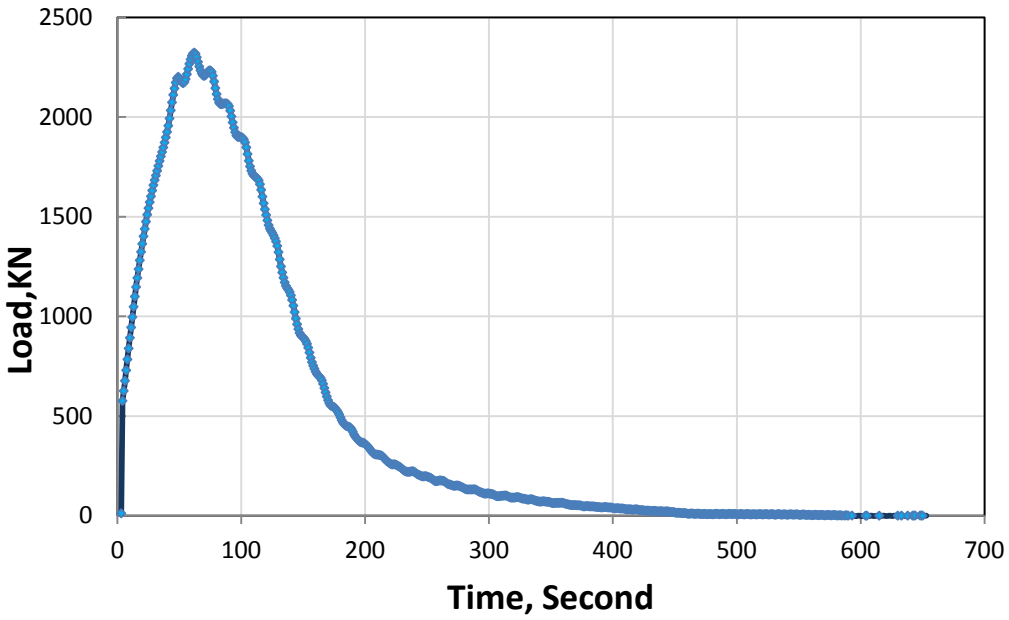

FIGURE 122 Indirect tensile strength for (3 P, 1 A) at 40 ºF.

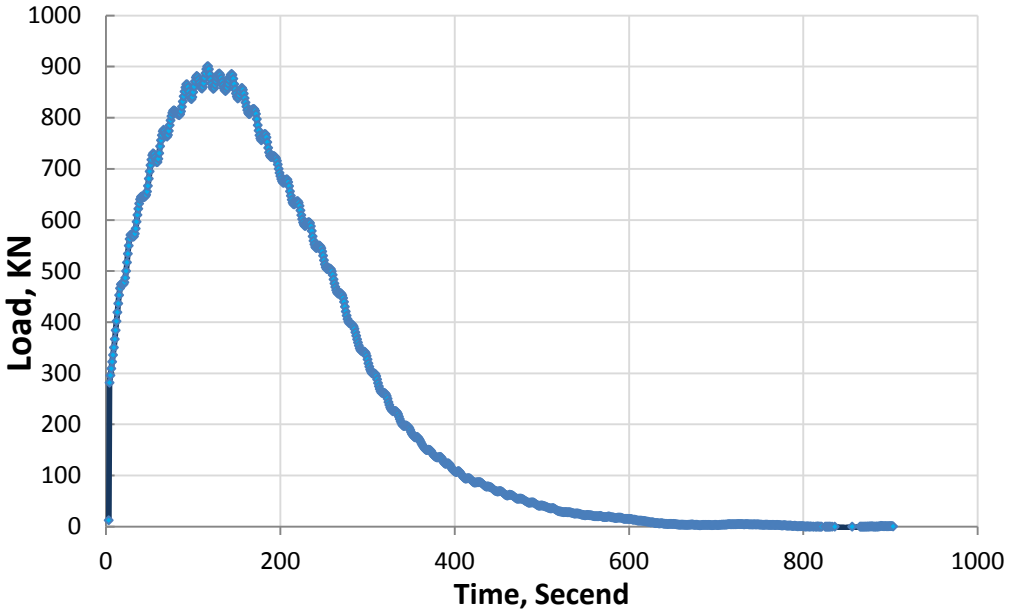

FIGURE 123 Indirect tensile strength for (3 P, 1 A) at 70 ºF.

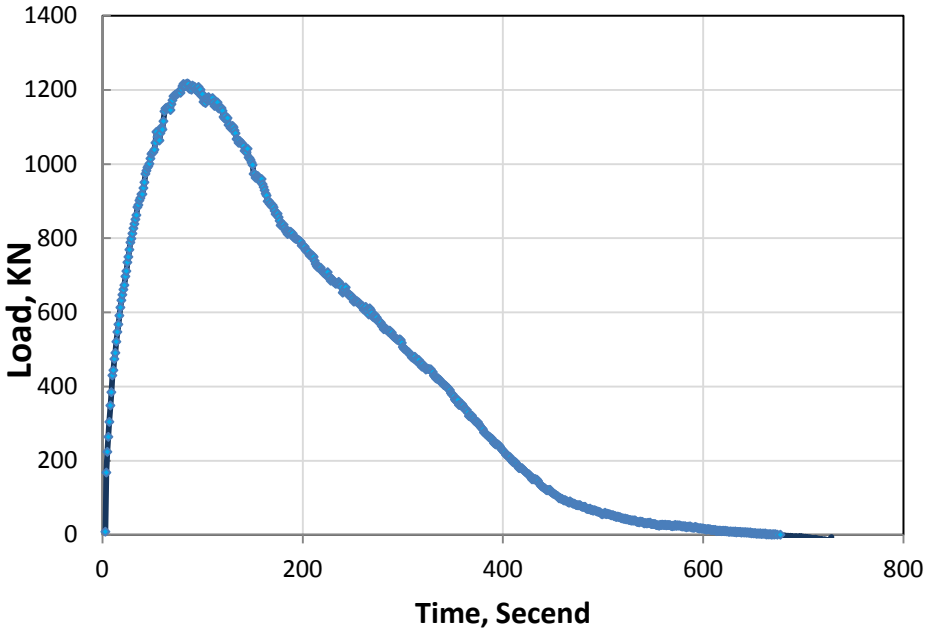

FIGURE 124 Indirect tensile strength for (3 P, 1 A) at 100 ºF.

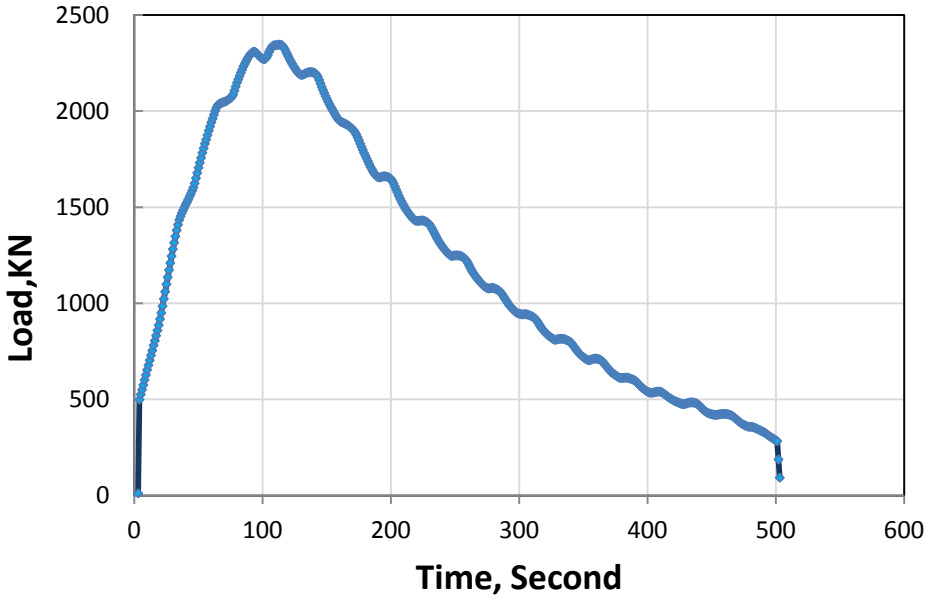

FIGURE 125 Indirect tensile strength for (3 P, 2 A) at 40 ºF.

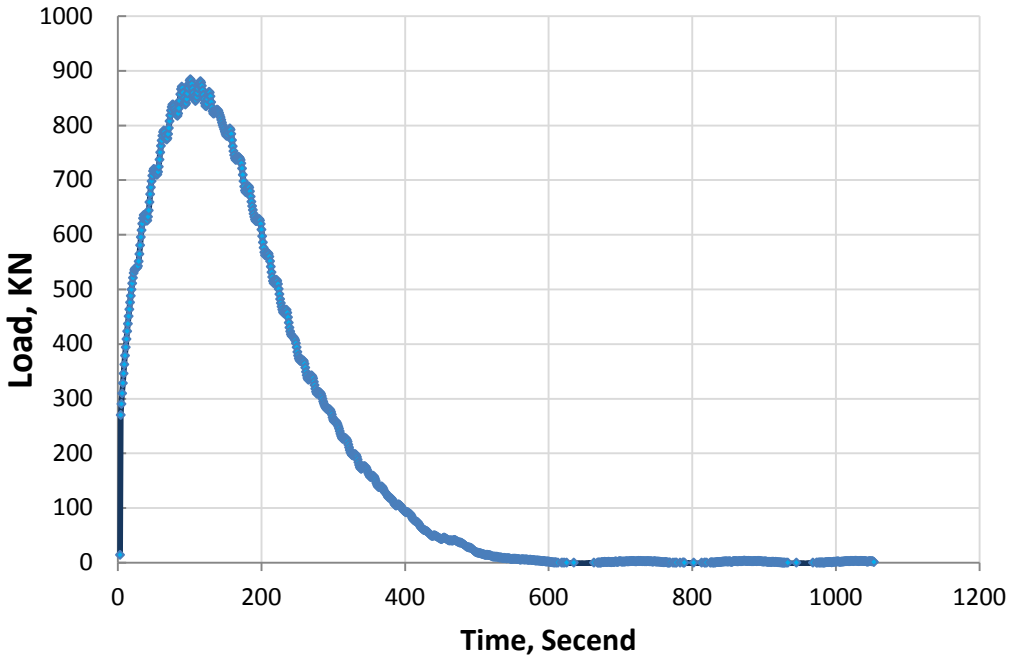

FIGURE 126 Indirect tensile strength for (3 P, 2 A) at 70 ºF.

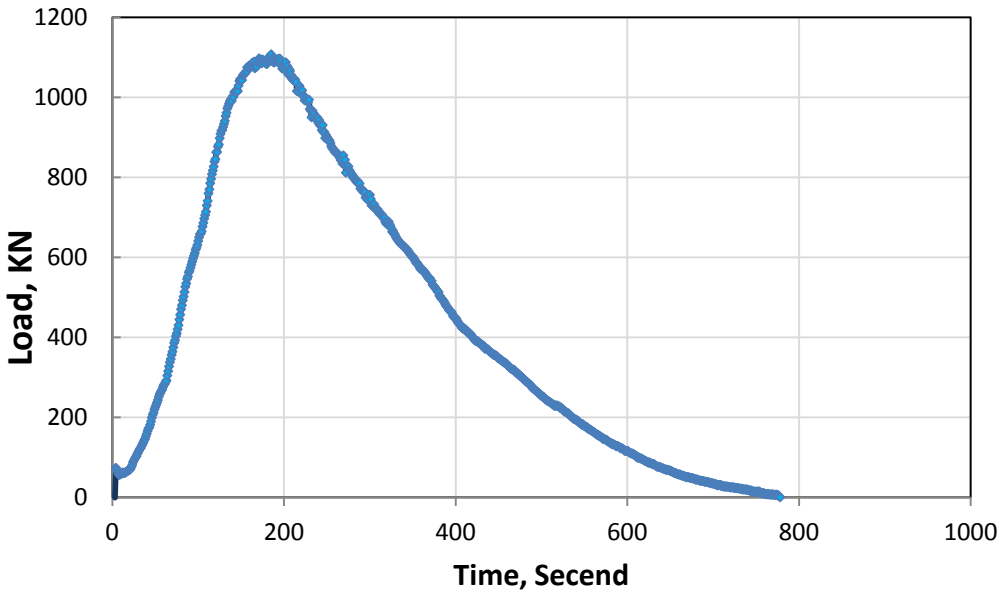

FIGURE 127 Indirect tensile strength for (3 P, 2 A) at 100 ºF.

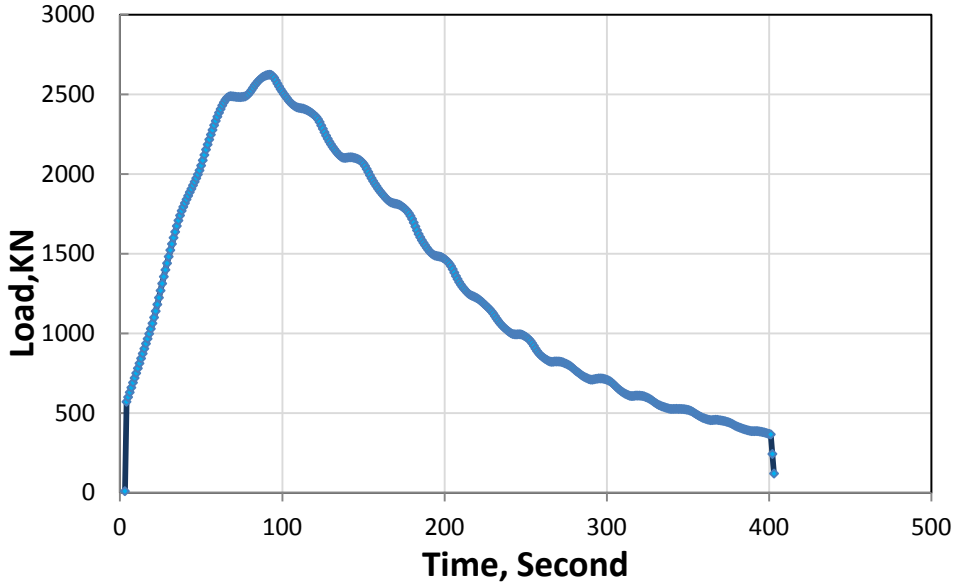

FIGURE 128 Indirect tensile strength for (3 P, 3 A) at 40 ºF.

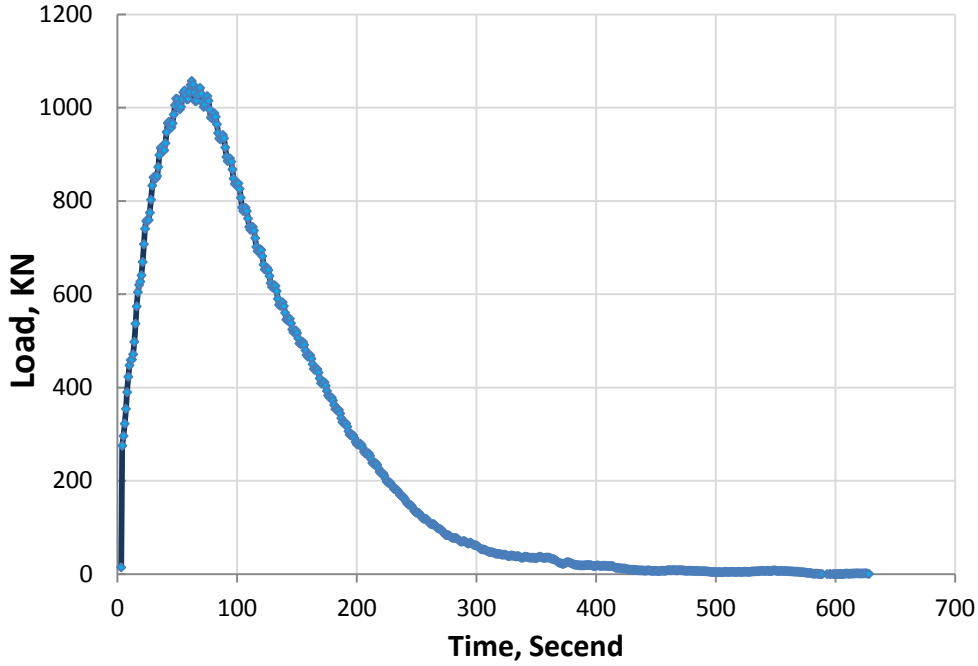

FIGURE 129 Indirect tensile strength for (3 P, 3 A) at 70 ºF.

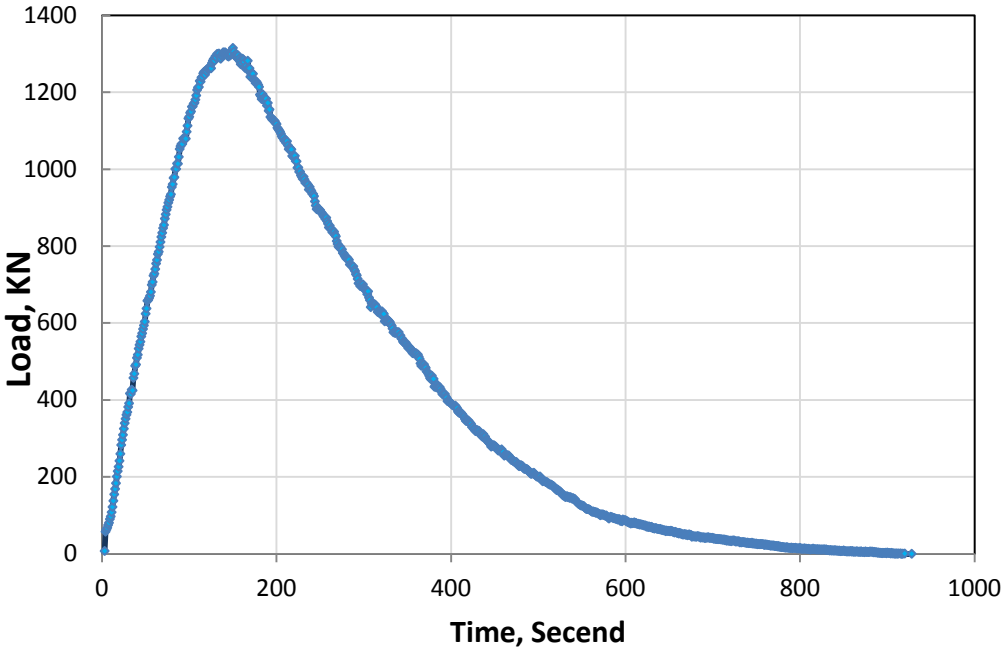

FIGURE 130 Indirect tensile strength for (3 P, 3 A) at 100 ºF.